

**1,3-DIPOLAR CYCLOADDITION REACTIONS OF SOME
AZOMETHINE IMINES AND
AZOMETHINE YLIDES**

by

MUSTAFA KEMAL BAYAZIT

**THESIS SUBMITTED TO
THE GRADUATE SCHOOL OF NATURAL AND APPLIED SCIENCES
OF
THE ABANT İZZET BAYSAL UNIVERSITY
IN PARTIAL FULLFILLMENT OF THE REQUIREMENTS FOR THE
DEGREE OF MASTER OF SCIENCE IN THE DEPARTMENT OF
CHEMISTRY**

AUGUST 2005

ABSTRACT

1,3-DIPOLAR CYCLOADDITION REACTIONS OF SOME AZOMETHINE IMINES AND AZOMETHINE YLIDES

BAYAZIT, Mustafa Kemal

M.Sc. , Department of Chemistry

Supervisor : Prof.Dr. Nihat ÇELEBİ

July 2005, 105 pages

In this work, 1,3-dipolar cycloaddition reactions of three azomethine imines (betaines) and, three azomethine ylides, which are the new in the literature, to the different dipolarophiles such as; dimethyl acetylene dicarboxylate, diethyl acetylenedicarboxylate, vinyl acetate, diphenyl acetylene, phenylacetylene and vinylene carbonate are described. To our best knowledge of literature survey, six new azomethine ylide cycloadducts have been synthesized. Purification of the title compounds have been performed by means of preparative thin layer chromatography and column chromatography on silica gel. Also much attention was focused on the theoretical calculations of HOMO, LUMO energy levels of both azomethine ylides and dipolarophiles. In addition, the probability of formation of azomethine ylide based cycloadducts were discussed depending on the theoretical calculations. The

structures of pyridinium ylide cycloadducts were elucidated by means of IR, NMR and physical characteristics (melting points and retardation factors).

Keywords: 1,3-Dipolar cycloaddition reactions, azomethine imine, azomethine ylide

ÖZET

BAZI AZOMETİN İMİNLER VE AZOMETİN İLİDLERİN 1,3-DİPOLAR HALKASAL KATILMA REAKSİYONLARI

BAYAZIT, Mustafa Kemal

Yüksek Lisans Tezi , Kimya Bölümü

Tez Danışmanı : Prof.Dr. Nihat ÇELEBİ

Temmuz 2005, 105 sayfa

Bu çalışmada, literatürde yeni olmak üzere üç adet azometin imine ve üç adet azometin ilid dipolünün farklı dipolarofil reaktifler olan dimetil asetilendikarboksilat, dietil asetilendikarboksilat, vinil asetat, difenil asetilen, fenil asetilen ve vinilen karbonat ile 1,3 dipolar halkalı katılma tepkimeleri tanımlanmaktadır. En son literatür araştırması esas alınarak 6 adet yeni halkasal azometin ilid bileşiğinin sentezi gerçekleştirildi. Ürünlerin tepkime karışımından saf olarak ayrılmaları silika jel üzerinde preparatif ince tabaka kromatografisi ve kolon kromatografisi ile yapıldı. Ayrıca azometin ilidler ve dipolarofillerin HOMO, LUMO enerji seviyelerinin teorik hesaplamaları üzerinde odaklanıldı. Buna ilaveten, teorik hesaplamalar kullanılarak halkasal azometin ilid bileşiklerinin teorik olarak oluşma ihtimali tartışıldı. Bileşiklerin yapı tayinleri IR, NMR ve bazı fiziksel sabitler (erime noktası, Rf değerleri) yardımıyla gerçekleştirildi.

Anahtar Kelimeler: 1,3-Dipolar halkasal katılma reaksiyonları, azometin imin, azometin ilid.

TO MY PARENTS AND SISTERS

ACKNOWLEDGEMENTS

I would like to thank my supervisor, Prof. Dr. Nihat ÇELEBİ for his guidance, encouragements and his enthusiasm throughout this study and writing up. It has been a privilege and pleasure to work for him.

I would also like to special thank Assoc.Prof. Dr. Özdemir ÖZARSLAN for his generous support over the entire course of this thesis. In particularly I am thankful to my friends and colleagues, Erhan BUDAK, Cevher ALTUĞ, Muhammet YILDIRIM, and, of course, Metin ALKAN for their support whenever I need it.

Gratitude is also extended to the Chemistry Department of A.İ.B.U. for providing the necessary equipment and chemicals which made this work possible and thanks to Assoc. Prof. Dr. F. Devrim ÖZDEMİRHAN for NMR data.

I would like to thank my family for their strong support and encouragement of my studies.

Finally, I would like to thank Hilal, who brings immeasurable joy to my life by simply being a part of it.

TABLE OF CONTENTS

| | |
|---|--------------|
| ABSTRACT | iii |
| ÖZET | v |
| ACKNOWLEDGEMENTS | viii |
| TABLE OF CONTENTS | ix |
| FORMULAE | xiv |
| LIST OF TABLES | xxiii |
| LIST OF FIGURES | xxiv |
| LIST OF SYMBOLS AND ABBREVIATIONS | xxvii |
| 1. INTRODUCTION | 1 |
| 1.1. Electrocyclic Reactions..... | 2 |
| 1.2. Sigmatropic Reactions..... | 2 |
| 1.3. Ene Reactions..... | 3 |
| 1.4. Cycloaddition and Cyclo-elimination reactions..... | 4 |
| 2. THEORY OF CYCLOADDITION REACTIONS | 5 |
| 2.1. Cycloaddition Reactions..... | 5 |
| 2.1.1. Definition and Classification | 5 |
| 2.1.2. Mechanisms | 7 |

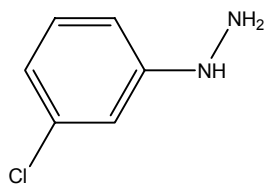
| | |
|--|----|
| 2.1.2.1. Concerted Mechanism..... | 9 |
| 2.1.2.2. Stepwise Mechanism..... | 10 |
| 2.1.3. 1,3-Dipolar Cycloaddition Reactions..... | 10 |
| 2.1.3.1. The 1,3-Dipoles..... | 12 |
| 2.1.3.2. The Dipolarophiles..... | 14 |
| 2.1.3.3. Frontier Molecular Orbital Interactions..... | 15 |
| 2.1.3.4. The Selectivities of 1,3-Dipolar Cycloaddition Reactions.. | 17 |
| 2.1.3.5. Simplified Molecular Orbital Theories and Computational Methods..... | 20 |
| 2.1.3.6. Azomethine Imine and Azomethine Ylide..... | 24 |
| 2.1.3.6.1. Azomethine Imines..... | 24 |
| 2.1.3.6.1.1. Crystalline N(β)-Cyano (Azomethine Imines)..... | 24 |
| 2.1.3.6.1.2. Azomethine Imines of the 3,4- Dihydroisoquinoline Series..... | 25 |
| 2.1.3.6.1.3. N-Imines of Pyridine, Quinoline, and Isoquinoline..... | 26 |
| 2.1.3.6.1.4. 2-Methylindazole..... | 27 |
| 2.1.3.6.1.5. Sydnone..... | 27 |
| 2.1.3.6.1.6. 1,2-Disubstituted Hydrazines and Carbonyl Compounds | 28 |
| 2.1.3.6.2. Azomethine Ylides | 29 |

| | |
|---|-----------|
| 2.1.4. Aim of this work..... | 30 |
| 3. EXPERIMENTAL..... | 31 |
| 3.1. Preparation of Mainly Used Solvents..... | 31 |
| 3.1.1. Tetrahydrofuran (THF) | 31 |
| 3.1.2. Acetone..... | 31 |
| 3.1.3. Chloroform..... | 31 |
| 3.2. Synthesis of starting compounds of Azomethine Imines..... | 32 |
| 3.2.1. Preparation of <i>m</i> -chlorophenylhydrazine hydrochloride (2a)..... | 32 |
| 3.2.2. Preparation of <i>p</i> -chlorophenylhydrazine hydrochloride (2b)..... | 33 |
| 3.2.3. Synthesis of 4,6-Bis-[<i>N</i> -(3-chloro-phenyl)-hydrazinocarbonyl]- isophthalic acid and 2,5-Bis-[<i>N</i> -(3-chloro-phenyl-hydrazinocarbonyl)- isophthalic acid (2c) (2c') | 34 |
| 3.2.4. Synthesis of 2,6-Bis-(3-chloro-phenyl amino)-pyrrolo[3,4- <i>f</i>]isoindole-1,3,5,7,tetraone (2d)..... | 35 |
| 3.2.5. Synthesis of 2,6-Bis-(3-chloro-phenylamino)-3,7-dihydroxy-2,3,6,7- tetrahydro-pyrrolo[3,4- <i>f</i>]isoindole-1,5-dione (2e) and 2,6-Bis-(3-chloro- phenylamino)-3,5-dihydroxy-2,3,5,6-tetrahydro-pyrrolo[3,4- <i>f</i>]isoindole- 1,7-dione (2e')..... | 35 |
| 3.2.6. Synthesis of 4,6-Bis-[<i>N</i> -(4-chloro-phenyl)-hydrazinocarbonyl] isophthalic acid, 2,5-Bis-[<i>N</i> -(4-chloro-phenyl)-hydrazinocarbonyl]- isophthalic acid (2f) (2f')..... | 37 |

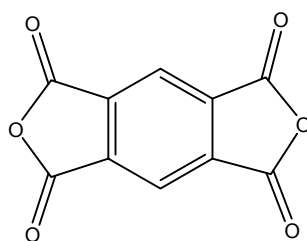
| | |
|---|----|
| 3.2.7. Synthesis of 2,6-Bis-(4-chloro-phenyl amino)-pyrrolo[3,4- <i>f</i>] isoindole-1,3,5,7,tetraone (2g)..... | 38 |
| 3.2.8. Synthesis of 2,6-Bis-(4-chloro-phenylamino)-3,7-dihydroxy-2,3,6,7- tetrahydro-pyrrolo[3,4- <i>f</i>]isoindole-1,5-dione (2h) and 2,6-Bis-(4-chloro- phenylamino)-3,5-dihydroxy-2,3,5,6-tetrahydro-pyrrolo[3,4- <i>f</i>]isoindole- 1,7-dione (2h')..... | 39 |
| 3.2.9. Synthesis of 4,6-Bis-[<i>N</i> -phenylhydrazinocarbonyl]-isophthalic acid, 4,6-Bis-[<i>N</i> -phenylhydrazinocarbonyl]-isophthalic acid (2i) (2i')..... | 40 |
| 3.2.10. Synthesis of 2,6-Bis-(phenylamino)-pyrrolo[3,4- <i>f</i>]isoindole- 1,3,5,7,tetra one (2j)..... | 41 |
| 3.2.11. Synthesis of 2,6-Bis-(phenylamino)-3,7-dihydroxy-2,3,6,7- tetrahydro pyrrolo[3,4- <i>f</i>]isoindole-1,5-dione(2k) and 2,6-Bis- (phenylamino)-3,5-dihydroxy-2,3,5,6-tetrahydro-pyrrolo[3,4- <i>f</i>]isoindole- 1,7-dione(2k')..... | 42 |
| 3.2.12. Synthesis of 3-chlorophenylhydrazine substituted olate (2l) (2l')..... | 43 |
| 3.2.13. Synthesis of 4-chlorophenylhydrazine substituted olate (2m) (2m')..... | 44 |
| 3.2.14. Synthesis of phenylhydrazine substituted olate (2n) (2n')..... | 45 |
| 3.3. Synthesis of starting compounds of azomethine ylides and their cycloadducts..... | 46 |

| | |
|---|-----------|
| 3.3.1. Synthesis of unsubstituted pyridinium bromide (3a)..... | 46 |
| 3.3.2. Synthesis of 3-cyanopyridinium bromide (3b)..... | 47 |
| 3.3.3. Synthesis of 4 -cyanopyridinium bromide (3c)..... | 47 |
| 3.3.4. Synthesis of unsubstituted pyridinium ylide (3d)..... | 48 |
| 3.3.5. Synthesis of 3-cyanopyridinium ylide (3e) or (3e')..... | 48 |
| 3.3.6. Synthesis of 4-cyanopyridinium ylide (3f)..... | 49 |
| 3.3.7. Reaction of unsubstituted pyridinium ylide with DMAD..... | 49 |
| 3.3.8. Reaction of unsubstituted pyridinium ylide with DEAD..... | 51 |
| 3.3.9. Reaction of 3-cyanopyridinium ylide with DMAD..... | 52 |
| 3.3.10. Reaction of 3-cyanopyridinium ylide with DEAD..... | 53 |
| 3.3.11. Reaction of 4-cyanopyridinium ylide with DMAD..... | 54 |
| 3.3.12. Reaction of 4-cyanopyridinium ylide with DEAD..... | 55 |
| 4. RESULTS&DISCUSSION..... | 56 |
| 4.1. Synthesis of Azomethine Imines..... | 56 |
| 4.2. Synthesis of Azomethine Ylides 3d, 3e, 3e' and 3f..... | 60 |
| 4.2.1. Characterization of Cycloadducts..... | 65 |
| 4.2.2. Molecular Orbital Consideration..... | 77 |
| 5. CONCLUSIONS..... | 88 |
| REFERENCES..... | 90 |
| APPENDIX : IR , ¹H NMR, ¹³C NMR FIGURES..... | 94 |

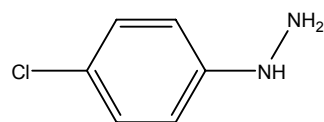
FORMULAE



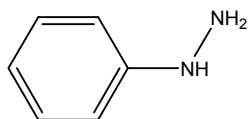
(1a)



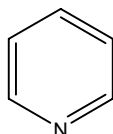
(1b)



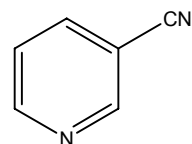
(1c)



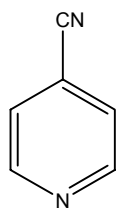
(1d)



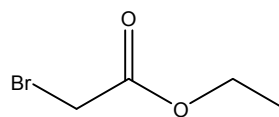
(1e)



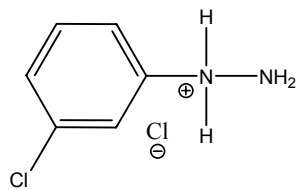
(1f)



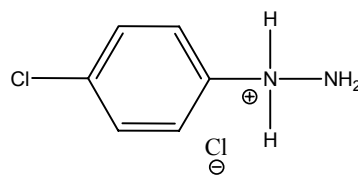
(1g)



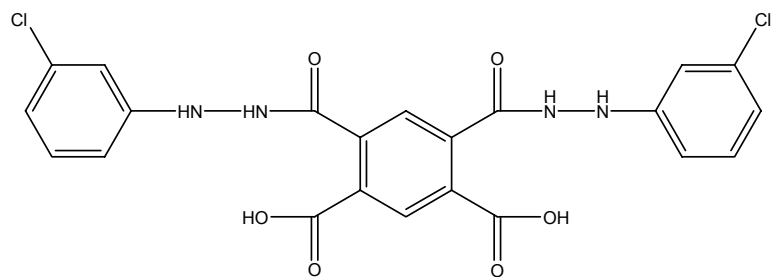
(1h)



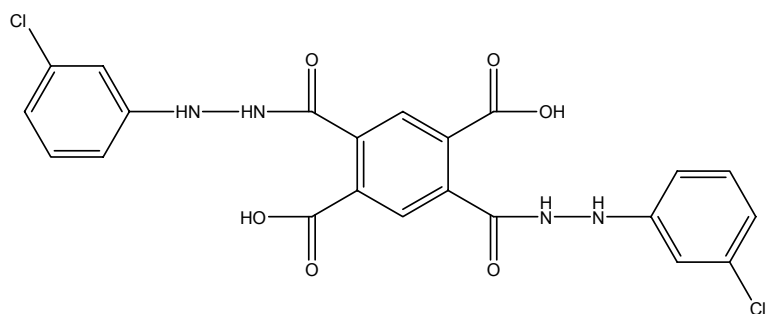
(2a)



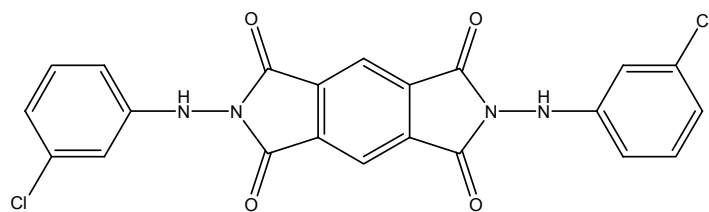
(2b)



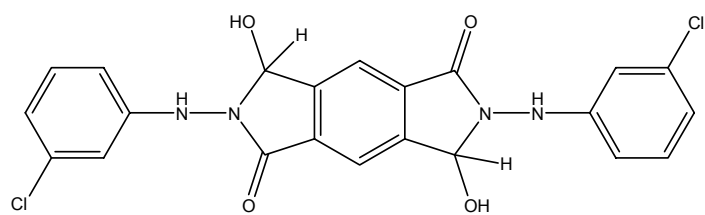
(2c)



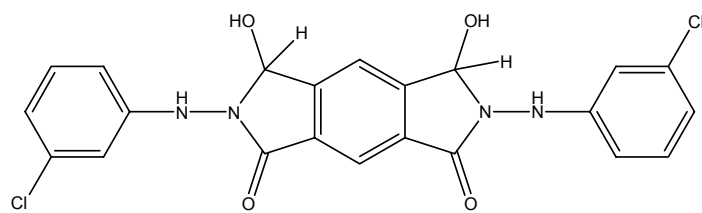
(2c')



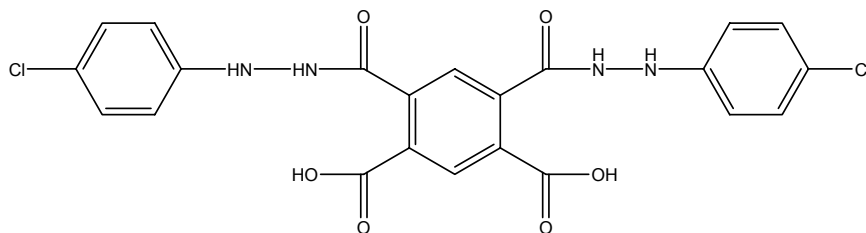
(2d)



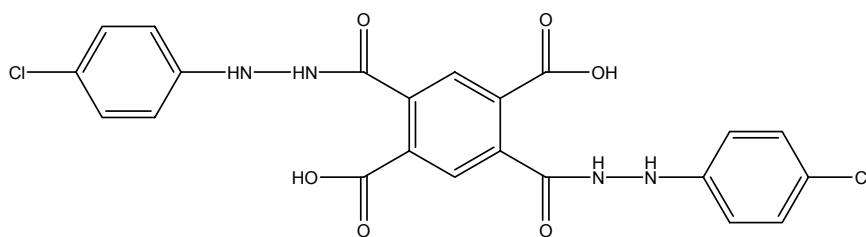
(2e)



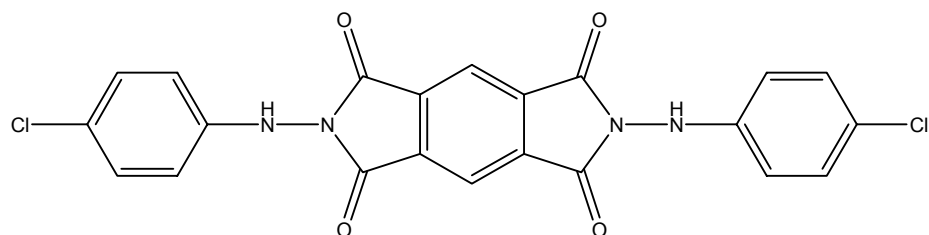
(2e')



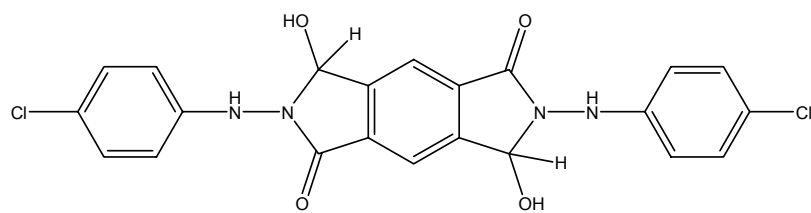
(2f)



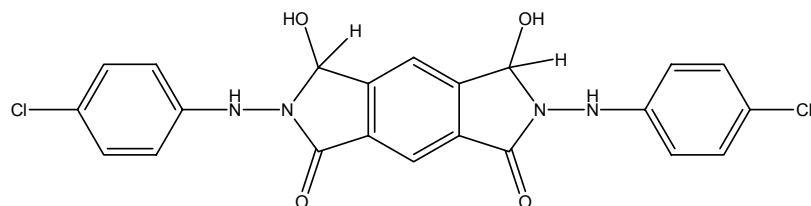
(2f')



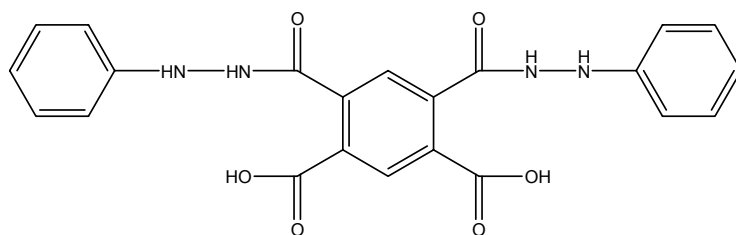
(2g)



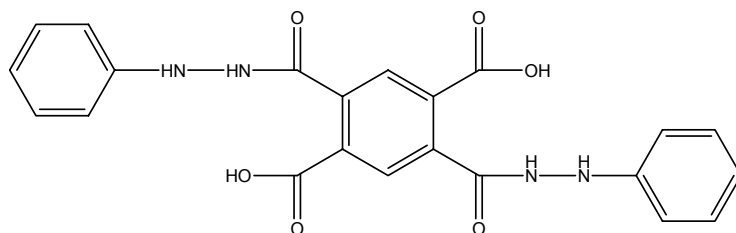
(2h)



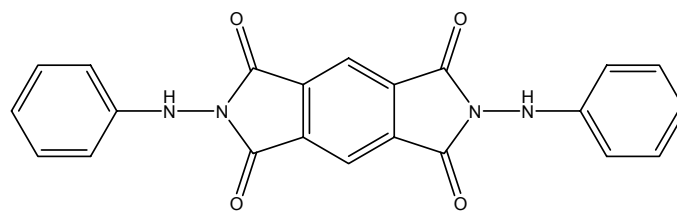
(2h')



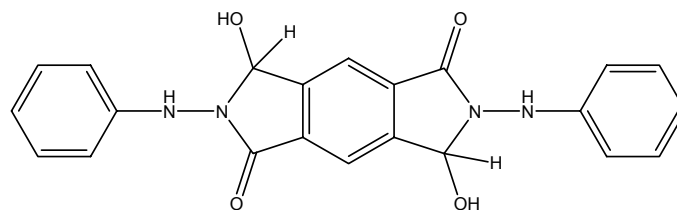
(2i)



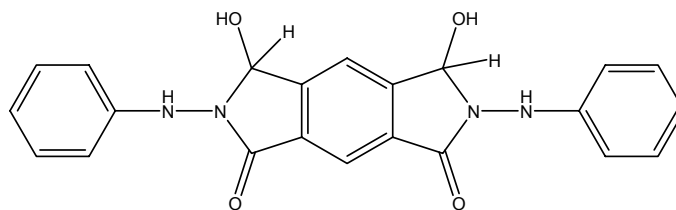
(2i')



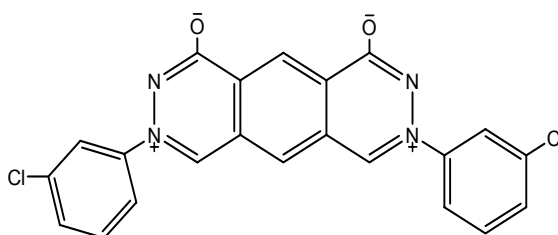
(2j)



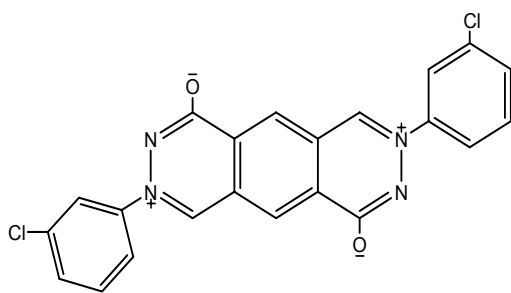
(2k)



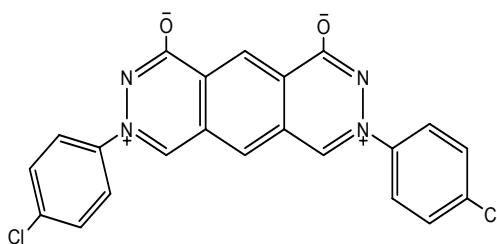
(2k')



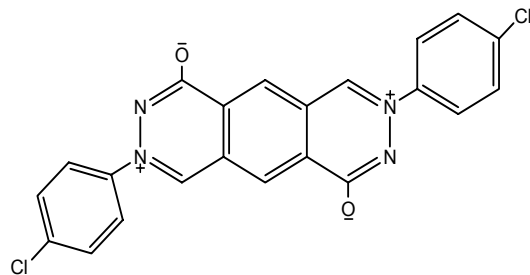
(2l)



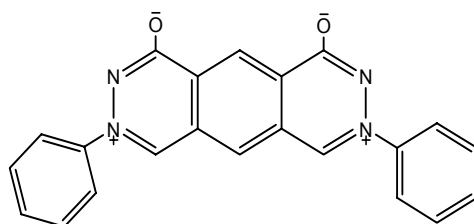
(2l')



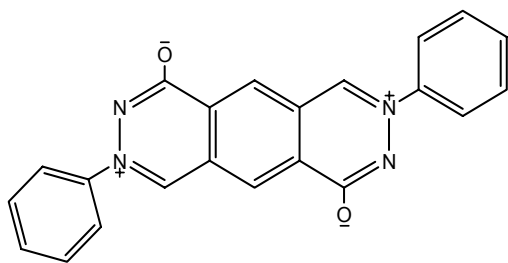
(2m)



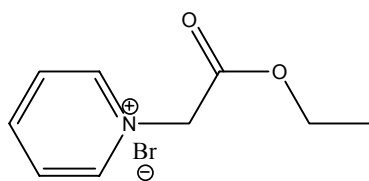
(2m')



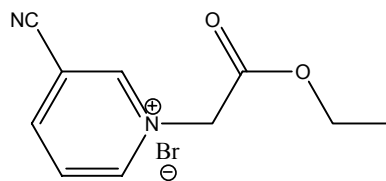
(2n)



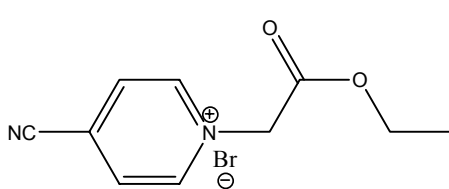
(2n')



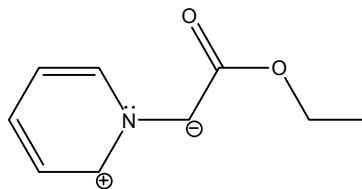
(3a)



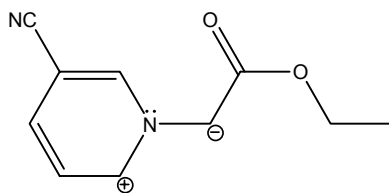
(3b)



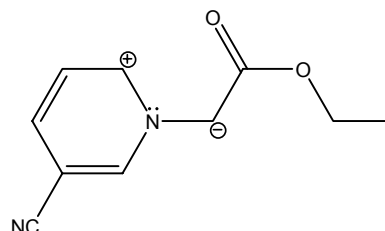
(3c)



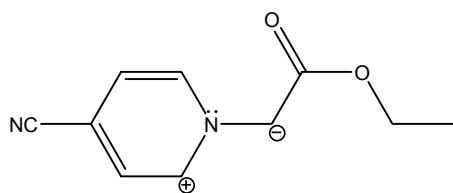
(3d)



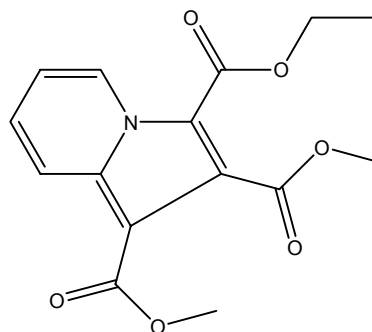
(3e)



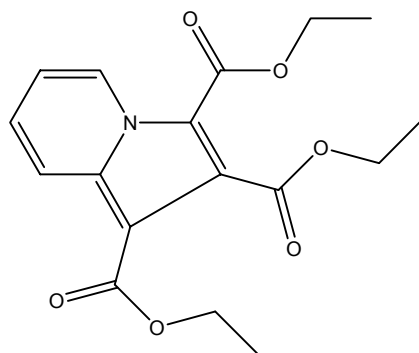
(3e')



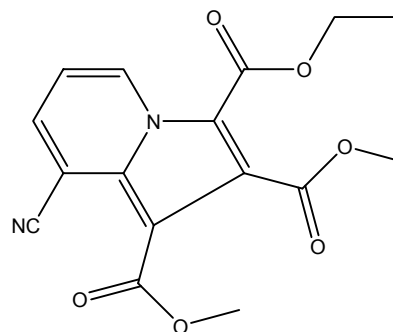
(3f)



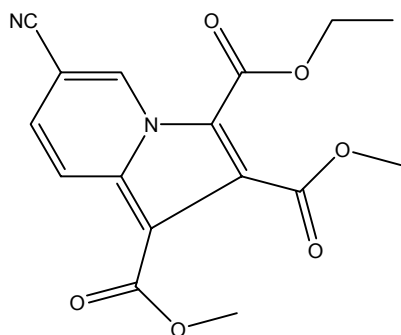
(3g)



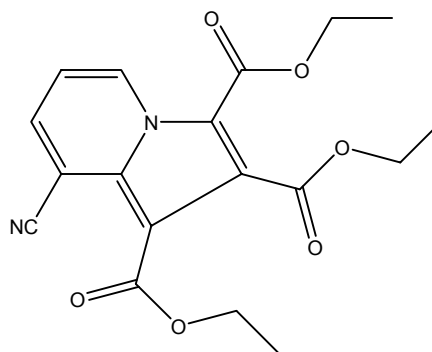
(3h)



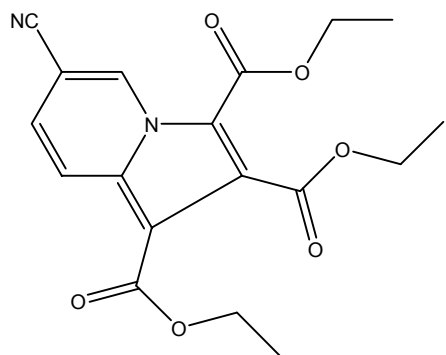
(3i)



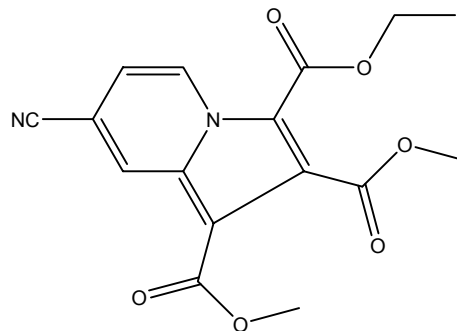
(3i')



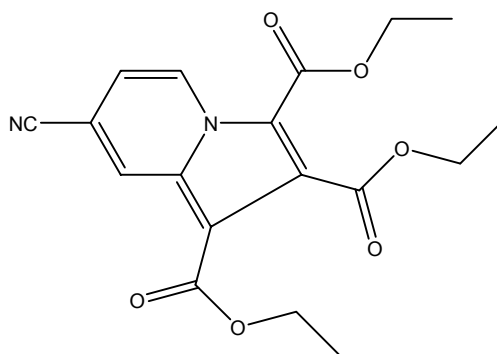
(3j)



(3j')



(3k)



(3l)

LIST OF TABLES

| | |
|--|-----------|
| Table 1. The FMO energies of the azomethine ylides in eV..... | 78 |
| Table 2. The HOMO and LUMO energies of dipolarophiles in eV..... | 79 |
| Table 3. The FMO coefficients of the azomethine ylides in eV..... | 83 |
| Table 4. The FMO coefficients of the dipolarophiles in eV..... | 84 |

LIST OF FIGURES

| | |
|--|----|
| Figure 1.1. A simple representation of Electrocyclic Reactions..... | 2 |
| Figure 1.2. A simple representation of Sigmatropic Reactions..... | 3 |
| Figure 1.3. A simple representation of Ene Reactions..... | 3 |
| Figure 1.4. A simple representation of Cycloaddition and Cyclo-elimination Reactions..... | 4 |
| Figure 2.1. The ring-forming cycloaddition and the ring-opening cycloreversion reactions..... | 6 |
| Figure 2.2. Energy profile of a Concerted Mechanism..... | 7 |
| Figure 2.3. Energy profile of a Stepwise Mechanism..... | 8 |
| Figure 2.4. A hypothetical fragmentation of a ring..... | 9 |
| Figure 2.5. 1,3-dipoles as (a) propargyl-allenyl and (b) allyl type..... | 13 |
| Figure 2.6. Canonical structures of common 1,3-dipoles..... | 13 |
| Figure 2.7. The simple representation of a 1,3-dipolar cycloaddition..... | 14 |
| Figure 2.8. Possible interactions between 1,3-dipole (A) and dipolarophile (B)..... | 16 |
| Figure 2.9. Two possible regioisomers of the 1,3-dipolar additions of an unsymmetrical 2π -system..... | 17 |
| Figure 2.10. Diastereoselectivity in a 1,3-dipolar cycloaddition reaction..... | 19 |
| Figure 2.11. Representation of (a) $[\pi 4_s + \pi 2_s]$ and (b) $[\pi 2_s + \pi 2_s]$ reactions..... | 21 |
| Figure 3.1. The i.r. spectrum of 2c,c' (In Nujol)..... | 95 |
| Figure 3.2. The i.r. spectrum of 2d (In Nujol)..... | 95 |
| Figure 3.3. The i.r. spectrum of 2e,e' (In Nujol)..... | 96 |

| | |
|--|------------|
| Figure 3.4. The i.r. spectrum of 2f,f' (In Nujol)..... | 96 |
| Figure 3.5. The i.r. spectrum of 2g (In Nujol)..... | 97 |
| Figure 3.6. The i.r. spectrum of 2h,h' (In Nujol)..... | 97 |
| Figure 3.7. The i.r. spectrum of 3b (In Nujol)..... | 98 |
| Figure 3.8. The i.r. spectrum of 3c (In Nujol)..... | 98 |
| Figure 3.9. The i.r. spectrum of cycloadduct 3h (In Nujol)..... | 99 |
| Figure 3.10. The ¹ H NMR spectrum of cycloadduct 3h..... | 99 |
| Figure 3.11. The ¹³ C NMR spectrum of cycloadduct 3h..... | 101 |
| Figure 3.12. The i.r. spectrum of cycloadduct 3j' (In Nujol)..... | 102 |
| Figure 3.13. The ¹ H NMR spectrum of cycloadduct 3j'..... | 102 |
| Figure 3.14. The i.r. spectrum of cycloadduct 3l (In Nujol)..... | 104 |
| Figure 3.15. The ¹ H NMR spectrum of cycloadduct 3l..... | 104 |
| Figure 4.1. The schematic representation of the synthesis of azomethine imines..... | 57 |
| Figure 4.2. The i.r. spectrum of 2i,2i' (In Nujol)..... | 59 |
| Figure 4.3. The i.r. spectrum of 2j (In Nujol)..... | 59 |
| Figure 4.4. The i.r. spectrum of 2k, 2k' (In Nujol)..... | 60 |
| Figure 4.5. The schematic representation of the synthesis of azomethine ylide 3d..... | 61 |
| Figure 4.6. The i.r. spectrum of 3a (In Nujol)..... | 62 |
| Figure 4.7. The ¹ H NMR of 3a..... | 63 |
| Figure 4.8. The ¹³ C NMR of 3a..... | 65 |
| Figure 4.9. The schematic representation of the synthesis of cycloadduct 3g..... | 66 |
| Figure 4.10. The i.r. spectrum of cycloadduct 3g (In Nujol)..... | 67 |

| | |
|--|-----------|
| Figure 4.11. The ^1H NMR spectrum of cycloadduct 3g..... | 68 |
| Figure 4.12. The ^{13}C NMR spectrum of cycloadduct 3g..... | 70 |
| Figure 4.13. The i.r. spectrum of cycloadduct 3i' (In Nujol)..... | 71 |
| Figure 4.14. The ^1H NMR spectrum of cycloadduct 3i'..... | 72 |
| Figure 4.15. The i.r. spectrum of cycloadduct 3k (In Nujol)..... | 74 |
| Figure 4.16. The ^1H NMR spectrum of cycloadduct 3k..... | 75 |
| Figure 4.17. The relative energy gaps of the pyridinium ylide and dipolarophiles.... | 80 |
| Figure 4.18. The relative energy gaps of the 3-cyanopyridinium ylide and dipolarophiles..... | 81 |
| Figure 4.19. The relative energy gaps of the 4-cyanopyridinium ylide and dipolarophiles..... | 82 |
| Figure 4.20. Bonding interactions between the ylides and dipolarophiles..... | 85 |

LIST OF SYMBOLS AND ABBREVIATIONS

| | |
|----------------------|---|
| DC | Dipolar Cycloaddition |
| DA | Diels-Alders |
| Δ | Heat |
| CNDO/2 | Complete Neglect of Differential Overlap |
| MINDO/3 | Modified Intermediate Neglect of Differential Overlap |
| LUMO | Lowest Unoccupied Molecular Orbital |
| HOMO | Highest Unoccupied Molecular Orbital |
| FMO | Frontier Molecular Orbitals |
| LCAO | Linear Combination of Atomic Orbitals |
| PMO | Perturbational Molecular Orbital |
| EH | Extended Huckel |
| MO | Molecular Orbitals |
| M.p. | Melting point |
| R_f | Retardation Factor |
| DMAD | Dimethyl acetylenedicarboxylate |
| DEAD | Diethyl acetylenedicarboxylate |
| VA | Vinyl acetate |
| DPA | Diphenylacetylene |
| PA | Phenylacetylene |
| VC | Vinylene carbonate |
| DMF | Dimethylformamide |
| EtOH | Ethyl Alcohol |

| | |
|--------------|-----------------------------|
| THF | Tetrahydrofuran |
| EtOAc | Ethyl Acetate |
| FT-IR | Fourier Transform Infra-Red |
| IR | Infra Red |
| NMR | Nuclear Magnetic Resonance |

1. INTRODUCTION

An important body of chemical reactions, differing from ionic or free radical reactions in a number of respects, has been recognized and extensively studied. Among the characteristics shared by these reactions, three in particular set them apart.:

1. They are relatively unaffected by solvent changes, the presence of radical initiators or scavenging reagents, or (with some exceptions) by electrophilic or nucleophilic catalysts.

2. They proceed by a simultaneous or concerted collection of bond breaking and bond making events, often with high stereospecificity.

3. In agreement with 1 & 2, no discernible ionic or free radical intermediates lie on the reaction path.

Since reactions of this kind often proceed by the simultaneous reorganization of bonding electron pairs by way of cyclic transition states, they have been termed pericyclic reactions. The four principle classes of pericyclic reactions are termed: Cycloaddition, Electrocyclic, Sigmatropic, and Ene Reactions [1].

1.1. Electrocyclic Reactions

An electrocyclic reaction involves the concerted formation of a σ bond between the two ends of a linear conjugated π system, or the reverse reaction in which the σ bond is broken to produce a linear conjugated system.

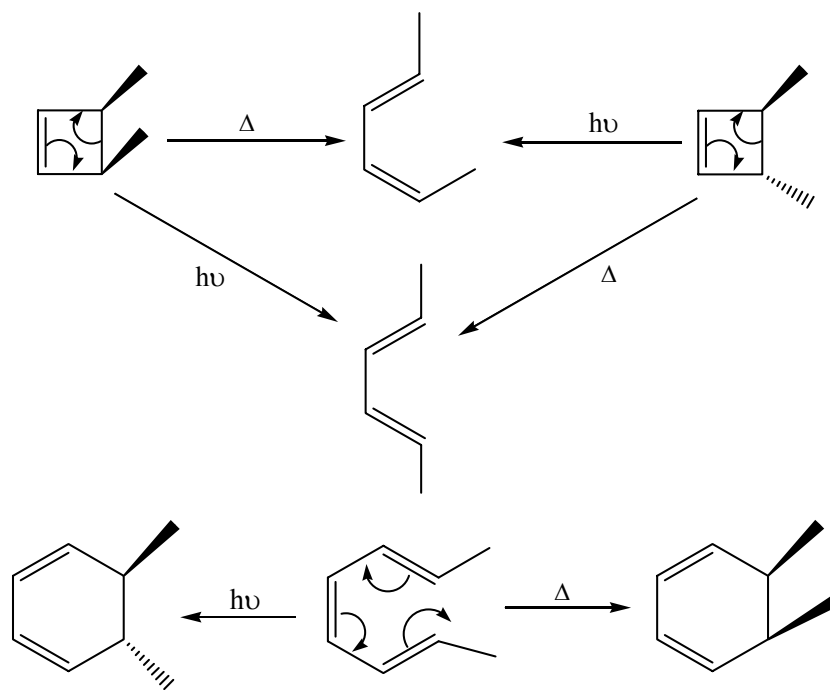


Figure 1.1. A simple representation of Electrocyclic Reactions

1.2. Sigmatropic Reactions

A sigmatropic reaction involves the concerted migration of an atom or group from one point of attachment to a conjugated system to another point of attachment, during which one σ bond is broken and another σ bond is made. A sigmatropic

reaction can be classified according to the length of the group that migrates, and the length of the backbone along which it migrates;

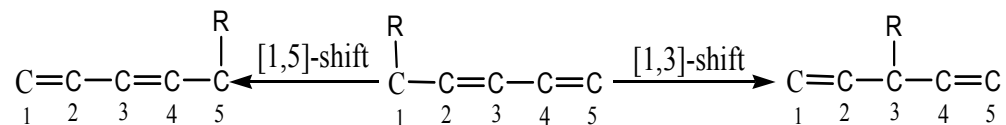


Figure 1.2. A simple representation of Sigmatropic Reactions

1.3. Ene Reactions

A general category which involves the formation and cleavage of unequal numbers of σ bonds in a concerted cyclic transition state.

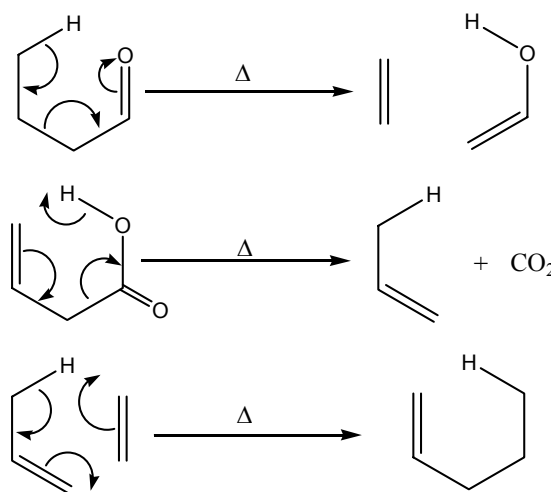


Figure 1.3. A simple representation of Ene Reactions

1.4. Cycloaddition and Cyclo-elimination Reactions

A cycloaddition reaction involves the concerted formation of two or more σ bonds between the termini of two or more conjugated π systems. Cycloaddition reactions are symmetry controlled reactions [2]. In general, cycloadditions can be designated by a bracket $[m+p]$ where m and p represent the number of π electrons in each participants [3]. The reverse reaction involves the concerted cleavage of two or more σ bonds to produced two or more conjugated π systems.

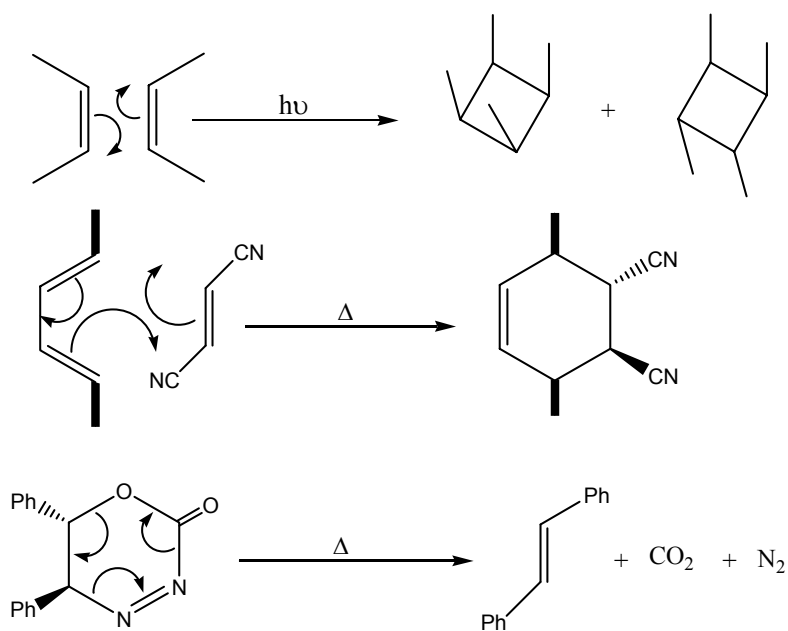


Figure 1.4. A simple representation of Cycloaddition and Cycloelimination Reactions

2. THEORY OF CYCLOADDITION REACTIONS

2.1. Cycloaddition Reactions

Cycloaddition reactions are one of the most important processes with both synthetic and mechanistic interest in organic chemistry. Current understanding of the underlying principles in the Diels-Alder (DA) reactions and the 1,3-dipolar cycloadditions (1,3-DC) has grown from a fruitful interplay between theory and experiment [4, 5, 6].

2.1.1. Definition and Classification

A concerted combination of two π -electron systems to form a ring of atoms having two new σ bonds and two fewer π bonds is called a cycloaddition reaction. The number of participating π -electrons in each component is given in brackets preceding the name, and the reorganization of electrons may be depicted by a cycle of curved arrows- each representing the movement of a pair of electrons. (Figure 2.1)

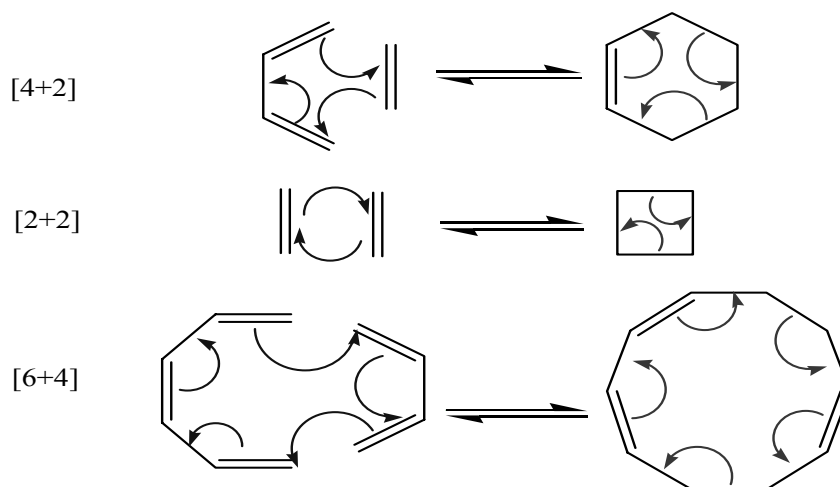


Figure 2.1. The ring-forming cycloaddition and the ring-opening cycloreversion reactions

According to the Huisgen a cycloaddition reaction has to fulfill with the following requirements [7].

- i) Cycloadditions are ring closures in which the number of σ -bonds increases.
- ii) Cycloadditions are not associated with the elimination of small molecules or ions. The cycloadduct corresponds to the whole integrity of the components.
- iii) Cycloadditions do not involve the cleavage of σ -bonds. The reverse is true for retroadditions.
- iv) Cycloadditions can be intramolecular, if a molecule contains the necessary number of π -bonds (σ -bonds for retroadditions) in its skeleton.
- v) When more than two components combine, only the reaction step leading to the ring formation is a cycloaddition.
- vi) The products of a cycloaddition need not be stable, or isolable, but the cycloadducts must occur at least as intermediates.

Generally, a cycloaddition reaction is the union of two molecules, each containing one or more conjugated double bonds. Their π -orbitals overlap and undergo cycloaddition.

2.1.2. Mechanisms

Reactions in which more than one bond is broken or formed can be divided into two classes [8]. The first is one in which all the bond forming and bond breaking processes occur simultaneously so that a one step transformation of reactants to products occurs without the intervention of an intermediate. Such reactions are called concerted since the bond changes occur in concert or at the same time at more than one centre. The energy curve for such processes as shown in Figure 2.2; it involves only one energy barrier and one transition state.

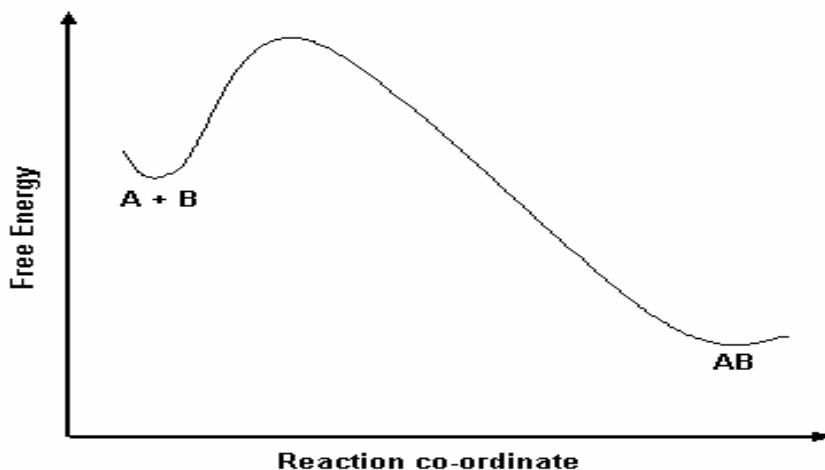


Figure 2.2. Energy profile of a Concerted Mechanism

The second broad class of reactions is one in which the bond forming and breaking processes occur consecutively so that one or more intermediates is involved. These intermediates may be stable molecules capable of isolation, or they may be highly reactive species of only transient existence. Where the intermediate is a stable molecule it is often more convenient to consider the overall process as two or more consecutive concerted reactions. Where the intermediates are unstable the process is normally considered as one reaction which proceeds in a stepwise manner. This distinction is purely arbitrary and one of convenience. The energy curve for simple stepwise reaction could be as in Figure 2.3.

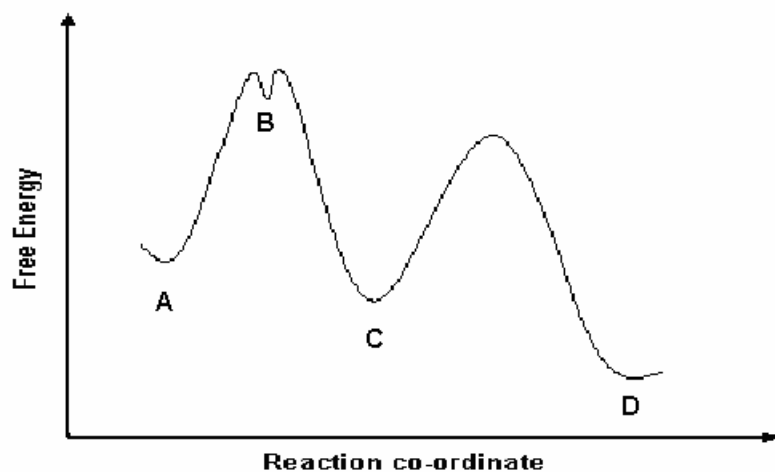


Figure 2.3. Energy profile of a Stepwise Mechanism

In such a reaction C is formed from A via an unstable intermediate B which has a discrete, though short, lifetime. The instability of B is indicated by the fact that it lies in a shallow energy well. It has only a small energy barrier to surmount in order to pass over the products or to revert to reactants. The more stable such an

intermediate is, the deeper the energy well. C is relatively stable and lies in a deep energy well.

Although C is the first isolable product to be formed, it may subsequently pass over to the more stable D in the reaction conditions. C is called the kinetically controlled product of reaction of A. D, which is the product isolated after the system reaches equilibrium, is called the thermodynamically controlled product. This is the type of situation where kinetic and thermodynamic control is most frequently encountered.

Cycloaddition reactions are regarded as proceeding in either a concerted or in a nonconcerted fashion involving biradical or dipolar intermediates.

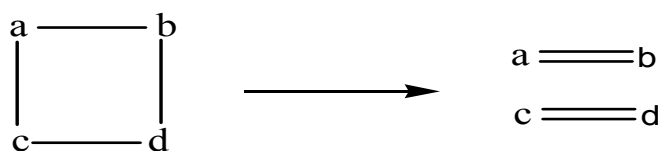


Figure 2.4. A hypothetical fragmentation of a ring

2.1.2.1. Concerted Mechanism

In the concerted fragmentation the breaking of the a-c bond is coupled with, and depends on, the breaking of the b-d bond, so that both processes are going on at the same time. The overall reaction does not involve an intermediate and the energy profile is of the type shown in figure 2.2. There is only one energy barrier with a transition state in which both σ -bonds are partially broken and the new π -bonds in $a=b$ and $c=d$ are partially formed. In an unsymmetrical concerted process the transition state has some of the character of the intermediates which are involved in

truly stepwise processes; the an unequal rates of formation of the two bonds leads to the development of dipolar or diradical character in the transition state.

Woodward and Hoffmann [9] have introduced the term pericyclic to cover all concerted reactions which involve a cyclic transition state, and define it as follows: ‘a pericyclic reaction in which all first order changes in bonding relationships take place in concert on a closed curve’.

2.1.2.2. Stepwise Mechanism

The bonds a-c and b-d may break in two successive independent steps. The reaction then involves an intermediate in which only one of the σ -bonds is broken. The energy profile will be as in Figure 2.3, with two transition states [10].

2.1.3. 1,3-Dipolar Cycloaddition Reactions

The 1,3-dipolar cycloaddition reaction is the single most important method for the construction of heterocyclic five-membered rings in organic chemistry [11]. A cycloaddition type $3+2\rightarrow 5$ leading to an uncharged 5-membered ring can not possibly occur with octet-stabilized reactants which have no formal charges. Rather, a 1,3-dipole, a-b-c, must be defined, such that atom (a) possesses an electron sextet, i.e. an incomplete valence shell combined with a positive formal charge, and that atom (c), the negatively charged center, has an unshared electron pair. Combination of such a 1,3-dipole with a multiple bond system d-e, termed the dipolarophile, is referred to as a 1,3-dipolar cycloaddition. The two components coalesce by means of a cyclic electron displacement with extinction of the formal charges to give a 5-

membered ring. The dipolarophile may be any double or triple bond. The general concept of 1,3-dipolar cycloadditions was introduced by Huisgen and co-workers in the early 1960s [12]. Huisgen's work stated the basis for the understanding of the mechanism of concerted cycloaddition reactions. The development of the 1,3-dipolar cycloaddition reactions has in recent years entered a new stage as control of the stereochemistry in the addition step is now the major challenge. The stereochemistry of these reactions may be controlled either by choosing the appropriate substrates or by controlling the reaction using a metal complex acting as catalyst [13].

Given the importance of these reactions, a strong effort has been directed toward the characterization of the reagents in these cycloadditions as well as the elucidation of its reaction mechanism. However, the nature of the 1,3-dipolar cycloaddition reaction mechanism is still an open problem in physical organic chemistry. For instance, the mechanism proposed primarily by Huisgen is that of a single step, four-centered reaction.

A five-membered instead of a six-membered ring should result from a [4+2] cycloaddition if the 4π -electrons in the diene component be compressed into only a three-atom skeleton. This is most commonly seen in the 1,3-dipolar additions. The term dipolar here refers to the necessary formal charges in the structure of the 4π -electron component. The 2π -electron component, or dipolarophile, is usually activated by being strained, highly polar or highly polarizable [14].

2.1.3.1. The 1,3-Dipoles

The 1,3-Dipoles consist of elements from main groups IV, V, VI. A dipole is a system of three atoms over which there are distributed four π -electrons. There are a wide variety of dipoles that include a combination of carbon, oxygen and nitrogen atoms within their structures.

Dipolar cycloaddition reactions take place between unsaturated hetero atom compounds, such as azomethine imines, azomethine ylides, diazoalkanes, alkyl and aryl azides, nitrile oxides and nitrones, and alkene or alkyne functions. Although the former reactants are neutral, their Lewis structures have formal charges, and may be written as 1,3-dipoles. The terminology used for these reactions may be confusing unless one pays careful attention to the electronic structures of the dipolar reactants.

In general, four resonance canonical structures may be written for each compound. Two have adjacent or 1,2-charge separation, and two have the 1,3-dipolar charge separation noted above. The 1,2-dipolar structures retain valence shell octets for all heavy atoms, suffer less charge separation, and have one more covalent bond than do the 1,3-dipolar structures. Therefore, the most representative Lewis structures for these compounds are 1,2-dipoles, not 1,3-dipoles.

Another factor in identifying the best structure for a given compound is electronegativity. Negative charge is best on the most electronegative atom, and positive charge on the least electronegative atom.

1,3-Dipolar cycloadditions always involve syn (suprafacial)-addition to both alkene and dipolarophile, and may be regioselective. Huisgen classified 1,3-dipoles as allyl (bent) and propargyl-allenyl type (linear) (Figure 2.5).

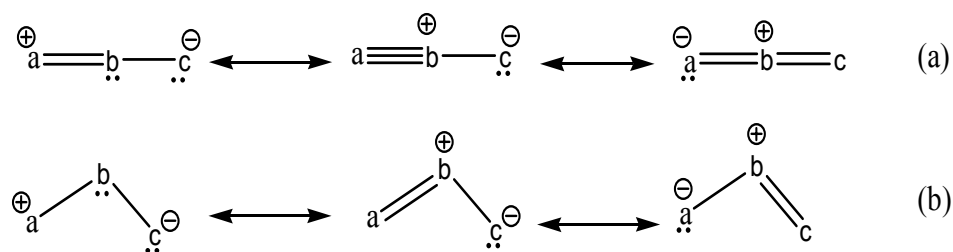


Figure 2.5. 1,3-dipoles as (a) propargyl-allenyl and (b) allyl type

In the propargyl-allenyl type, b atom must be nitrogen. No other element has an extra pair of electrons available while remaining in the triply bonded neutral state. In the allyl type, b atom can be occupied by either a nitrogen or an oxygen atom [15]

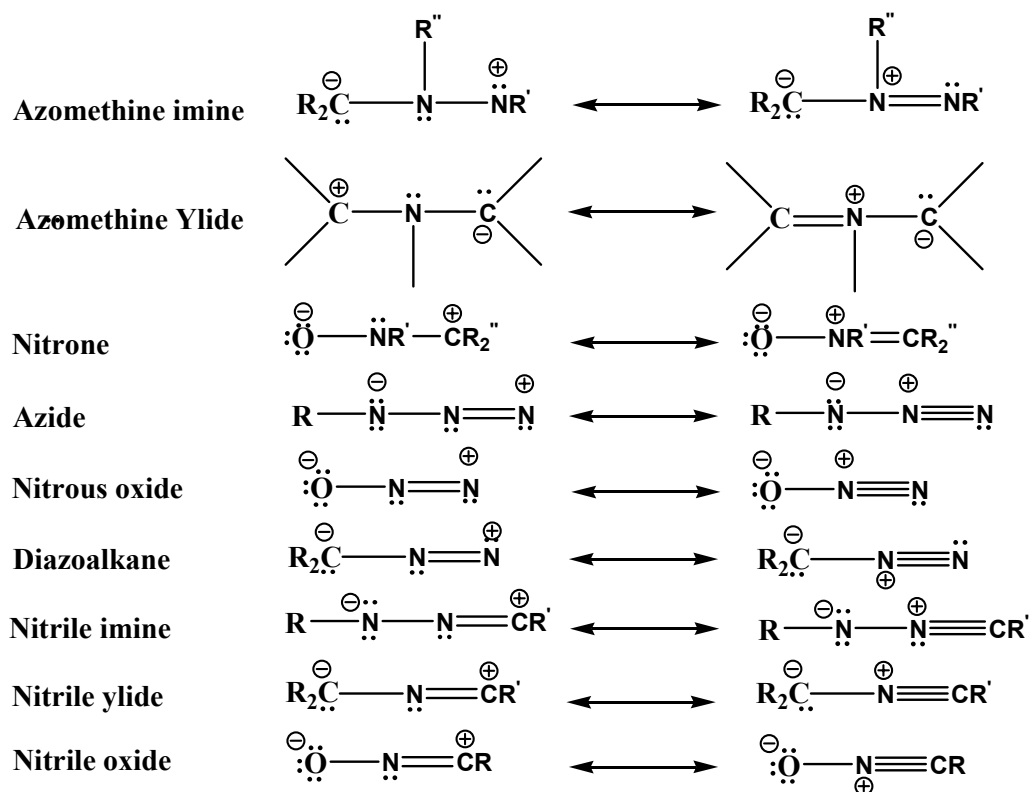


Figure 2.6. Canonical structures of common 1,3-dipoles

“Thus combination of such a zwitterionic molecule $a=b^+ - c^-$ (the dipole) with a multiple bond system $d=e$ (the dipolarophile) is referred to 1,3-dipolar cycloaddition shown in Figure 2.7.

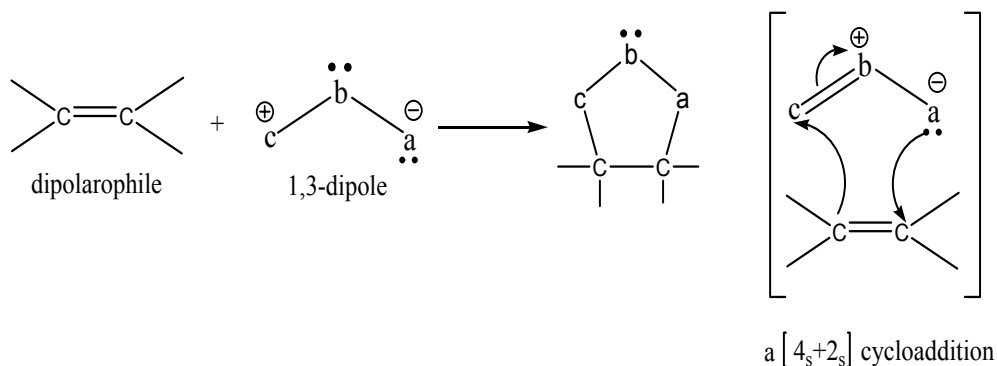


Figure 2.7. The simple representation of a 1,3-dipolar cycloaddition.

2.1.3.2. The Dipolarophiles

The alkene and alkyne functions to which the dipoles add are called dipolarophiles. The dipolarophiles can be substituted alkenes or alkynes. The dipolarophile in a 1,3-dipolar cycloaddition is a reactive alkene moiety containing 2π electrons. Thus, depending on which dipole that is present, α, β -unsaturated aldehydes, ketones, and esters, allylic alcohols, allylic halides, vinylic ethers and alkynes are examples of dipolarophiles that react readily. It must be noted, however, that other 2π -moieties such as carbonyls and imines also can undergo cycloaddition with dipoles. The alkene moiety can be mono-, di-, tri- or even tetrasubstituted. However, mostly due to steric factors, tri- and tetrasubstituted ones often display very low reactivity in reactions with dipoles.

Olefinic and acetylenic dipolarophiles are more reactive when they bear conjugating groups. Hetero-dipolarophiles are generally less reactive than the corresponding C—C dipolarophiles, possibly because the energy gained from forming the two new σ bonds is less in the former case. This follows because C—C or C-hetero-atom σ bonds are stronger than hetero-hetero-atom bonds [8].

2.1.3.3. Frontier Molecular Orbital Interactions

The transition state of the concerted 1,3-dipolar cycloaddition reaction is controlled by the frontier molecular orbitals (FMO) of the substrates. The $\text{LUMO}_{\text{dipole}}$ interacts with the $\text{HOMO}_{\text{alkene}}$ and the $\text{HOMO}_{\text{dipole}}$ interacts with the $\text{LUMO}_{\text{alkene}}$ [16, 17].

Sustmann has classified 1,3-dipolar cycloaddition reactions into three types, based on the relative FMO energies between the dipole and dipolarophile (Figure 2.8) [18, 19]. In the type I reactions the dominant FMO interaction is that of the $\text{HOMO}_{\text{dipole}}$ with the $\text{LUMO}_{\text{dipolarophile}}$. For type II reactions the similarity of the dipole and dipolarophile FMO energies implies that both HOMO-LUMO interactions are important. Cycloaddition reactions of type III are dominated by the interaction between the $\text{LUMO}_{\text{dipole}}$ and the $\text{HOMO}_{\text{dipolarophile}}$.

Reactions of type I are typical for azomethine ylides and carbonyl ylides, whereas 1,3-dipolar cycloaddition reactions of nitrones are normally classified as type II [20]. Reactions of the nitrile oxides are also classified as borderline to type III, since nitrile oxides have relatively low LUMO energies of -11 to -10 eV. It should be taken into account that the classification of a reaction is also dependent on the other reactant. Introduction of electron-donating or electron-withdrawing

substituents on the dipole or the dipolarophile can alter the relative FMO energies, and therefore the reaction type, dramatically [19, 21].

In this case both $\text{HOMO}_{\text{dipole}}\text{-LUMO}_{\text{dipolarophile}}$ and $\text{LUMO}_{\text{dipole}}\text{-HOMO}_{\text{dipolarophile}}$ interactions may be important in determining the reactivity and regiochemistry of the process.

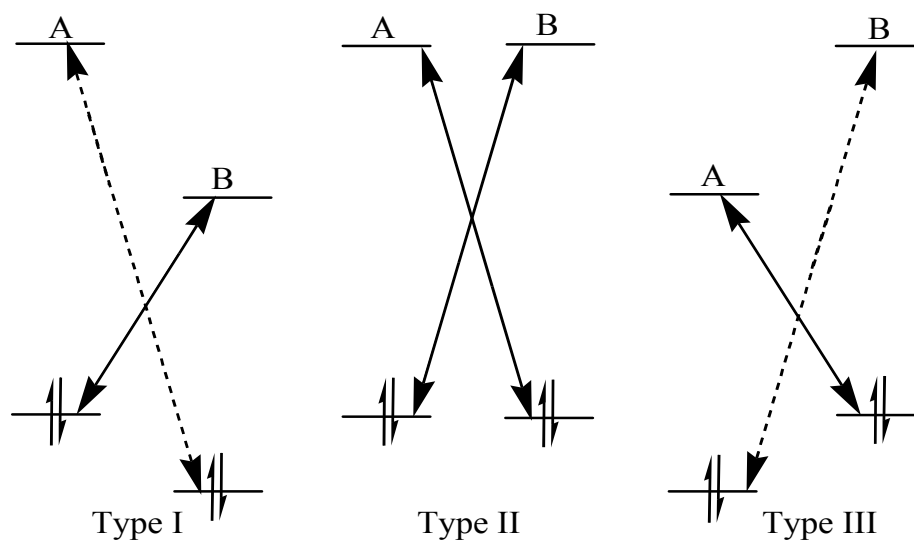


Figure 2.8. Possible interactions between 1,3-dipole (A) and dipolarophile (B).

There are two types of orientation of addition (regioselectivity) of 1,3-dipoles to unsymmetrically substituted dipolarophiles (Figure 2.9).

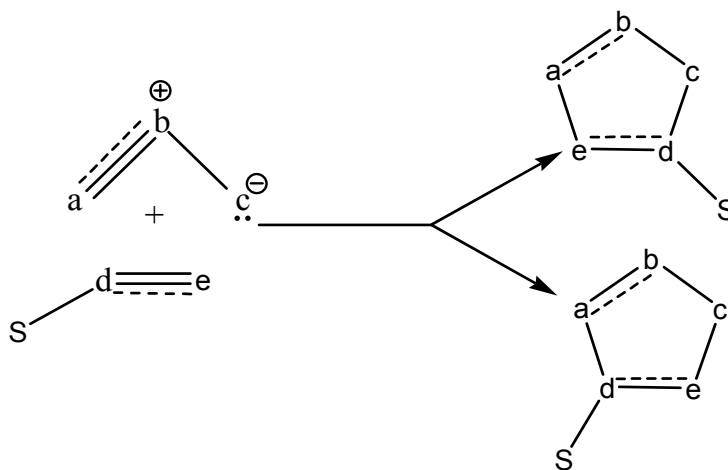


Figure 2.9. Two possible regioisomers of the 1,3-dipolar additions of an unsymmetrical 2π-system.

2.1.3.4. The Selectivities of 1,3-Dipolar Cycloaddition Reactions

Three types of selectivity must be considered in 1,3-dipolar cycloaddition reactions—regioselectivity, diastereoselectivity, and enantioselectivity. The regioselectivity is controlled by both steric and electronic effects [17, 22]. For the addition to terminal alkenes the sterically most crowded functionality of the 1,3-dipole tends to add to the terminal carbon atom of the alkene, giving the 5-substituted isomer. The steric effects may, however, be overruled by strong electronic effects [11-b]. In the cycloaddition reaction of electron-rich or electron-neutral alkenes with nitrones, the 5-substituted isomer is obtained. The reaction is primarily controlled by the $LUMO_{\text{dipole}}-HOMO_{\text{dipolarophile}}$ interaction. The $LUMO_{\text{dipole}}$ has the largest coefficient at the carbon atom and the $HOMO_{\text{alkene}}$ has the largest coefficient at the terminal carbon atom. Thus, the nitron and alkene combine in a regioselective manner to give the 5-isoxazolidine. This is obviously supported by the steric factors.

For terminal alkenes with an electron-withdrawing group, the reaction is primarily controlled by the $\text{HOMO}_{\text{dipole}}\text{-LUMO}_{\text{dipolarophile}}$ interaction. The $\text{HOMO}_{\text{dipole}}$ has the largest coefficient at the oxygen atom, whereas the $\text{LUMO}_{\text{dipolarophile}}$ has the largest coefficient at the terminal carbon atom. This favors the formation of the 4-isomer, but since steric factors oppose this, a mixture of regioisomers is often obtained [22].

In the 1,3-dipolar cycloaddition reactions of especially allyl anion type 1,3-dipoles with alkenes the formation of diastereomers has to be considered. In reactions of allyl type dipoles with terminal alkene the dipole can approach the alkene in an endo or an exo fashion giving rise to two different diastereomers. The nomenclature endo and exo is well known from the Diels-Alder reaction [16].

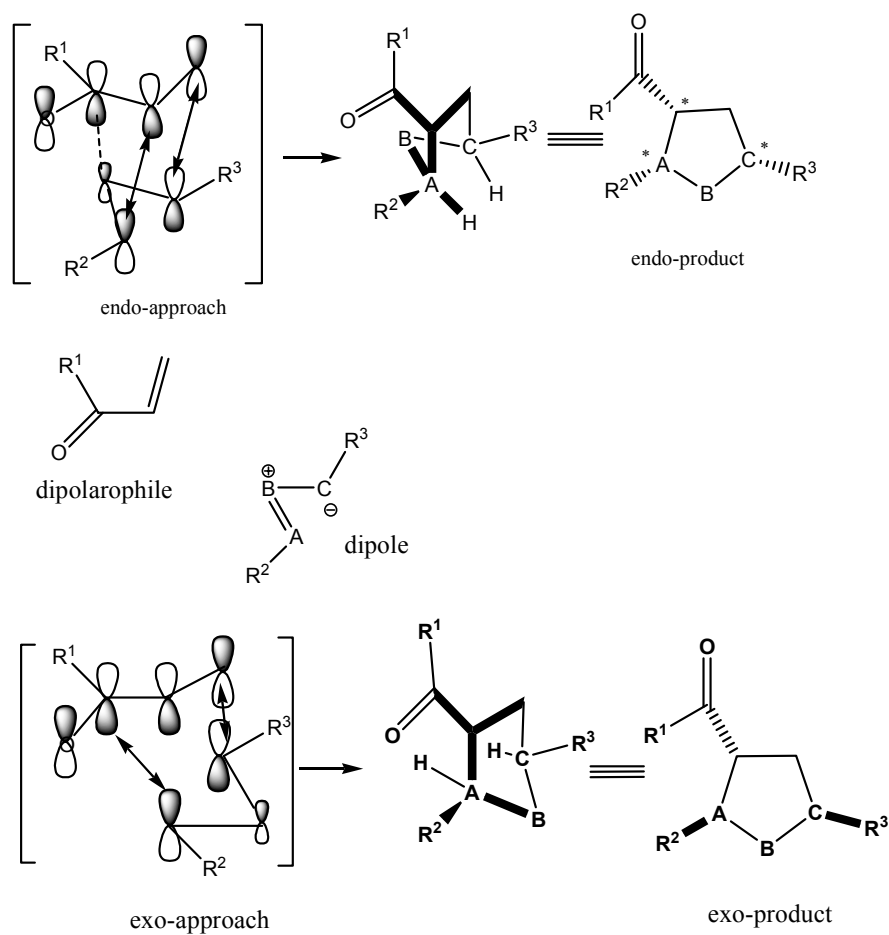


Figure 2.10. Diastereoselectivity in a 1,3-dipolar cycloaddition reaction

Finally, there is the enantioselectivity of the 1,3-dipolar cycloaddition reactions. The only factor present for control of the enantioselectivity is therefore the chiral catalyst.

2.1.3.5. Simplified Molecular Orbital Theories and Computational methods

Molecular orbital theory explains the reactivities of cycloaddition reactions by using the energy differences between the reactants and the transition states. Linear combination of atomic orbitals (LCAO) method is used in molecular orbital calculations.

Interactions between two conjugated molecules with overlapping p orbitals is described in terms of the π electrons of the separate system. The orbitals that interact have been called the frontier orbitals by Fukui [23].

Frontier orbitals are given the names, highest occupied molecular orbital (HOMO) and lowest unoccupied molecular orbital (LUMO).

The principle of conservation of orbital symmetry, explained by Fukui, Woodward and Hoffmann [24,25], provides a fruitful theoretical basis for concerted reactions.

Whether a concerted reaction is allowed or not, can be predicted by orbital symmetry rules, which are also known as Woodward-Hoffmann rules [26]. The orbital symmetry rules are related to the Huckel aromaticity. The selection rules for cycloaddition reactions can be derived from consideration of the aromaticity of the transition state. In applying the orbital symmetry, sign inversions are taken into account. System with zero and even number of sign inversions are called Huckel systems. A thermal pericyclic reaction involving a Huckel system is allowed only if the total number of electrons is $4n+2$. Systems with an odd number of sign inversions are called Möbius systems, in which a thermal pericyclic reaction is allowed, if the total number of electrons is $4n$. For photochemical reactions these rules are reversed [27].

In concerted reactions, if the new bonds are formed from the same face of the π system, the reaction is a suprafacial-suprafacial process. For $[\pi 4_{s+\pi} 2_s]$, Diels-Alder reactions suprafacial-suprafacial process is symmetry allowed according to Woodward-Hoffmann rules [24]. In symmetry allowed $[\pi 2_{s+\pi} 2_s]$ cyclization reactions the new σ bonds are formed from the opposite faces of the π system. This manner of bond formation is called antarafacial-suprafacial.

For the $[\pi 4_{s+\pi} 2_s]$ suprafacial-suprafacial cycloaddition the transition state is aromatic, while for $[\pi 2_{s+\pi} 2_s]$ suprafacial-suprafacial mode it is anti-aromatic and suprafacial-antarafacial mode is aromatic (Figure 2.11).

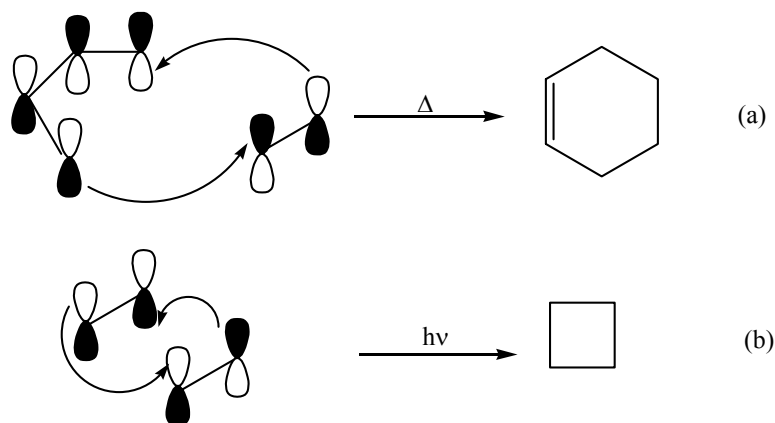


Figure 2.11. Representation of (a) $[\pi 4_{s+\pi} 2_s]$ and (b) $[\pi 2_{s+\pi} 2_s]$ reactions.

The regioselectivity and reactivity [19,28,29,30,31], the mechanism [32,33,34], the electroselectivity [35,36], the stereoselectivity [37], the regiospecificity [38] of cycloadditions were explained on the basis of molecular orbital theories.

As two conjugated systems approach each other along the lowest energy path, the greatest stabilization upon the interaction is provided. The magnitude of this

stabilization depends upon the nature of the interacting molecular orbitals of the conjugated systems and can be estimated by using the perturbational molecular orbital (PMO) and frontier molecular orbital (FMO) theories.

The most popular of the available methods are Extended Huckel (EH), CNDO/2, and the MINDO/3 methods.

By using CNDO/2 method, the coefficients and the energy levels of frontier orbital can be calculated. The CNDO (complete neglect of differential overlap) method [39,40] makes the approximation that the product $\phi_i \phi_j$ is always zero if ϕ_i and ϕ_j are located on the same center. The MINDO (modified intermediate neglect of differential overlap) method restores several of the integrals neglected in the CNDO method.

Huckel molecular orbital theory utilizes the treatment of conjugated systems. It is based on the approximation that the π system can be treated independently of the σ framework conjugated planar molecules and that is the π system has a great importance in determining the chemical and spectroscopic properties of conjugated polyenes and aromatic compounds. The rationalization for treating the σ and π as independent of each other is based on their orthogonality.

How a change in structure, perturbation, will affect the MO's can be understood by the help of PMO. In a PMO a system under analysis is compared to another related system for which the MO pattern is known.

In molecular orbital theory, reactivity is related to the relative energies and shapes of the orbitals, which are involved during the transformation of reactants to products. The shapes of the orbitals, which affect the energy of the reactions, are quantified by atomic coefficients.

PMO incorporates the concept of frontier orbital theory, which proposed that the most important reactions between the highest molecular orbital of one reactant and the lowest molecular orbital of the other reactant.

A basic postulate of PMO theory is that the strongest overlap occurs, when the interacting orbitals, with the same sign, on two reaction centers have the highest coefficients on the participating atoms. Another postulate of PMO theory is that only MO's of matching symmetry can interact for the bond formation. Thus, relative energies and symmetry of the frontier orbitals are taken into account in PMO theory.

The relative energies of the frontier orbitals can be approximated by first order perturbation theory.

$$\Delta E_u = \sum_i C_{ui}^2 \Delta \alpha_i + \sum_i \sum_j C_{ui} C_{uj} \Delta \beta_{ij}$$

The above equation, derived from the PMO approach to first order changes, indicates the change in energy of the u^{th} molecular orbital as a function of changes in Coulomb integral (electronegativity or ionization potential and resonance integrals (bond energy)). The PMO theory utilizes ground state frontier eigenvalues and eigenvectors in the second order perturbation theory and provides knowledge of the energetics of the transition state between the two participating frontier orbitals [41].

Frontier molecular orbital theory (FMO) provides the basic framework for analysis of the effect that symmetry of orbitals has upon reactivity.

Cycloaddition reactions are allowed only when all overlaps between the HOMO of one reactant and the LUMO of the other are such that a positive lobe overlaps with another positive lobe and a negative lobe only with another negative lobe.

To apply FMO theory, the coefficients and energies of the frontier orbitals are necessary. The interaction energy between the HOMO of one reactant and the

LUMO of the second is calculated by using the second order perturbation theory [42]. The total interaction energy (ΔE) is a measure of the transition state stabilization (or destabilization) in the direction of maximum overlap.

According to Fukui [42], reactions take place in the direction of maximal HOMO-LUMO overlap. In concerted cycloadditions that orientation should be favored in which the centers with the largest atomic coefficients interact.

The use of these generalized frontier orbitals within the framework of qualitative perturbation molecular orbital theory provides a qualitative explanation of differential reactivity, regioselectivity and periselectivity in cycloadditions [43,44].

2.1.3.6. Azomethine Imines and Azomethine Ylides

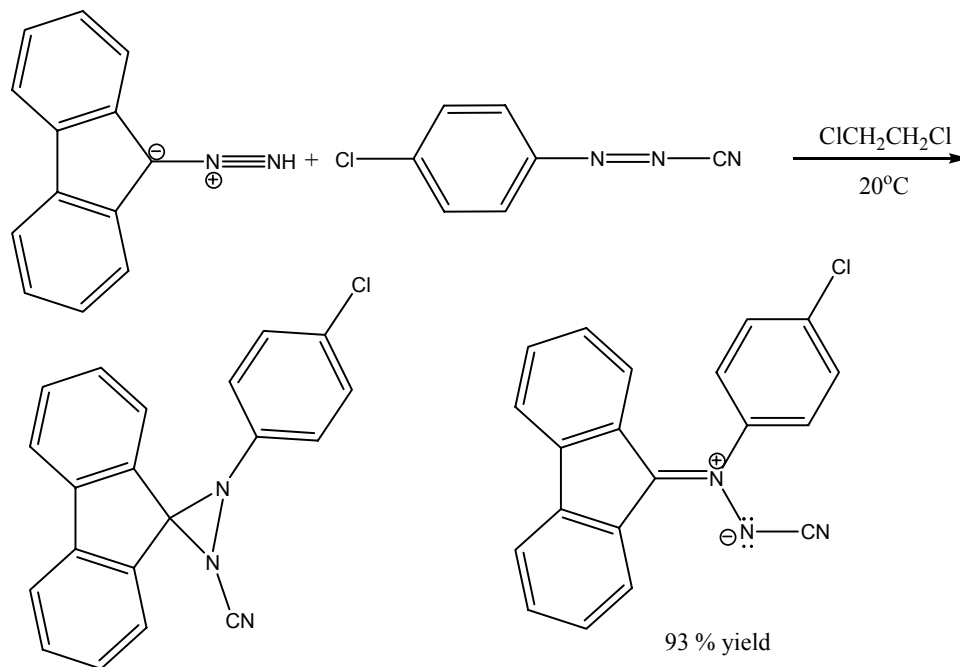
The compounds containing C=N double bond obtained in reactions of aldehydes and ketones with amines are referred to as Schiff bases, imines, or azomethines. Azomethine imines and azomethine ylides are both 1,3-dipoles without a double bond but with internal octet stabilization [45].

2.1.3.6.1. Azomethine Imines

2.1.3.6.1.1. Crystalline N(β)-Cyano (Azomethine Imines)

Aromatic diazocyanides are electrophilic and react with diazoalkanes by evolving one equivalent of nitrogen. Exothermic combination of *p*-chlorobenzenediazocyanide with diazofluorene affords a 93% yield of the orange-red crystals [46,47]. Degradation reactions and especially the physical properties

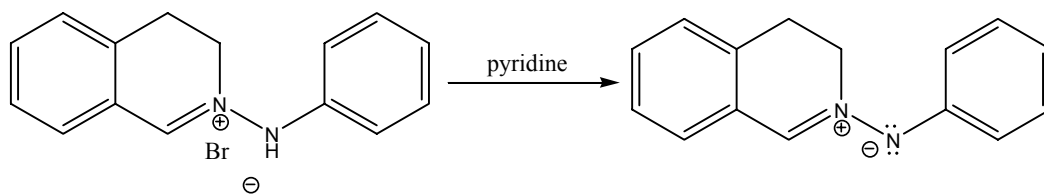
demonstrate that this is the open-chain azomethine imine and not the isomeric diaziridine. This is exemplified in Scheme 2.1.



Scheme 2.1. Exothermic combination of *p*-chlorobenzene diazocyanide with diazofluorene

2.1.3.6.1.2. Azomethine Imines of the 3,4-Dihydroisoquinoline Series

N-Arylamino-3,4-dihydroisoquinolinium salts, which are accessible from 2-(β -bromoethyl)benzaldehyde and arylhydrazines [48,49], are intramolecular alkylation products of arylaldehyde arylhydrazones. Whereas normally hydrazone alkylation occurs at N-(β), the closure of a 6-membered ring here favors N(α)-alkylation. A mere deprotonation with base at the nitrogen suffices to yield a class of highly reactive azomethine imines. This is exemplified in Scheme 2.2.



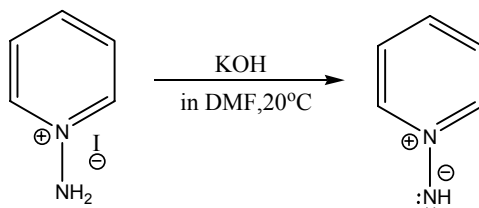
Scheme 2.2. Synthesis of azomethine imines of the 3,4-dihydroisoquinoline series

These azomethine imines of the 3,4-dihydroisoquinoline series combine so smoothly with all kinds of alkenes that they may be recommended as analytical reagents for the identification of liquid olefins, and possibly for the separation of olefin mixtures as well.

2.1.3.6.1.3. N-Imines of Pyridine, Quinoline, and Isoquinoline

Experiments with azomethine imines in which the C=N double bond is an integral part of an aromatic ring give convincing proof of the driving force behind 1,3-dipolar additions. Since this addition involves loss of the aromatic mesomerism, very active dipolarophiles are required.

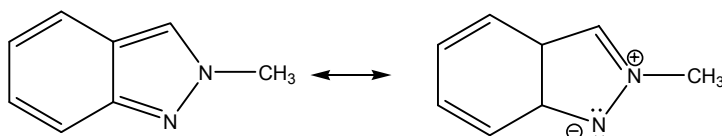
The *N*-aminopyridinium salt, which is readily obtained from pyridine and hydroxylamine-*O*-sulfonic acid [50], yields solutions of pyridine-*N*-imines when treated with alkali in dimethylformamide. Scheme 2.3 includes this transformation.



Scheme 2.3. Synthesis of pyridine-*N*-imines

2.1.3.6.1.4. 2-Methylindazole

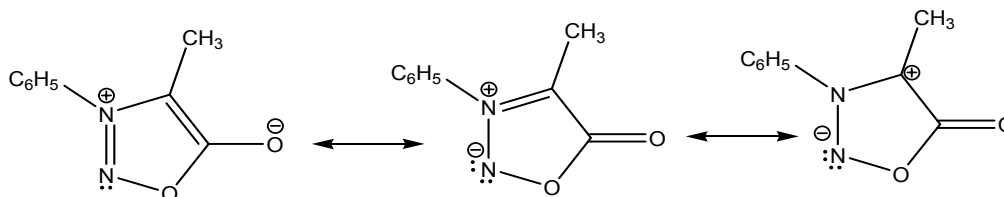
Another aspect of the problem appears when the entire 1,3-dipole is built into an aromatic ring. 2-Methylindazole is undoubtedly aromatic. Even though it can be described only by one neutral structure. Its resonance energy is only about 2,4 kcal/mole lower than that of 1-methylindazole [51]. Scheme 2.4 indicates the resonance forms of 2-methylindazoles.



Scheme 2.4. Resonance forms of 2-methylindazole

2.1.3.6.1.5. Sydnones

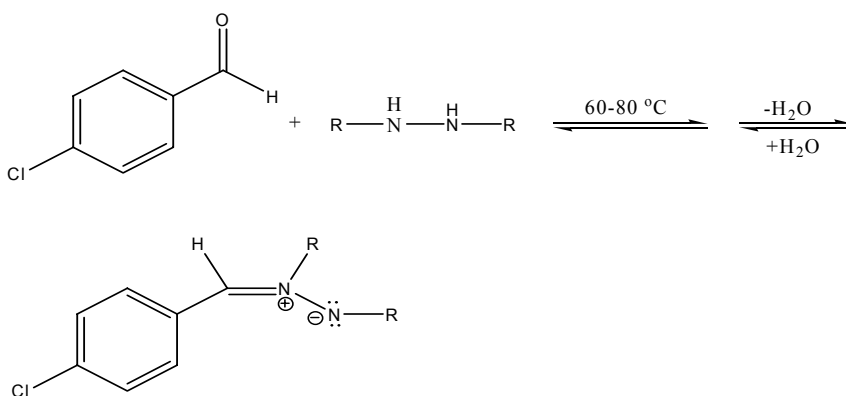
The problem of mechanistic ambiguity does not exist in the reactive behaviour of the sydnones formed from *N*-nitrosoalkyl or *N*-nitrosoarylamino-carboxylic acids and acetic anhydride. These are aromatic compounds which can be described only by zwitterionic resonance structures, as can be judged from their spectral properties and high dipole moments [52]. The resonance structures of *N*-phenyl-*C*-methyl-sydnone is given in scheme 2.5.



Scheme 2.5. Resonance forms of *N*-phenyl-*C*-methyl-sydnone

2.1.3.6.1.6. 1,2-Disubstituted Hydrazines and Carbonyl Compounds

The interaction of 1,2-disubstituted hydrazines with aldehydes may possibly open a general synthetic route to azomethine imines. At equilibrium, the 1,3-dipole could exist together with the α -hydrazinocarbinal in such a system. However, the characteristic ability of the dipole to undergo addition would be evident even at modest equilibrium concentrations. An example of such a cycloaddition [53] is the reaction of *N,N*-di-(*p*-methoxyphenyl)hydrazine with *p*-chlorobenzaldehyde in acrylonitrile or carbon disulfide. This is exemplified in Scheme 2.6. However valuable this synthetic scheme may appear to be, its mechanism has not been established unequivocally.

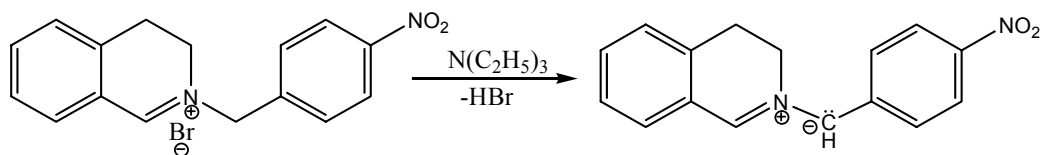


Scheme 2.6. Synthetic route for azomethine imines via 1,2-Disubstituted Hydrazines and Carbonyl Compounds

2.1.3.6.2. Azomethine Ylides

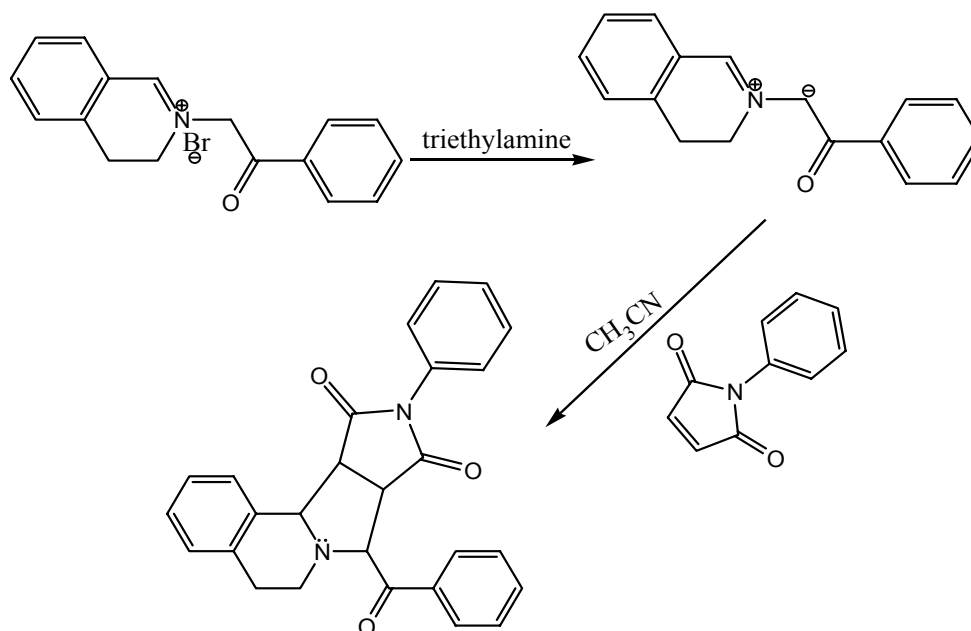
When azomethine ylides are liberated from immonium salts with base, it is necessary to avoid both addition of the base onto the α -carbon atom and abstraction

of a β -proton with formation of an enamine. The first azomethine ylide was prepared from *N*-(*p*-nitrobenzyl)-3,4-dihydroisoquinolinium bromide with triethylamine in hot pyridine. This is exemplified in Scheme 1.7. It is not stable enough to be isolated but adds readily to dimethyl fumarate in situ [54].



Scheme 2.7. An example for the synthesis of *N*-(*p*-nitrobenzyl)-3,4-dihydroisoquinolinium ylide via elimination of HBr

Another short-lived azomethine ylide, which is obtained from *N*-phenylacetyl-3,4-dihydroisoquinolinium bromide with triethylamine, also undergoes cycloadditions with olefinic dipolarophiles; with *N*-phenylmaleimide in acetonitrile a 73% yield of the 1:1 adduct is obtained [54]. This synthesis is represented in scheme 2.8.



Scheme 2.8. Synthesis of *N*-phenylacetyl-3,4-dihydroisoquinolinium ylide

2.1.4. Aim of this work

The aim of this work can be ordered as follows:

- To synthesize some new betaine and azomethine ylide structures and also providing an account for the reactivity and cycloaddition properties of those dipoles.
- To provide an application of the PMO and FMO methods leading to discussion of the reactivities of the azomethine ylides.
- To compare the experimental results with the theoretical predictions.
- To introduce new cyclic compounds to the heterocyclic chemistry.

3. EXPERIMENTAL

Melting points were determined with Electrothermal apparatus. Spectra were recorded with a JASCO 430 FT/IR and BRUCKER 400 MHz NMR spectrophotometers. Compounds were purified using preparative t.l.c and column chromatography techniques until they were observed as single spots on t.l.c. (Kieselgel PF 254; Chloroform, Ethyl acetate, Hexane as eluant). The solvents, that were mainly used, were dried before using.

3.1. Preparation of Mainly Used Solvents

3.1.1. Tetrahydrofuran (THF)

Solvent was stirred with CuCl about 3 hours, then filtered and distilled.

3.1.2. Acetone

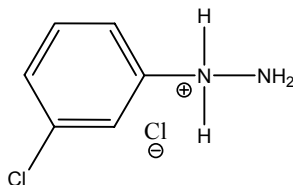
Solvent was refluxed with small quantity of KMnO_4 until violet color persists. Dried with anhydrous K_2SO_4 or CaSO_4 , then filtered and distilled.

3.1.3. Chloroform

Drying agents were added to the commercially available solvent.

3.2. Synthesis of starting compounds of Azomethine Imines

3.2.1. Preparation of *m*-chlorophenylhydrazine hydrochloride (2a)



Concentrated HCl (130 mL) was added to a 1L of beaker equipped with a mechanical stirrer and immersed in a freezing mixture of ice and salt. When the temperature has fallen to about 0 °C, pure *m*-chloroaniline (65.061g, 54.217 mL, 0.510 mol) was added to HCl solution during about 5 minutes. And then, 60 g of crushed ice was added to the mixture. After that, the solution of sodium nitrite, which was prepared by dissolving 35 g (0.510 mol) in 75 mL H₂O, was cooled to 0-3 °C and run in the cold mixture of *m*-chloroaniline. Then, the solution, prepared by using 0.59 mol sodium sulfite, was cooled by adding crushed ice and was run in the ice-cooled diazonium salt solution as rapidly as possible. After heating the solution to 60-70 °C on water bath about 30-60 minutes, the solution was acidified using concentrated HCl and was heated on water bath about 4-6 hours. Finally, 500 mL of concentrated HCl was added to the clear solution. Then, the *m*-chlorophenylhydrazine HCl crystals were separated as yellow to pink.

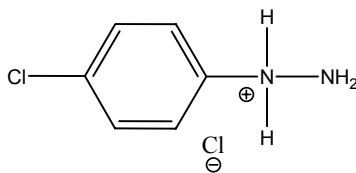
Color : White to pink

Color : White to light pink (In Litt.)

M.p. : 243-245 °C

M.p. : 242 °C (In Litt.)

3.2.2. Preparation of *p*-chlorophenyldiazine hydrochloride (2b)



Concentrated HCl (130 mL) was added to a 1L of beaker equipped with a mechanical stirrer and immersed in a freezing mixture of ice and salt. When the temperature has fallen to about 0 °C, pure *p*-chloroaniline (65.061g, 0.510 mol) was added to HCl solution during about 5 minutes. And then, 60 g of crushed ice was added to the mixture. After that, the solution of sodium nitrite, which was prepared by dissolving 35 g (0.510 mol) in 75 mL H₂O, was cooled to 0-3 °C and run in the cold mixture of *p*-chloroaniline. Then, the solution, prepared by using 0.59 mol sodium sulfite, was cooled by adding crushed ice and was run in the ice-cooled diazonium salt solution as rapidly as possible. After heating the solution to 60-70 °C on water bath about 30-60 minutes, the solution was acidified using concentrated HCl and was heated on water bath about 4-6 hours. Finally, 500 mL of concentrated HCl was added to the clear solution. Then, the *p*-chlorophenyldiazine HCl crystals were separated as yellow to pink.

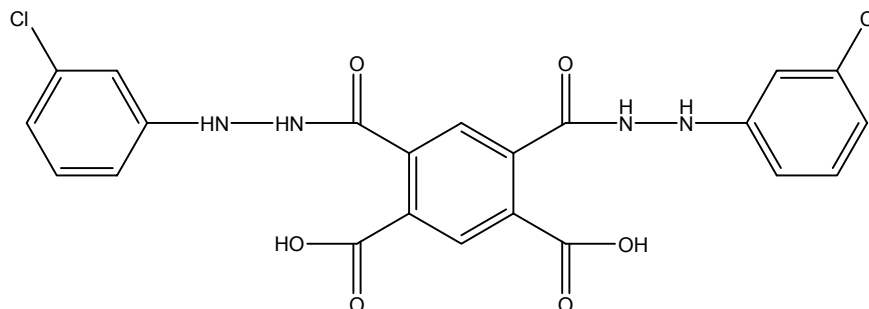
Color : Yellow to pink

Color : White to pink (In Litt.)

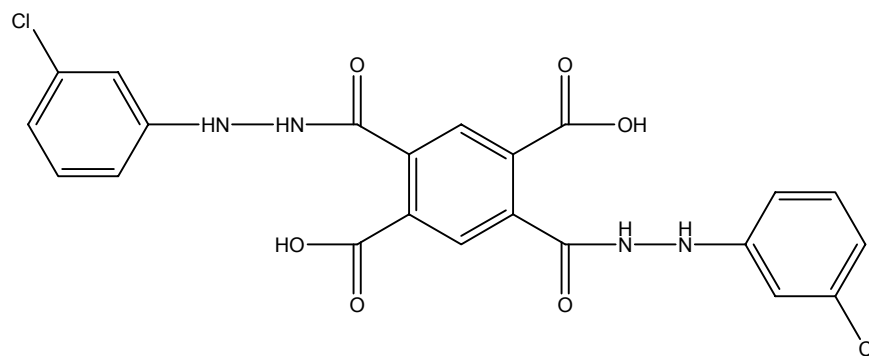
M.p. : 199-201 °C

M.p. : 203 °C (In Litt.)

3.2.3. Synthesis of 4,6-Bis-[N-(3-chloro-phenyl-hydrazinocarbonyl)]-isophthalic acid (2c) and/or 2,5-Bis-[N-(3-chloro-phenyl-hydrazinocarbonyl)]-terephthalic acid (2c')



2c



2c'

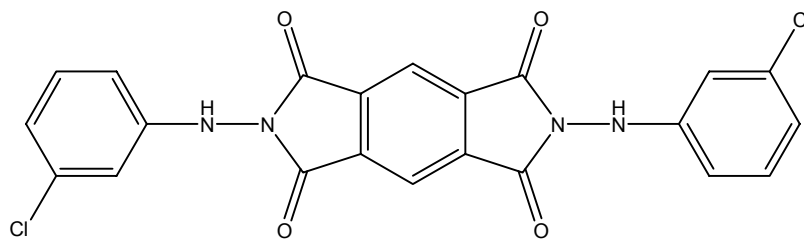
m-chlorophenyldiazine **1a** (5.70 g, 0.040 mol, 4.350 mL) in DMF (25 mL) was added to pyromellitic dianhydride **1b** (4.362 g, 0.02 mol) in DMF (50 mL) and the mixture was kept at 20 °C for 3 h. Excess distilled water was added to the solution. The precipitated 4,6-Bis-[N-(3-chloro-phenyl)-hydrazinocarbonyl] isophthalic acid **2c** and/or **2c'** was filtered off as pale yellow crystals and air dried. The yield was 90% (9.059 g).

M.p. : Not specified (Converted into imide)

R_f : 0.3 (EtOAc)

IR (Nujol): ν (cm⁻¹): 3328, 3250, 1707, 1657, 1595

3.2.4. Synthesis of 2,6-Bis-(3-chloro-phenyl amino)-pyrrolo[3,4-*f*]isoindole-1,3,5,7,tetraone (2d)



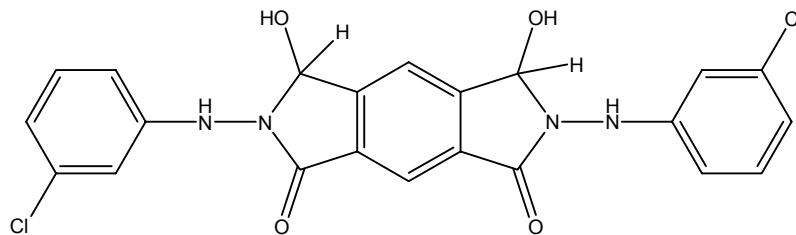
Bis-[*N*-(3-chloro-phenyl)-hydrazinocarbonyl]-isophthalic or terephthalic acid **2c,c'** (5.00 g, 0.010 mol) was heated at 160-170 °C in an oven for 24 hours to give 2,6-Bis-(3-chloro-phenyl amino)-pyrrolo[3,4-*f*]isoindole-1,3,5,7,tetraone **2d** as yellow powders. The product was crystallized from ethanol. The yield was 85% (4.25 g).

M.p. : 315-318 °C

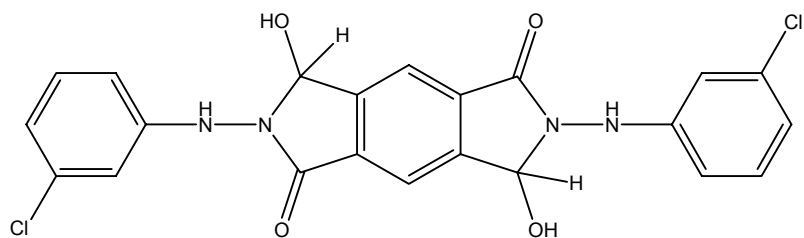
R_f : 0.70 (EtOAc-*n*-Hexane; 4:1)

IR (Nujol): ν (cm⁻¹): 3328, 1784, 1721, 1597

3.2.5. Synthesis of 2,6-Bis-(3-chloro-phenylamino)-3,7-dihydroxy-2,3,6,7-tetrahydro-pyrrolo[3,4-*f*]isoindole-1,5-dione (2e') and/or 2,6-Bis-(3-chloro-phenylamino)-3,5-dihydroxy-2,3,5,6-tetrahydro-pyrrolo[3,4-*f*]isoindole-1,7-dione (2e)



2e



2e'

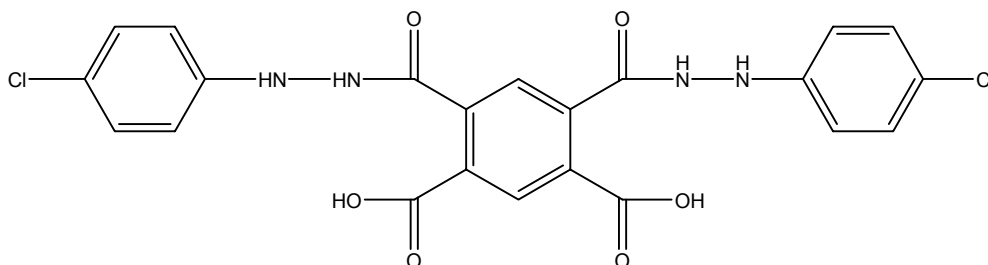
NaBH₄ (1.513 g, 0.04 mol) in [CH₂]₄O (10 mL) was added quickly and with vigorous stirring to 2,6-Bis-(3-chloro-phenyl amino)-pyrrolo[3,4-*f*]isoindole-1,3,5,7,tetraone **2d** (0.467 g, 0.001 mol) in [CH₂]₄O (10 mL) and distilled water (1mL) at 20 °C. After 2 h, the excess of NaBH₄ was decomposed with a large excess of dry acetone. The solution was stirred for 0.5 h more, filtered, and evaporated under vacuum and an oily product **2e** and/or **2e'** was obtained. The yield was 78% (0.368 g).

M.p. : Not specified (Product was oily)

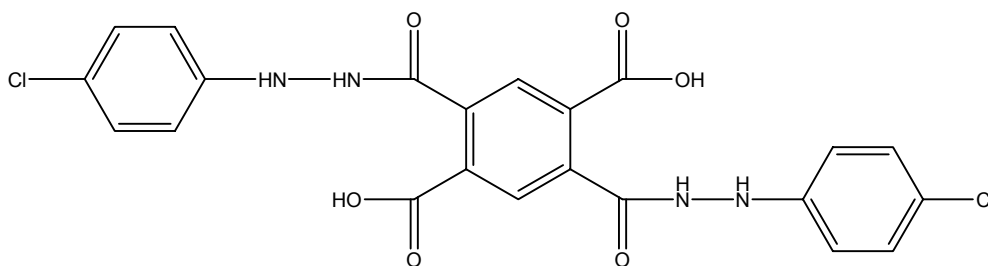
R_f : 0.55 (EtOAc)

IR (Nujol): ν (cm⁻¹) : 3285, 1704, 1598

3.2.6. Synthesis of 4,6-Bis-[N-(4-chloro-phenyl)-hydrazinocarbonyl]-isophthalic acid (2f) and/or 2,5-Bis-[N-(4-chloro-phenyl)-hydrazinocarbonyl]-terephthalic acid (2f')



2f



2f'

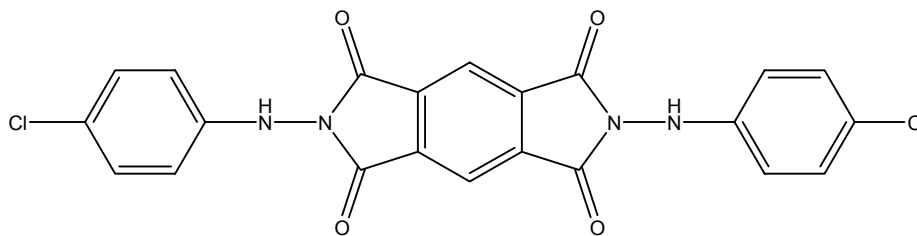
p-chlorophenylhydrazine **1c** (5.70 g, 0.040 mol, 4.350 mL) in DMF (25 mL) was added to pyromellitic dianhydride **1b** (4.362 g, 0.02 mol) in DMF (50 mL) and the mixture was kept at 20 °C for 3 h. Excess distilled water was added to the solution. The precipitated 4,6-Bis-[N-(4-chloro-phenyl)-hydrazinocarbonyl] isophthalic acid **2f** and/or **2f'** was filtered off as pale brown crystals and air dried. The yield was 80% (8.053 g).

M.p. : Not specified (Converted into imide)

R_f : 0.33 (EtOAc)

IR (Nujol): ν (cm⁻¹): 3327, 3252, 1696, 1657, 1596

3.2.7. Synthesis of 2,6-Bis-(4-chloro-phenyl amino)-pyrrolo[3,4-*f*]isoindole-1,3,5,7,tetraone (2g)



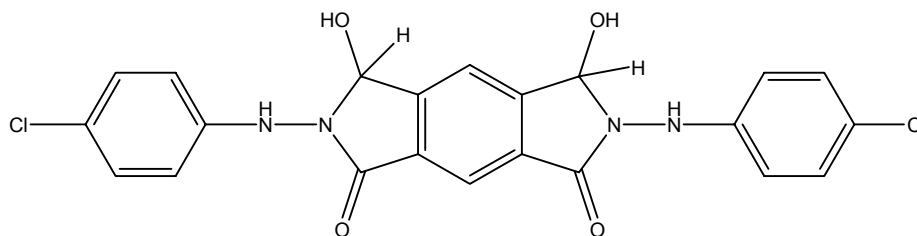
Bis-[*N*-(3-chloro-phenyl)-hydrazinocarbonyl]-isophthalic or terephthalic acid **2f,f'** (5.00 g, 0.010 mol) was heated at 160-170 °C in an oven for 24 hours to give 2,6-Bis-(4-chloro-phenyl amino)-pyrrolo[3,4-*f*]isoindole-1,3,5,7,tetraone **2g** as brick-red powders. The yield was 85% (4.25 g).

M.p. : 320-324 °C

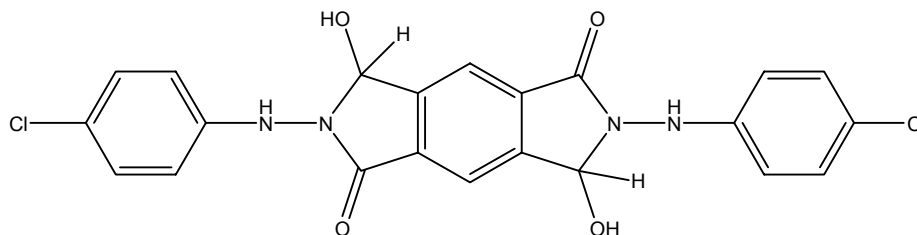
R_f : 0.73 (EtOAc-n-Hexane; 4:1)

IR (Nujol): ν (cm⁻¹) : 3367 , 1785 , 1729, 1596

3.2.8. Synthesis of 2,6-Bis-(4-chloro-phenylamino)-3,7-dihydroxy-2,3,6,7-tetrahydro-pyrrolo[3,4-*f*]isoindole-1,5-dione (2h**) and/or 2,6-Bis-(4-chloro-phenylamino)-3,5-dihydroxy-2,3,5,6-tetrahydro-pyrrolo[3,4-*f*]isoindole-1,7-dione (**2h**)**



2h



2h'

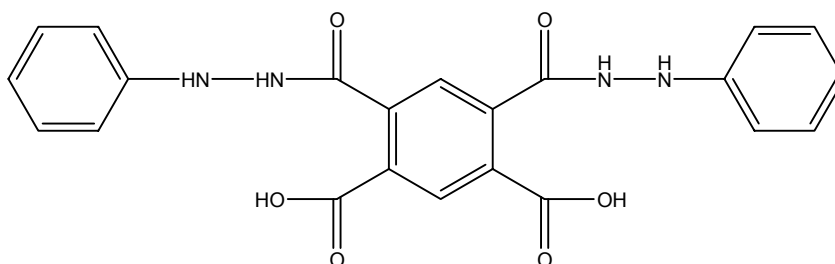
NaBH₄ (1.513 g, 0.04 mol) in [CH₂]₄O (10 mL) was added quickly and with vigorous stirring to 2,6-Bis-(4-chloro-phenyl amino)-pyrrolo[3,4-*f*]isoindole-1,3,5,7,tetraone **2g** (0.467 g, 0.001 mol) in [CH₂]₄O (10 mL) and distilled water (1 mL) at 20 °C. After 2 h, the excess of NaBH₄ was decomposed with a large excess of dry acetone. The solution was stirred for 0.5 h more, filtered, and evaporated under vacuum and an oily product **2h** and/or **2h'** was obtained. The yield was 75% (0.353 g).

M.p. : Not specified (Product was oily)

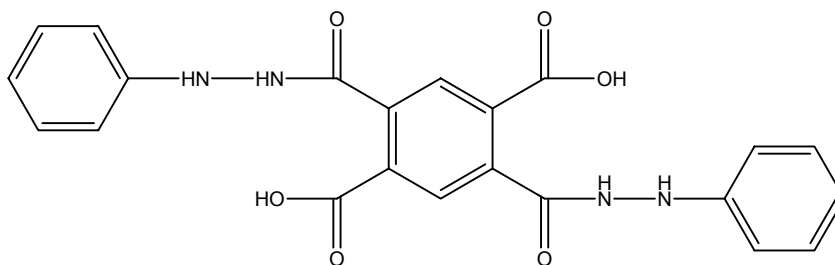
R_f : 0.60 (EtOAc)

IR (Nujol): ν (cm⁻¹) : 3278 , 1708, 1597

3.2.9. Synthesis of 4,6-Bis-[N -phenylhydrazinocarbonyl]-isophthalic acid (2i) and/or 2,5-Bis-[N -phenylhydrazinocarbonyl]-terephthalic acid (2i')



2i



2i'

Phenylhydrazine **1d** (8.651 g, 0.080 mol, 7.860 mL) in CHCl₃ (10 mL) was added to pyromellitic dianhydride **1b** (8.725 g, 0.04 mol) in THF-CHCl₃ (165 mL-50mL) and the mixture was kept at 20 °C for 3 h. The precipitated 4,6-Bis-[N-

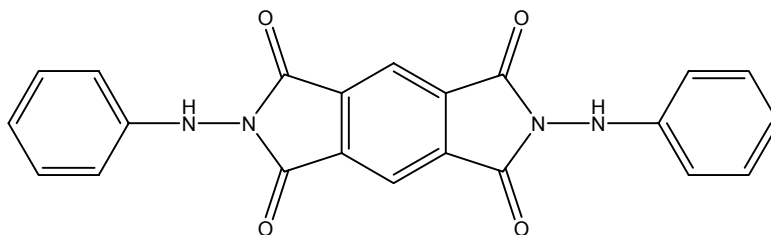
phenylhydrazinocarbonyl]-isophthalic acid **2i** and/or **2i'** was filtered off as brick-red crystals and air dried. The yield was 75% (13.032 g).

M.p. : Not specified (Converted into imide)

R_f : 0.4 (EtOAc)

IR (Nujol): ν (cm⁻¹) : 3271 , 1696 , 1655, 1595

3.2.10. Synthesis of 2,6-Bis-(phenylamino)-pyrrolo[3,4-*f*]isoindole-1,3,5,7, tetraone (**2j**)



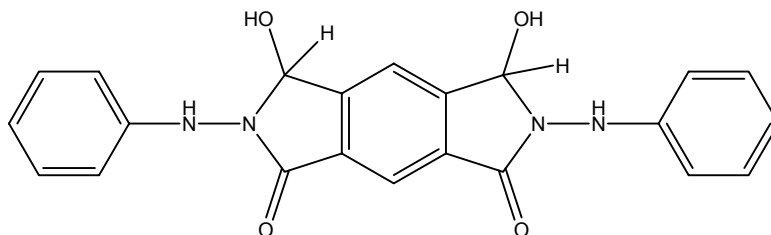
Bis-[*N*-phenylhydrazinocarbonyl]-isophthalic or terephthalic acid **2i,i'** (5.00 g, 0.012 mol) was heated at 160-170 °C in an oven for 24 hours to give 2,6-Bis-(phenylamino)-pyrrolo[3,4-*f*]isoindole-1,3,5,7,tetraone **2j** as yellow powders. The yield was 82% (4.100 g).

M.p. : 320-324 °C

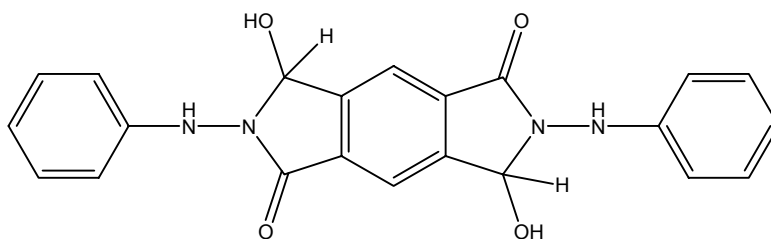
R_f : 0.73 (EtOAc-n-Hexane; 4:1)

IR (Nujol): ν (cm⁻¹) : 3328 , 1785 , 1721, 1605

3.2.11. Synthesis of 2,6-Bis-(phenylamino)-3,7-dihydroxy-2,3,6,7-tetrahydro-pyrrolo[3,4-f]isoindole-1,5-dione (2k) and/or 2,6-Bis-(phenylamino)-3,5-dihydroxy-2,3,5,6-tetrahydro-pyrrolo[3,4-f]isoindole-1,7-dione (2k')



2k



2k'

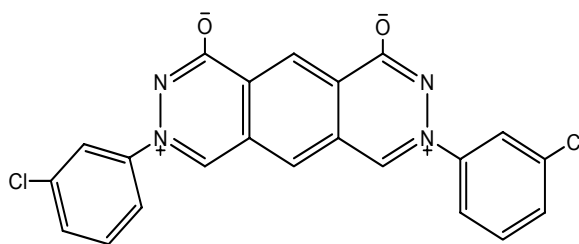
NaBH₄ (0.251 g, 0.007 mol) in [CH₂]₄O (10 mL) was added quickly and with vigorous stirring to 2,6-Bis-(phenylamino)-pyrrolo[3,4-f]isoindole-1,3,5,7-tetraone **2j** (0.500g, 0.001 mol) in THF (20 mL) and distilled water (1.255 mL) at 20 °C. After 2 h, the excess of NaBH₄ was decomposed with a large excess of dry acetone. The solution was stirred for 0.5 h more, filtered, and evaporated under vacuum and an oily product **2k** and/or **2k'** was obtained. The yield was 74 % (0.298 g).

M.p. : Not specified (Product was oily)

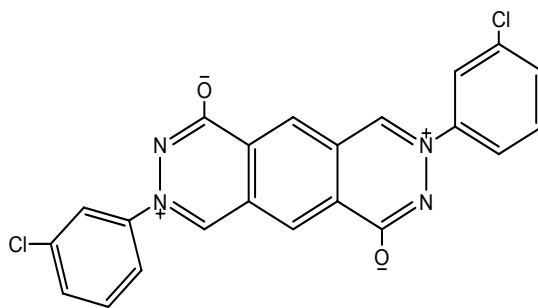
R_f : 0.60 (EtOAc)

IR (Nujol): ν (cm⁻¹): 3261, 1706, 1602

3.2.12. Attempts to synthesize 3-chlorophenylhydrazine substituted bis-1-olates (2l) and/or (2l')



2l

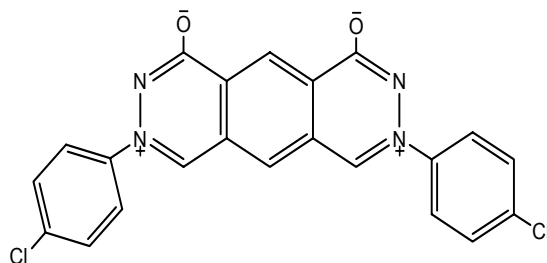


2l'

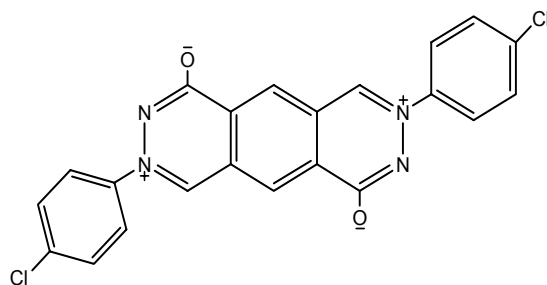
The oily residue **2e** and/or **2e'** was heated at 130-140 °C for 30 min to obtain the betaines **2l** and/or **2l'** as it was done for the preparations of 3-arylphthalazinium-1-olates [57,58].

3.2.13. Attempts to synthesize 4-chlorophenylhydrazine substituted bis-1-olates

(**2m**) and/or (**2m'**)



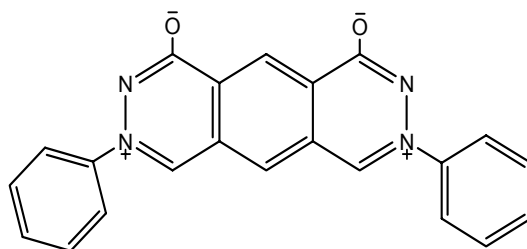
2m



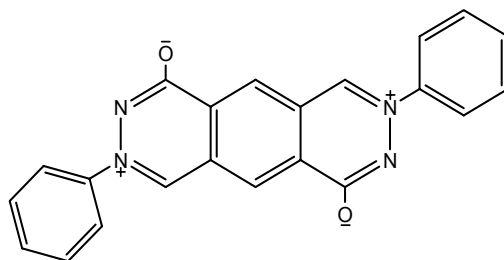
2m'

The oily residue **2h** and/or **2h'** was heated at 130-140 °C for 30 min to obtain the betaines **2m** and/or **2m'** as it was done for the preparations of 3-arylphthalazinium-1-olates [57,58].

3.2.14. Attempts to synthesize 4-chlorophenylhydrazine substituted bis-1-olates (**2n**) and/or (**2n'**)



2n

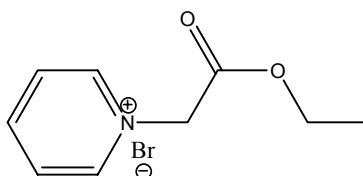


2n'

The oily residue **2k** and/or **2k'** was heated at 130-140 °C for 30 min to obtain the betaines **2n** and/or **2n'** as it was done for the preparations of 3-arylphthalazinium-1-olates [57,58].

3.3. Synthesis of starting compounds of azomethine ylides and their cycloadducts

3.3.1. Synthesis of unsubstituted pyridinium bromide (3a)



3a

Ethyl 2-bromoacetate **1h** (3.468, 0.021 mol, 2.300 mL) was added to pyridine **1e** (1.642 g, 0.021 mol, 1.672 mL) and the mixture was kept at 20 °C for 2 h. The precipitated pyridinium bromide **3a** was obtained. The precipitate was washed with ether. The yield was 95 % (4.909 g).

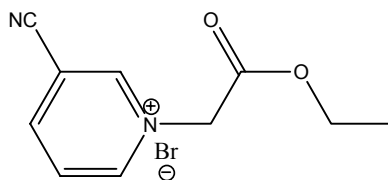
M.p. : 101-103 °C

IR (Nujol): ν (cm⁻¹): 1737, 1637, 1577

¹H NMR (δ_{H} , 400 MHz, CDCl₃): 9.49-9.55 (d, 2H), 8.62-8.53 (t, 2H), 8.16-8.09 (t, 1H), 6.34 (s, 2H), 4.33-4.25 (q, 2H), 1.35-1.28 (t, 3H).

¹³C NMR (δ_{C} , 400MHz, CDCl₃): 165.8, 146.7, 146.1, 127.7, 63.4, 61.1, 14.1

3.3.2. Synthesis of 3-cyanopyridinium bromide (**3b**)



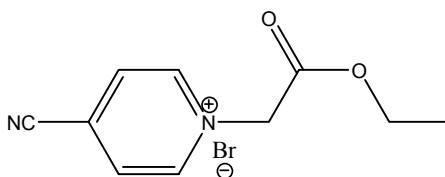
3b

Ethyl 2-bromoacetate **1h** (3.468, 0.021 mol, 2.300 mL) was added to 3-cyanopyridine **1f** (2.162 g, 0.021 mol, 2.00 mL) and the mixture was kept at 20 °C for 2 days. The precipitated 3-cyanopyridinium bromide **3b** was filtered off. The precipitate was washed with diethylether. The yield was 85 % (4.839 g).

M.p. : 145-146 °C

IR (Nujol): ν (cm⁻¹): 2247, 1749, 1641, 1582

3.3.3. Synthesis of 4-cyanopyridinium bromide (**3c**)



3c

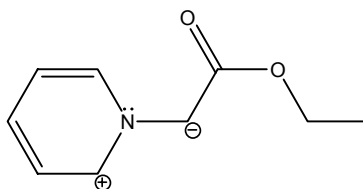
Ethyl 2-bromoacetate **1h** (3.468, 0.021 mol, 2.300 mL) was added to 4-cyanopyridine **1g** (2.162 g, 0.021 mol, 2.00 mL) and the mixture was kept at 20 °C

for 2 days. The precipitated 4-cyanopyridinium bromide **3c** was filtered off. The precipitate was washed with diethylether. The yield was 90 % (5.124 g).

M.p. : 212-213 °C

IR (Nujol): ν (cm⁻¹): 2240, 1735, 1644, 1566

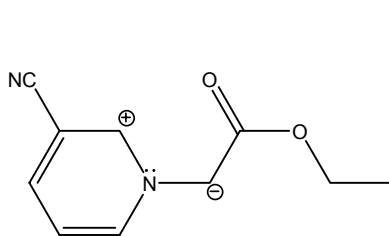
3.3.4. Synthesis of unsubstituted pyridinium ylide (**3d**)



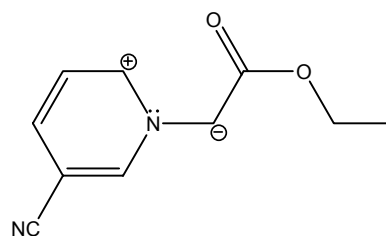
3d

Azomethine ylide **3d** was prepared in situ by adding (0.282 g, 0.0028 mol, 0.388 mL) triethyl amine to pyridinium bromide **3a** (0.726 g, 0.0028 mol) in 10 mL CHCl₃.

3.3.5. Synthesis of 3-cyanopyridinium ylide (**3e**) or (**3e'**)



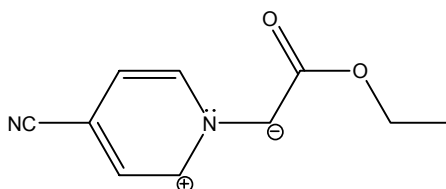
3e



3e'

Azomethine ylide **3e**, **3e'** was prepared in situ by adding (0.247 g, 0.0024 mol, 0.341 mL) triethyl amine to 3-cyanopyridinium bromide **3b** (0.698 g, 0.0024 mol) in 10 mL CHCl₃.

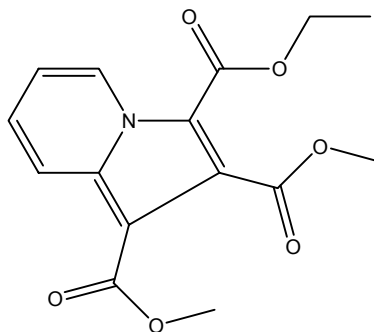
3.3.6. Synthesis of 4-cyanopyridinium ylide (**3f**)



3f

Azomethine ylide **3f** was prepared in situ by adding (0.247 g, 0.0024 mol, 0.341 mL) triethyl amine to 4-cyanopyridinium bromide **3c** (0.698 g, 0.0024 mol) in 10 mL CHCl₃.

3.3.7. Reaction of unsubstituted pyridinium ylide with Dimethyl acetylenedicarboxylate (DMAD)



3g

Dimethyl acetylenedicarboxylate (0.397 g, 0.0028 mol, 0.342 mL) was added to azomethine ylide **3d** (prepared by using 0.726 g **3a** and 0.388 mL N(CH₂CH₃)₃ in 10 mL CHCl₃) and the mixture was stirred 2 h at room temperature. The solvent was removed under vacuum and the product 3-ethyl-1,2-dimethyl-1,2,3,8a-tetrahydroindolizine-1,2,3-tricarboxylate **3g** was separated by preparative t.l.c. (silica gel; CHCl₃). Elution with chloroform gave a yellow product (75%, 0.641 g) as needles.(from diethyl ether)

M.p. : 115.5-116.5 °C

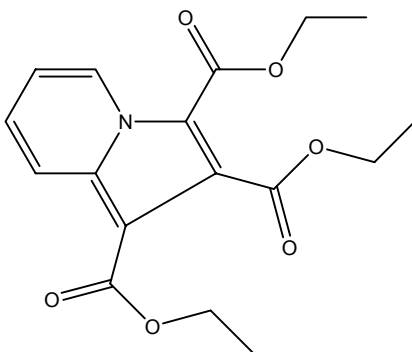
R_f : 0.47 (CHCl₃)

IR (Nujol): ν (cm⁻¹): 1740, 1708, 1693, 1600

¹H NMR (δ _H, 400 MHz, CDCl₃): 9.50-9.45 (d, 1H), 8.30-8.23(d, 1H), 7.35-7.27 (t, 1H), 7.00-6.94 (t, 1H), 4.33-4.27 (q, 2H), 3.92 (s, 3H), 3.82 (s, 3H), 1.35-1.28 (t, 3H).

¹³C NMR (δ _C, 400 MHz, CDCl₃): 165.2, 162.3, 159.1, 136.8, 129.5, 126.9, 125.6, 118.9, 114.3, 101.9, 59.9, 51.7, 50.6, 13.1

3.3.8. Reaction of unsubstituted pyridinium ylide with Diethyl acetylenedicarboxylate (DEAD)



3h

Diethyl acetylenedicarboxylate (0.505 g, 0.0028 mol, 0.475 mL) was added to azomethine ylide **3d** (prepared by using 0.726 g **3a** and 0.388 mL $N(\text{CH}_2\text{CH}_3)_3$ in 10 mL CHCl_3) and the mixture was stirred 2 h at room temperature. The solvent was removed under vacuum and the product triethyl-1,2,3,8a-tetrahydroindolizine-1,2,3-tricarboxylate **3h** was separated by preparative t.l.c. (silica gel; CHCl_3). Elution with chloroform gave a major product (70%, 0.653 g) as yellow powders.(from diethyl ether)

M.p. : 101-103 °C

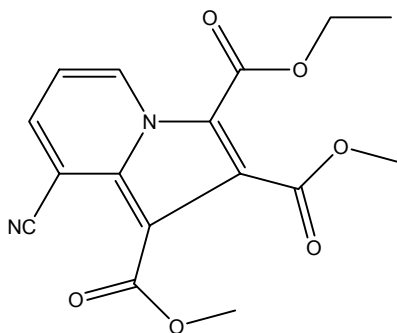
R_f : 0.47 (CHCl_3)

IR (Nujol): ν (cm^{-1}) : 1732, 1688

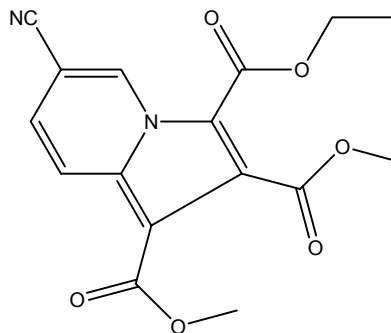
^1H NMR (δ_{H} , 400 MHz, CDCl_3): 9.50-9.46 (d, 1H), 8.31-8.27 (d, 1H), 7.33-7.27 (t, 1H), 6.99-6.93 (t, 1H), 4.41-4.35 (q, 2H), 4.34-4.27 (q, 4H), 1.38-1.28 (t, 9H).

^{13}C NMR (δ_{C} , 400 MHz, CDCl_3): 165.2, 162.3, 159.1, 136.8, 129.5, 126.9, 125.6, 118.9, 114.3, 101.9, 59.9, 51.7, 50.6, 13.1

3.3.9. Reaction of 3-cyanopyridinium ylide with Dimethyl acetylenedicarboxylate (DMAD)



(3i)



(3i')

Dimethyl acetylenedicarboxylate (0.348 g, 0.0024 mol, 0.300 mL) was added to azomethine ylide **3e** and **3e'** (prepared by using 0.698 g **3b** and 0.341 mL $N(\text{CH}_2\text{CH}_3)_3$ in 10 mL CHCl_3) and the mixture was stirred 2 h at room temperature. The solvent was removed under vacuum and the product 3-ethyl-1,2-dimethyl-8-cyanoindolizine-1,2,3-tricarboxylate **3i**, 3-ethyl-1,2-dimethyl-6-cyano indolizine-1,2,3-tricarboxylate **3i'** was separated by column chromatography (silica gel; Hexane-Ethyl acetate 2:1). Elution with Hexane-Ethyl acetate gave a product **3i'** (30%, 0.238 g) and **3i** (45%, 0.357 g) as yellow powder from chloroform.

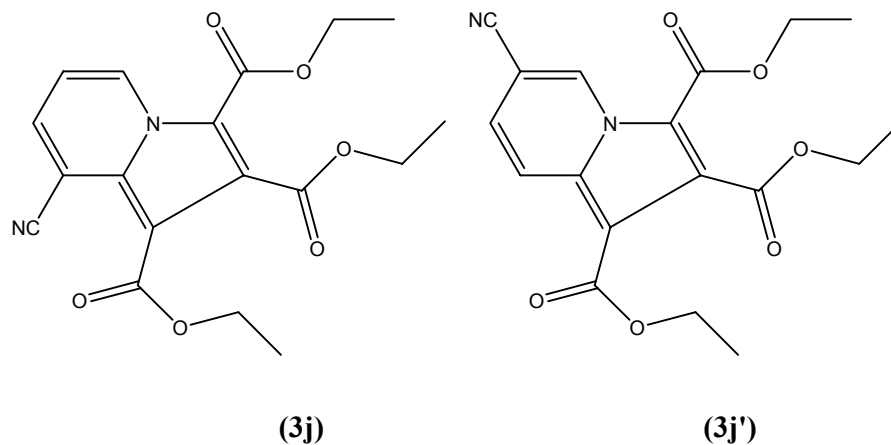
M.p. : 125.5-127 °C

R_f : 0.52 (CHCl_3)

IR (Nujol): ν (cm^{-1}): 2238, 1741, 1695, 1629

^1H NMR (δ_{H} , 400 MHz, CDCl_3): 10.0 (s, 1H), 8.45-8.40 (d, 1H), 7.45-7.39 (d, 1H), 4.45-4.38 (q, 2H), 4.00 (s, 3H), 3.92 (s, 3H), 1.42-1.37 (t, 3H).

3.3.10. Reaction of 3-cyanopyridinium ylide with Diethyl acetylenedicarboxylate (DEAD)



Diethyl acetylenedicarboxylate (0.417 g, 0.0024 mol, 0.392 mL) was added to azomethine ylide **3e** and **3e'** (prepared by using 0.698 g **3b** and 0.341 mL $N(\text{CH}_2\text{CH}_3)_3$ in 10 mL CHCl_3) and the mixture was stirred 2 h at room temperature. The solvent was removed under vacuum and the product triethyl-8-cyanoindolizine-1,2,3-tricarboxylate **3j** and triethyl-6-cyanoindolizine-1,2,3-tricarboxylate **3j'** was separated by column chromatography (silica gel; Hexane-Ethyl acetate 2:1). Elution with Hexane-Ethyl acetate gave a product **3j'** (35%, 0.301 g) and **3j** (42%, 0.361 g) as yellow powder from chloroform.

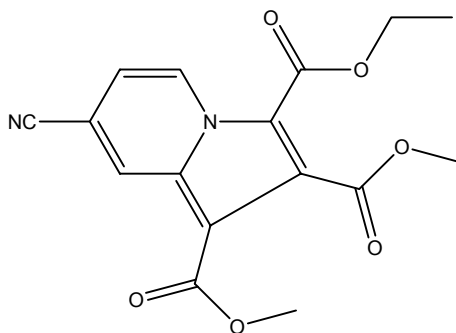
M.p. : 125.5-127 °C

R_f : 0.52 (CHCl_3)

IR (Nujol): ν (cm^{-1}) : 2233, 1750, 1700, 1628

^1H NMR (δ_{H} , 400 MHz, CDCl_3): 9.96-9.92 (s, 1H), 8.41-8.35 (d, 1H), 7.37-7.32 (d, 1H), 4.42-4.29 (q, 6H), 1.40-1.29 (t, 9H).

3.3.11. Reaction of 4-cyanopyridinium ylide with Dimethyl acetylenedicarboxylate (DMAD)



3k

Dimethyl acetylenedicarboxylate (0.348 g, 0.0024 mol, 0.300 mL) was added to azomethine ylide **3f** (prepared by using 0.698 g **3c** and 0.341 mL $N(CH_2CH_3)_3$ in 10 mL $CHCl_3$) and the mixture was stirred 2 h at room temperature. The solvent was removed under vacuum and the product 3-ethyl-1,2-dimethyl-7-cyanoindolizine-1,2,3-tricarboxylate **3k** was separated by column chromatography (silica gel; Hexane-Ethyl acetate 2:1). Elution with Hexane-Ethyl acetate gave a product (75%, 0.594 g) as white powder from chloroform-hexane.

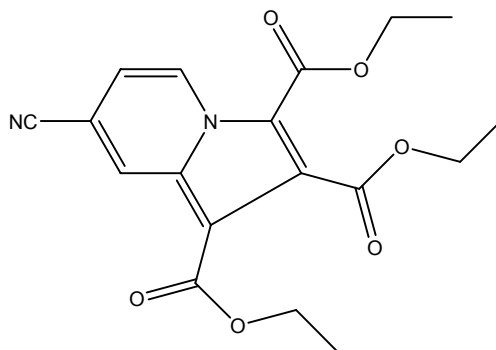
M.p. : 184-186 °C

R_f : 0.51 ($CHCl_3$)

IR (Nujol): ν (cm^{-1}): 2232, 1751, 1740, 1714, 1687

1H NMR (δ_H , 400 MHz, $CDCl_3$): 9.65-9.60 (d, 1H), 8.78-8.70 (s, 1H), 7.18-7.10 (d, 1H), 4.47-4.37 (q, 2H), 4.02 (s, 3H), 3.98 (s, 3H), 1.48-1.38 (t, 3H).

3.3.12. Reaction of 4-cyanopyridinium ylide with Diethyl acetylenedicarboxylate (DEAD)



31

Diethyl acetylenedicarboxylate (0.417 g, 0.0024 mol, 0.392 mL) was added to azomethine ylide **3f** (prepared by using 0.698 g **3c** and 0.341 mL $N(\text{CH}_2\text{CH}_3)_3$ in 10 mL CHCl_3) and the mixture was stirred 2 h at room temperature. The solvent was removed under vacuum and the product triethyl-7-cyanoindolizine-1,2,3-tricarboxylate **31** was separated by column chromatography (silica gel; Hexane-Ethyl acetate 2:1). Elution with Hexane-Ethyl acetate gave a product (71%, 0.610 g) as yellow powder from chloroform-hexane.

M.p. : 184-186 °C

R_f : 0.51 (CHCl_3)

IR (Nujol): ν (cm^{-1}): 2230, 1737, 1715, 1698, 1686

^1H NMR (δ_H , 400 MHz, CDCl_3): 9.62-9.59 (d, 1H), 8.76 (s, 1H), 7.13-7.09 (d, 1H), 4.49-4.38 (q, 6H), 1.46-1.37 (t, 9H).

4. RESULTS&DISCUSSION

This work covers the synthesis of different types of azomethine imines and azomethine ylides and also the study of cycloaddition properties of them towards the olefinic and acetylenic dipolarophiles. The more detailed method for the synthesis of dipoles were mentioned in the experimental part.

4.1. Synthesis of Azomethine Imines

Mesomeric betaines are widely utilized as useful synthetic intermediates in the construction of a variety of heteropolycycles involving natural products and biologically active compounds. Their utility derives from the fact that most act as 1,3-dipoles and lead to heteropolycycles by one-step reactions with dipolarophiles [55].

In this study, the synthesis of azomethine imines were tried to perform in four steps which were described in modified method of Lund [56] by Katritzky [57] and Çelebi [58].

In the first step, amic acids **2i,i'** were precipitated as brick-red powders by reacting pyromellitic dianhydride and phenyl hydrazine and then the precipitated amic acids were heated to 160-170°C for the corresponding imide **2j** structure. Reduction of imide by NaBH₄ in THF gave the reduced imide **2k,k'** as an oily product. Formation of azomethine imines **2n,n'** was tried by heating 130-140 °C.

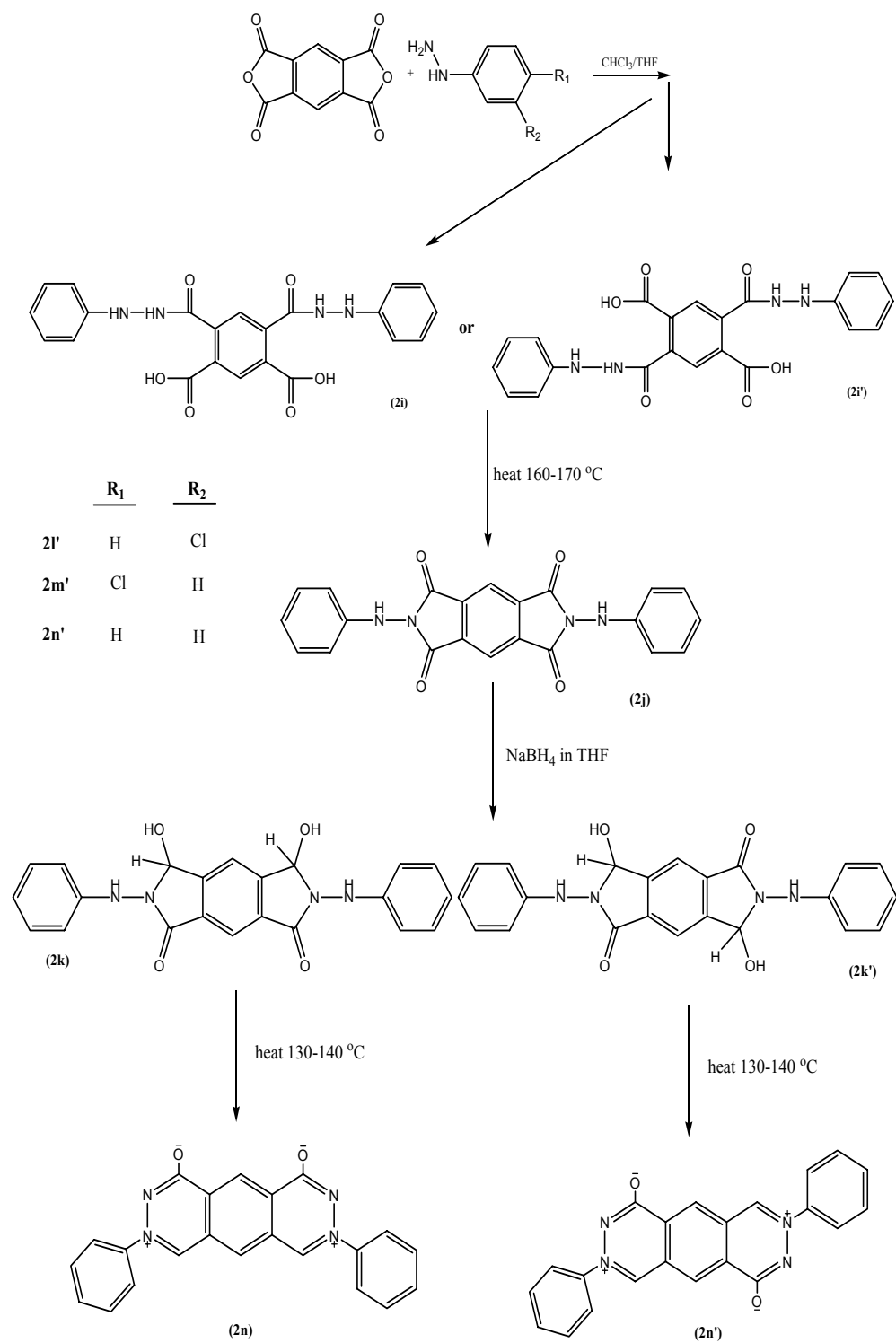


Figure 4.1. The schematic representation of the synthesis of azomethine imines 2n and 2n'.

During the working, synthesis of imides were always performed successfully. But, the selective reduction of imide was full with problems. The main reason, that we had problem in reduction of imide, was the twin structure of imide having four possible carbonyl groups. Although the imides synthesized by using with phthalic anhydride were reduced easily, the twin imides were not. At the end of the working, too excess usage of sodium borohydride gave us positive results about the reduced imide. But the yield was very low to convert it into betaine structure and to make a cycloaddition reaction. Because of those reasons we couldn't obtain any cycloadduct related with azomethine imine. And so, only the amic acid, imide, and possible reduced imide structures were characterized by using FTIR. While comparing the IR spectra of the amic acid, imide and reduced imide, the corresponding spectra of those compounds, given by Katritzky [57] and his co-workers, were used.

The amic acid **2i**, **2i'** structure is supported by the i.r. absorptions for α,β -unsaturated carboxylic acid groups [$\nu(\text{nujol})$ (C=O) 1696 cm^{-1}], amide groups [$\nu(\text{nujol})$ (C=O) 1655 cm^{-1}], aromatic stretching band [$\nu(\text{nujol})$ (C=C) 1595 cm^{-1}] and NH stretching [$\nu(\text{nujol})$ (NH) 3271 cm^{-1}]. (**Fig. 4.2**) The imide **2j** structure shows a strong carbonyl band and a shoulder [$\nu(\text{nujol})$ (C=O) 1721 and 1785 cm^{-1}], an aromatic stretching band [$\nu(\text{nujol})$ (C=C) 1605 cm^{-1}] and a NH stretching band [$\nu(\text{nujol})$ (NH) 3328 cm^{-1}]. (**Fig. 4.3**) These peaks are characteristic for an imide. And the reduced imide **2k**, **2k'** is supported by i.r. absorptions for five membered lactam carbonyl [$\nu(\text{nujol})$ (C=O) 1706 cm^{-1}], aromatic stretching band [$\nu(\text{nujol})$ (C=C) 1602 cm^{-1}] and OH band [$\nu(\text{nujol})$ (OH) 3400-3261 cm^{-1}]. (**Fig. 4.4**) The betaine structure shows aromatic stretching band [$\nu(\text{nujol})$ (C=C) 1600 cm^{-1}] and $\text{C}^+\text{-O}^-$ band [$\nu(\text{nujol})$ ($\text{C}^+\text{-O}^-$) 1565 cm^{-1}].

The studies on this topic is still going on to get a reasonable results in future.

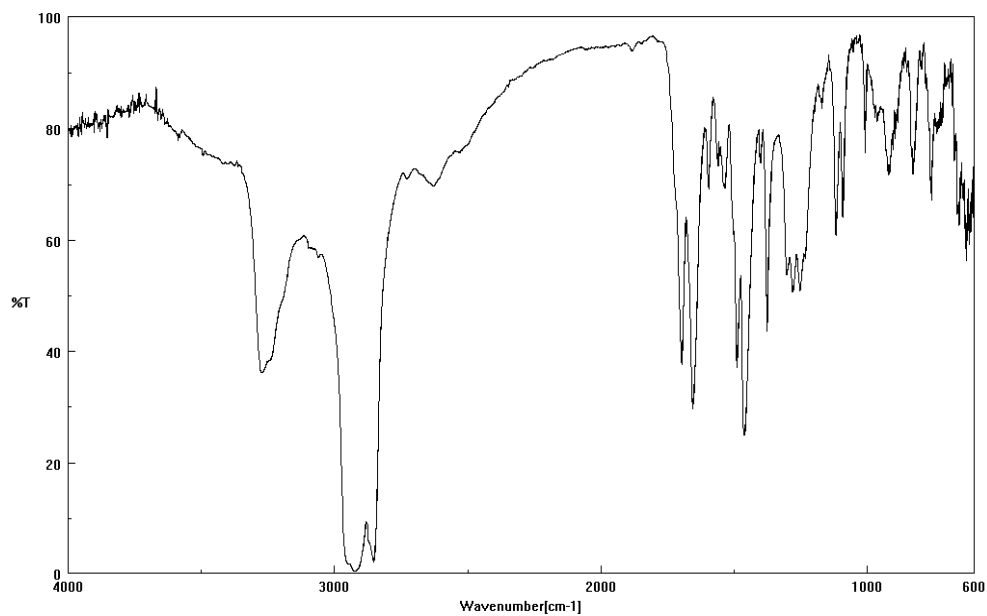


Figure 4.2. The i.r. spectrum of 2i, 2i' (In Nujol)

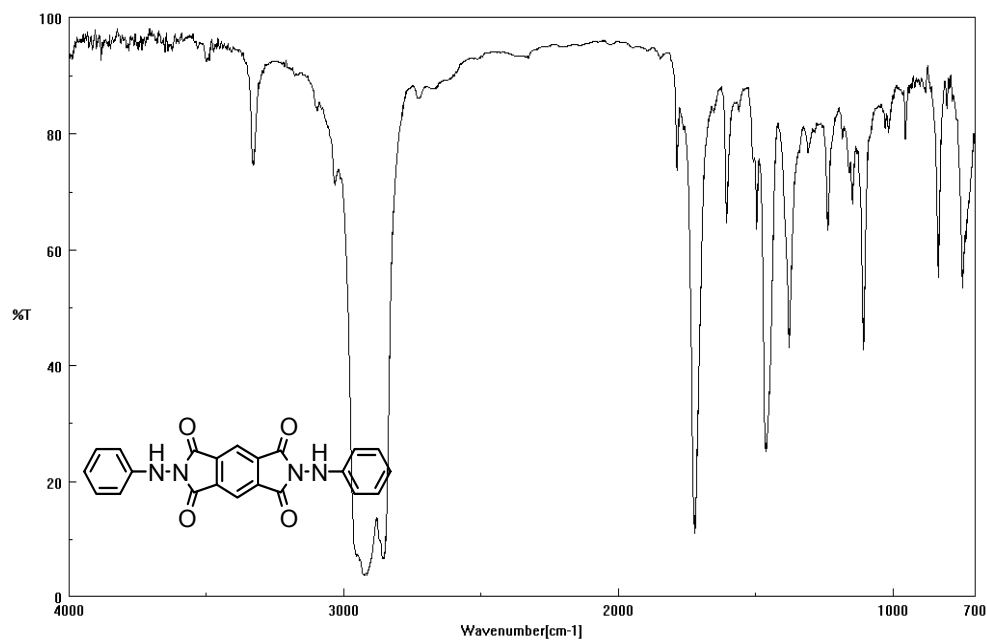


Figure 4.3. The i.r. spectrum of 2j (In Nujol)

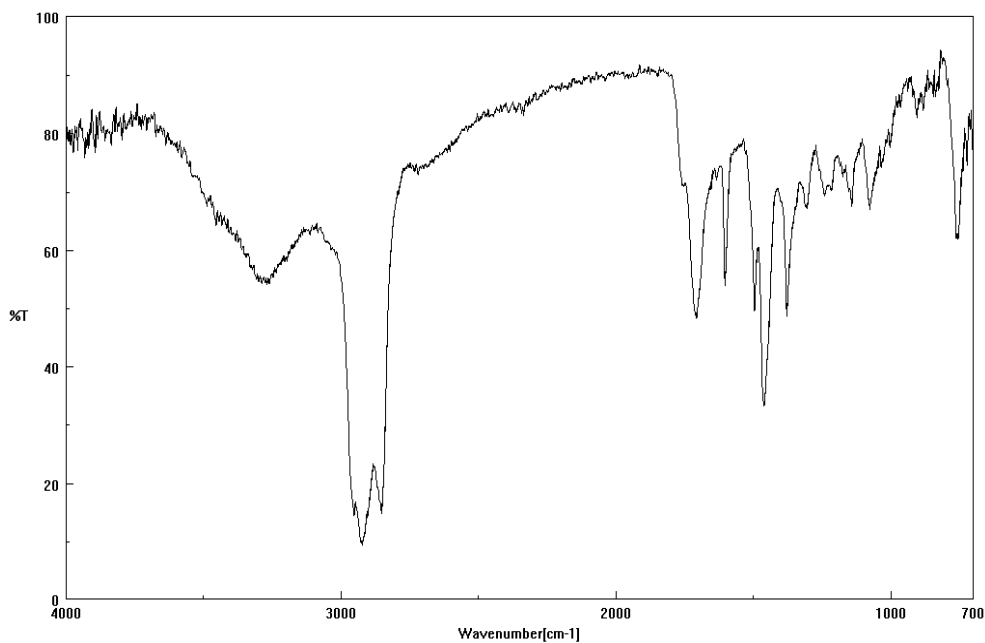


Figure 4.4. The i.r. spectrum of 2k, 2k' (In Nujol)

4.2. Synthesis of Azomethine Ylides 3d, 3e, 3e' and 3f

Pyridine was mixed with the ethyl 2-bromoacetate to yield the pyridinium bromide salt **3a**. Removing a proton from the methylene group by using base gave the corresponding azomethine ylide **3d** in CHCl_3 . Pyridinium ylides **3d**, **3e**, **3e'**, **3f**, prepared by us, are only moderately stable in solution and can not be isolated.

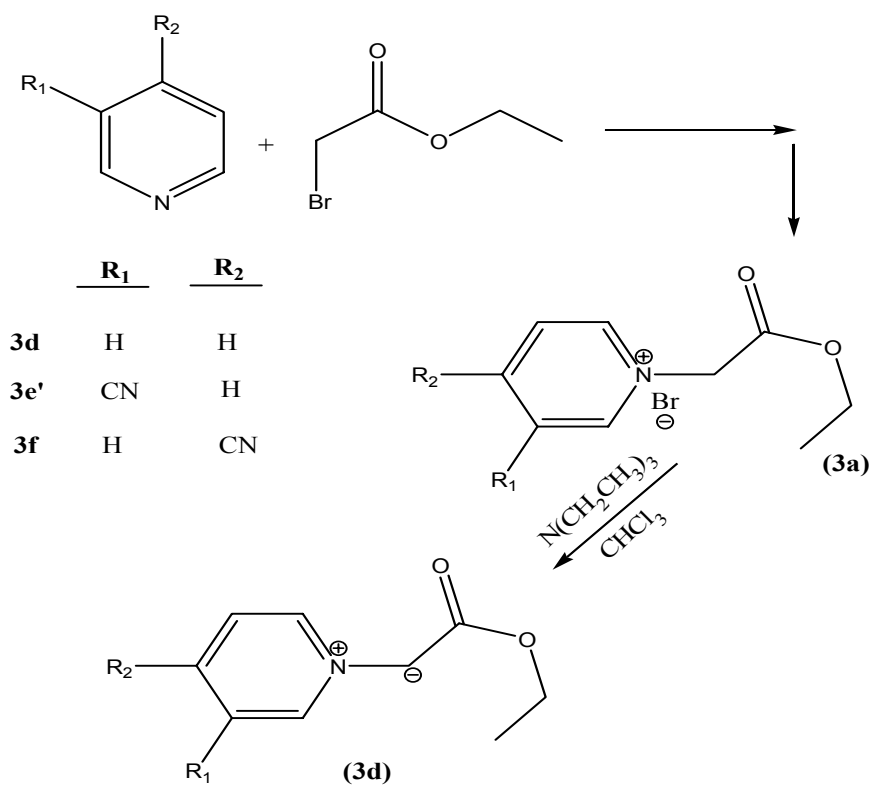


Figure 4.5. The schematic representation of the synthesis of azomethine ylide **3d**

The IR spectrum of **3a**, shows a saturated ester group [ν (nujol) (C=O) 1737 cm^{-1}], an imine stretching band [ν (nujol) (C=N) 1637 cm^{-1}], and an aromatic stretching band [ν (nujol) (C=C) 1577 cm^{-1}]. (**Fig. 4.6**)

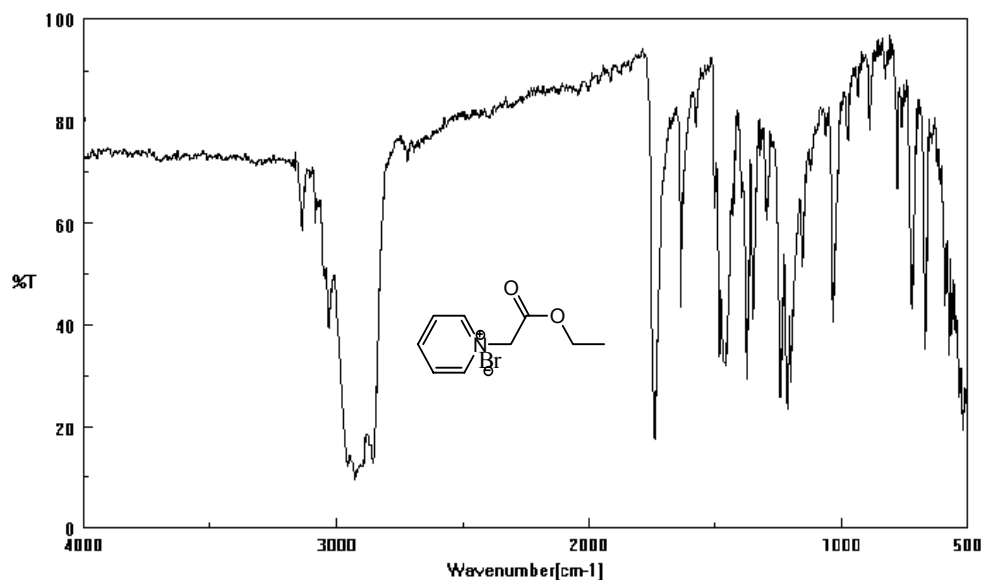


Figure 4.6. The i.r. spectrum of 3a (In Nujol)

The ^1H NMR spectrum of **3a**, shows a doublet for H_a centered at 9.52 ppm coupled with H_b ($J_{ab}=6.06$ Hz), a singlet for H_d at 6.34 ppm, a quartet for H_e centered at 4.29 ppm coupled with H_f ($J_{ef}=7.14$) and three triplets for H_b , H_c , H_f centered at 8.58 ppm, 8.13 ppm and 1.32 ppm, respectively. H_b protons couples with both H_a and H_c ($J_{ba}=7.81$ Hz) ($J_{bc}=7.80$ Hz). Also, H_f couples with H_e ($J_{fe}=7.05$ Hz). The coupling constants for J_{ab} and J_{ba} are quite different. Because the carbon atom belongs to H_a is bonded to an electronegative atom. Any electronegative atom bonded to carbon decreases the coupling constant. For the **3a** compound, there are two homotopic hydrogens H_a , H_b , having the same environment, so only one signal is observed for each proton a doublet and a triplet, respectively. The coupling constants are nearly the same around $J=7-8$, and so we can say that all coupling types are the same. These are vicinal couplings. (**Fig. 4.7**)

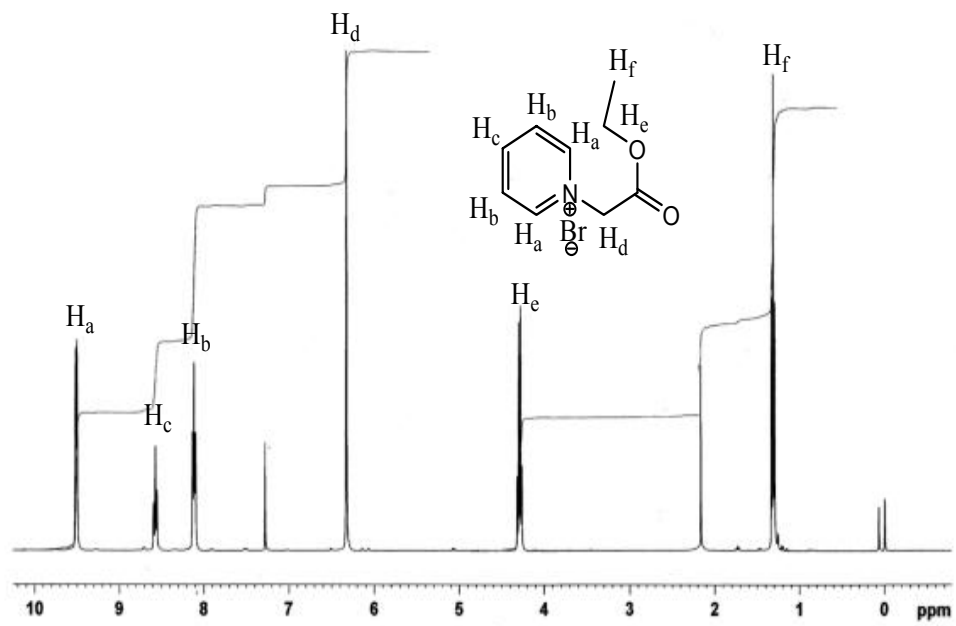


Figure 4.7. The ^1H NMR of 3a

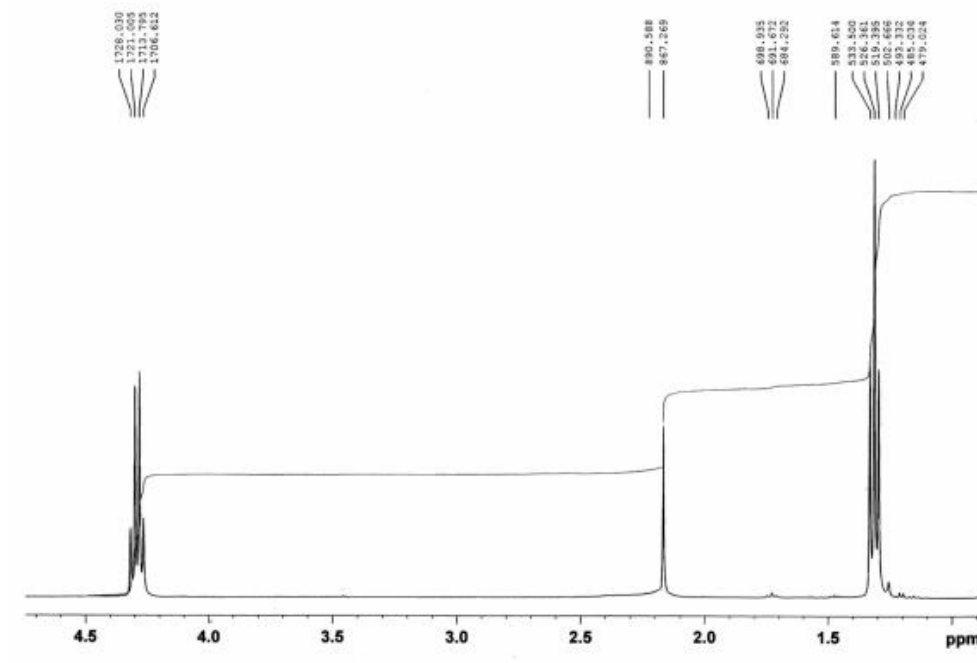


Figure 4.7. (continued)

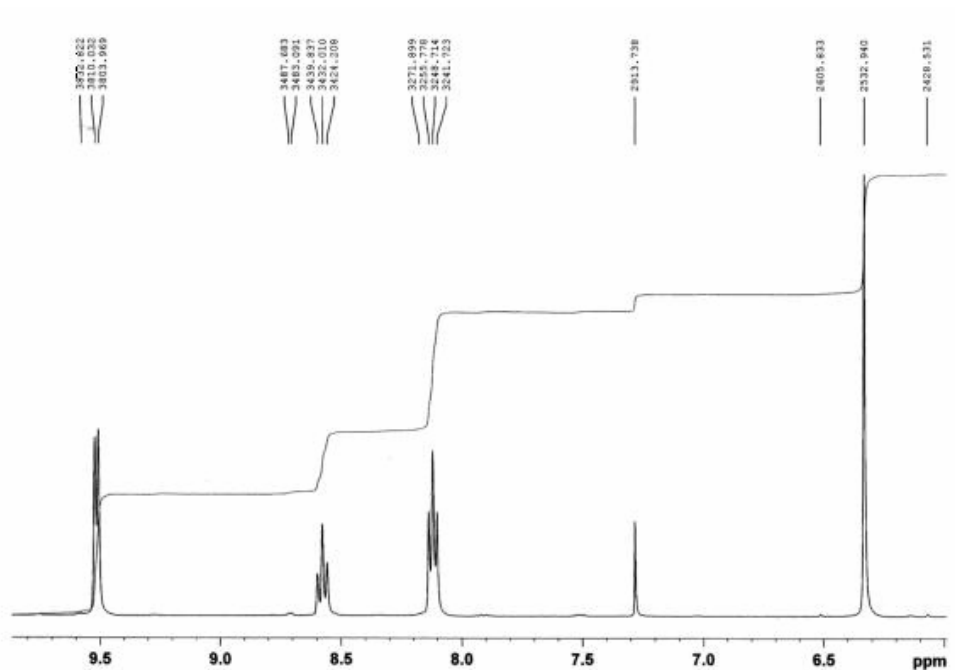


Figure 4.7. (continued)

The ^{13}C NMR spectrum shows signals for C_e carbon atom at 165.8 ppm, C_c carbon atom 146.7 ppm, C_a carbon atom at 146.1 ppm, C_b carbon atom at 127.7 ppm, C_d carbon atom at 63.4 ppm, C_f carbon atom at 61.1 ppm, C_g carbon atom 14.1 ppm. According to the ^{13}C spectrum, there are seven carbon atoms related to the structure. In fact, there are nine carbon atoms on **3a** structure but two of them H_a , H_b have the same environment and give the same chemical shifts. (**Fig. 4.8**)

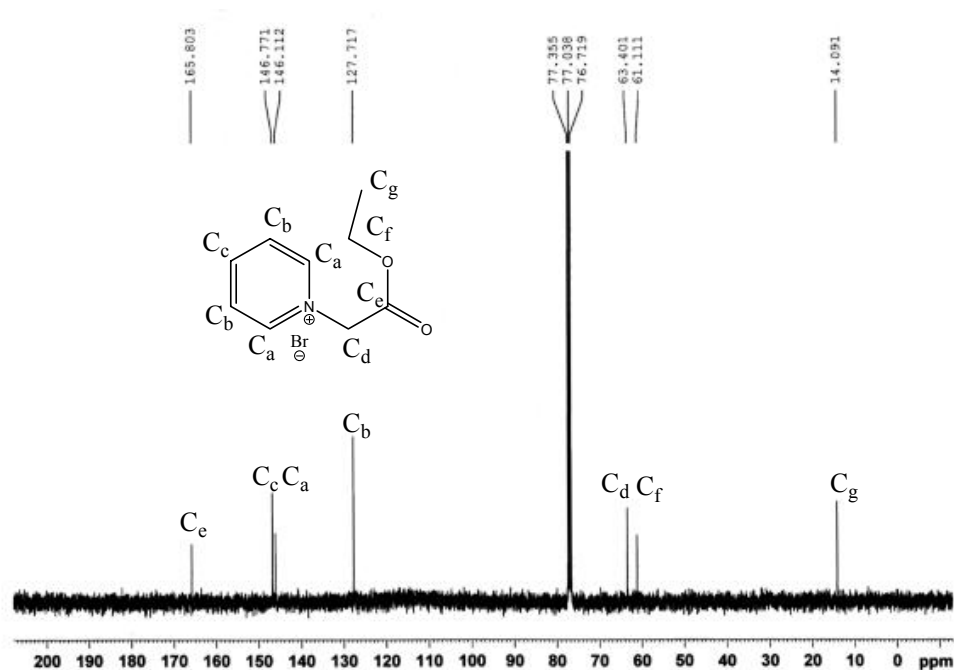


Figure 4.8. The ^{13}C NMR of 3a

4.2.1. Characterization of Cycloadducts

Pyridinium ylides **3d**, **3e**, **3e'**, **3f** prepared in situ were reacted with both acetylenic and olefinic dipolarophiles such as dimethyl acetylenedicarboxylate, diethyl acetylenedicarboxylate, diphenyl acetylene, phenyl acetylene, vinyl acetate and vinylene carbonate.

As a result of this working, dipoles show reactivity with DMAD and DEAD at room temperature in CHCl_3 . Although the reaction mixtures, including dipoles and dipolarophiles (DPA, PA, VA, VC), have been stirred for twelve days at reflux temperature in CHCl_3 , any reaction was not observed. The reason was explained by theoretically. And a new thing was noticed that acetylenecarboxylic esters were more reactive as dipolarophiles towards azomethine ylides than other olefinic esters and acetylenic dipolarophiles. Indeed, acetylenic esters interact rapidly with pyridinium

ylides giving high yields at room temperature. In addition, two of the products prepared by 4-cyano pyridinium ylide and DMAD, DEAD are UV active compounds. To our best knowledge of literature survey, these type of compounds have absorbance maximum at UV region and can be used as dyes in different areas. And also different studyings will be done on this topic. At the end of the reactions, six new heterocyclic compounds were purified and characterized by using IR, NMR data.

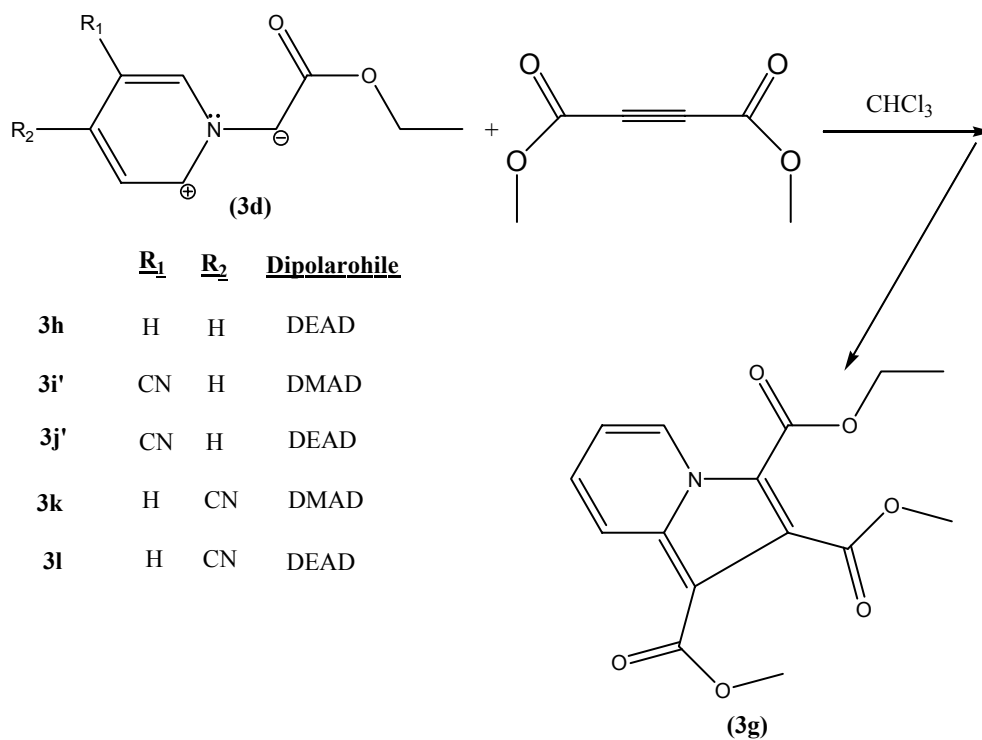


Figure 4.9. The schematic representation of the synthesis of cycloadduct 3g

The cycloadduct **3g** is supported by the i.r. absorptions for α,β -unsaturated ester groups [ν (nujol) (C=O) 1740 and 1708 cm^{-1}] and an aromatic stretching band [ν (nujol) (C=C) 1600 cm^{-1}]. (**Fig. 4.10**)

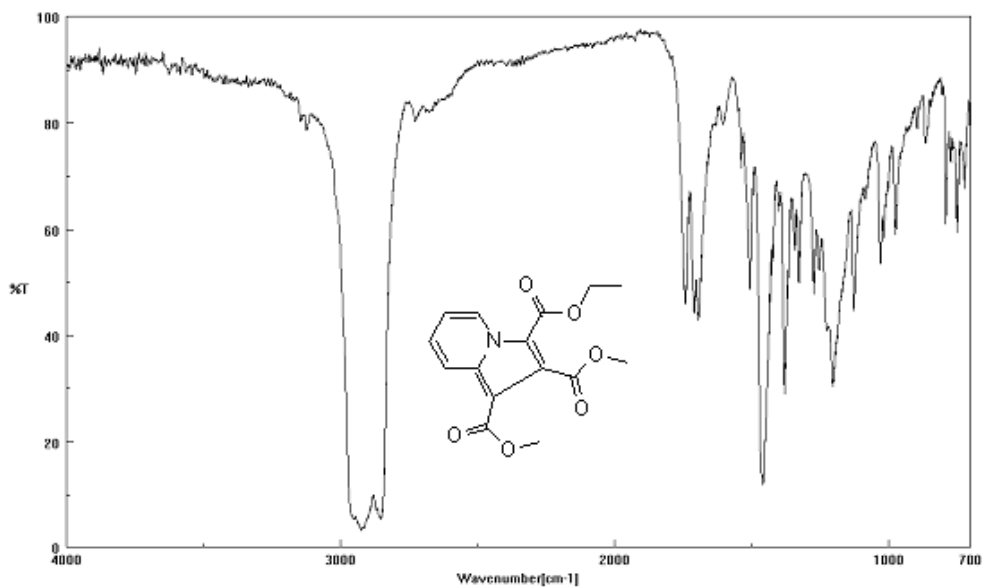


Figure 4.10. The i.r. spectrum of cycloadduct **3g** (In Nujol)

The ^1H NMR spectrum of **3g**, shows two doublets for H_a , H_d centered at 8.26 ppm and 9.47 ppm, respectively. H_a couples only with H_b ($J_{ab}=9.05$ Hz) and H_d couples with H_c ($J_{dc}=7.17$ Hz). When we compare the vicinal coupling constants of H_a and H_d , H_d has lower value than H_a . Because H_d carbon is bonded an atom more electronegative than carbon atom. Any electronegative atom bonded to a carbon atom decreases the vicinal coupling constants. There are three triplets for H_b , H_c , H_g centered at 7.31 ppm, 6.97 ppm, 1.32 ppm, respectively. H_b couples with H_a and H_c on three bonds, and with H_d on four bonds. This means that H_b makes vicinal couplings with H_a , H_b and long range coupling with H_d . H_b couples with H_c , H_a , H_d .

J_{bd} constant is 1.30 Hz and J_{bc} or J_{ba} is 6.89 Hz. H_c makes vicinal coupling with ($J_{cb}\sim 6.99$ Hz) ($J_{cd}\sim 6.99$ Hz) H_b and H_d , and long range coupling with H_a ($J_{ca}=1.30$ Hz). H_g couples with H_f . And also two singlets H_e and one quartet H_f comes at 3.92 ppm, 3.82 ppm, 4.30 ppm, respectively. H_f is splitted by methylene protons and couples with H_g ($J_{fg}=7.24$). Normally, methyl groups almost have the same environment. But singlets come at different fields. When we compare the environment of the both methyl protons, the methyl protons near to ethyl ester group is more shielded than the other because of the steric hindrance of the side group. It needs more magnetic field. This causes the signal shifting towards high magnetic field. So it comes upfield in the spectrum (3.82 ppm). (Fig. 4.11)

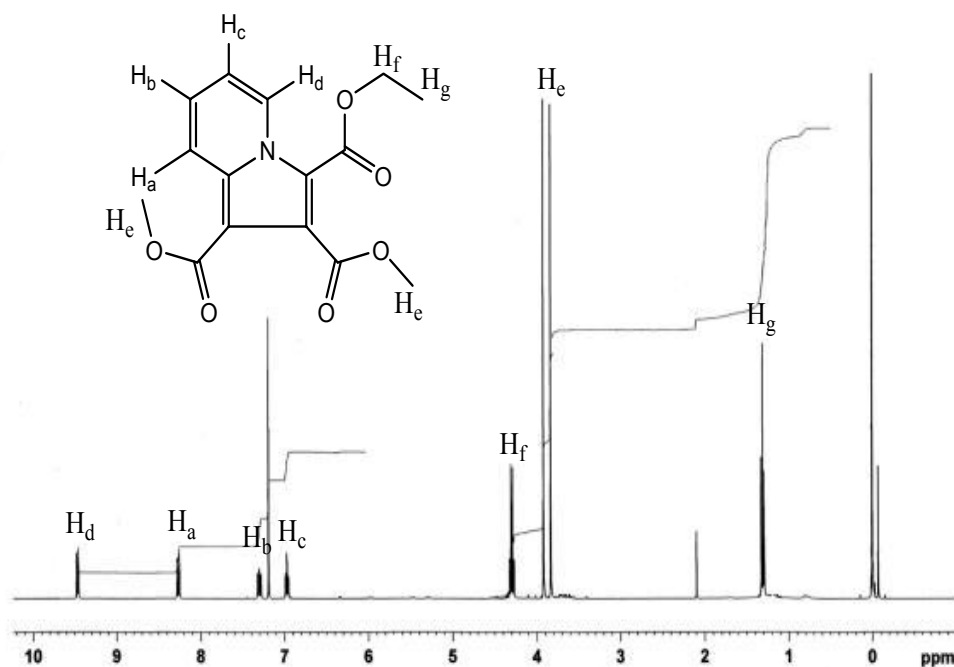


Figure 4.11. The ^1H NMR spectrum of cycloadduct 3g

The same side effects are valid for ^{13}C NMR. So the position of signals are different. The ^{13}C NMR spectrum shows signals for C_n carbon atom at 165.2 ppm, C_l carbon atom 162.3 ppm, C_i carbon atom at 159.1 ppm, C_e carbon atom at 151.3 ppm, C_d carbon atom at 136.8 ppm, C_g carbon atom at 129.5 ppm, C_a carbon atom 126.9 ppm, C_b carbon atom at 125.6 ppm, C_h carbon atom at 118.9 ppm, C_c carbon atom at 114.3 ppm, C_f carbon atom at 101.9 ppm, C_j carbon atom at 59.9 ppm, C_o carbon atom at 51.7 ppm, C_m carbon atom at 50.6 ppm and C_k carbon atom at 13.1 ppm. According to the ^{13}C spectrum, there are fifteen carbon atoms related to the structure. And we can say that ^{13}C NMR spectrum is also supporting the **3g** cycloadduct. (**Fig. 4.12**)

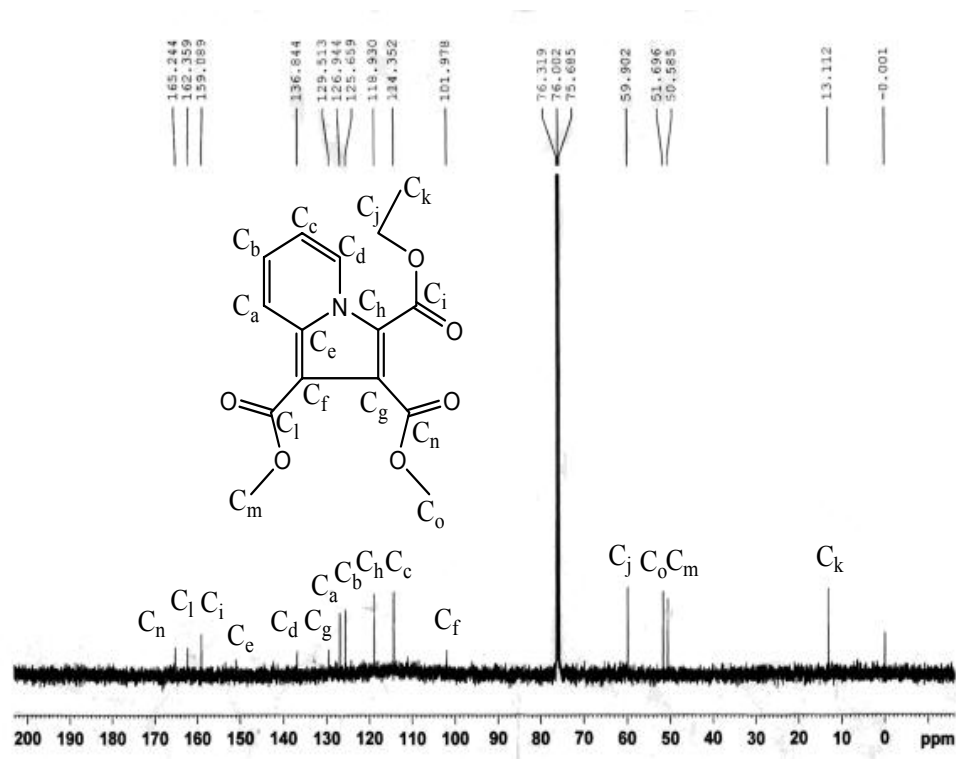


Figure 4.12. The ^{13}C NMR spectrum of cycloadduct **3g**

The cycloadduct **3i'** is supported by the i.r. absorptions for α,β -unsaturated ester groups [$\nu(\text{nujol})$ (C=O) 1741 cm^{-1}], a vinyl stretching band [$\nu(\text{nujol})$ (C=C) 1695 cm^{-1}] and a nitrile band [$\nu(\text{nujol})$ (C \equiv N) 2238 cm^{-1}]. (**Fig. 4.13**)

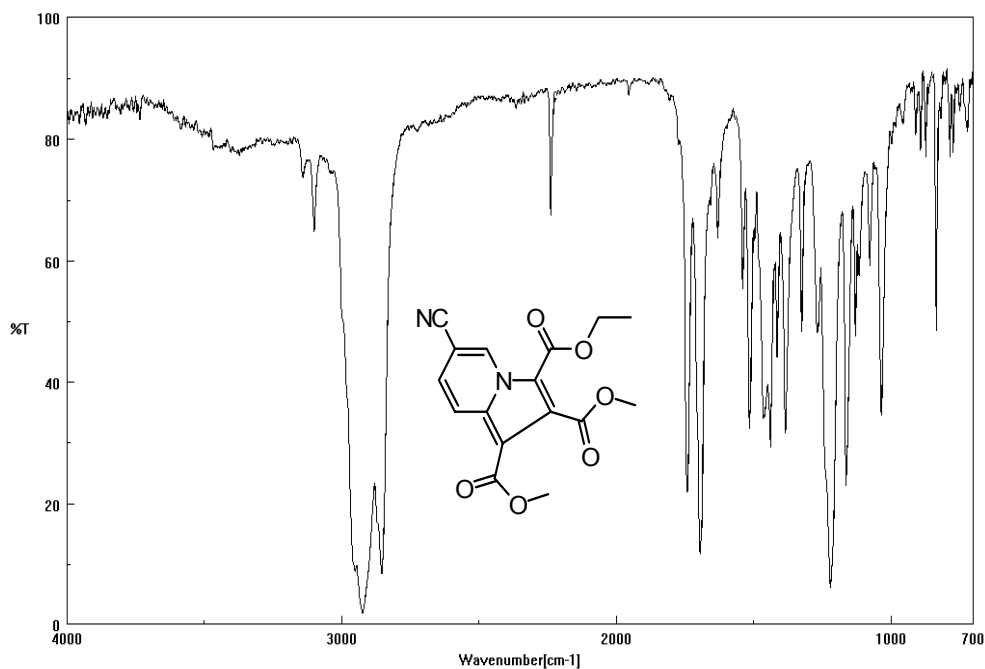


Figure 4.13. The i.r. spectrum of cycloadduct **3i'** (In Nujol)

The ^1H NMR spectrum of cycloadduct **3i'** shows one singlet related with H_c proton centered at 10.0 ppm, two singlets H_d protons almost having the same chemical shifts at 4.00 ppm and 3.92 ppm, two doublets for H_a and H_b protons centered at 8.43 ppm and 7.42 ppm, one triplet for H_f protons centered at 1.39 ppm and a quartet for H_e protons centered at 4.42 ppm. H_a proton only makes vicinal coupling with H_b ($J_{ab}=9.46$ Hz). This shows us that the dihedral angle between the protons are near to 0° . H_b makes vicinal coupling with H_a ($J_{ba}=9.24$ Hz) and long range coupling with H_c ($J_{bc}=1.28$ Hz). This shows, dihedral angle between H_b and H_a

is near to 0°. In addition, the position of the signal for H_d protons change because of the side group effects on these protons. The more shielded protons, near to ethyl ester group, comes at high field at 3.92 ppm.

On the other hand, there was an another possibility to get a different isomeric product **3i**. At the end of the reaction, this product was formed and isolated. It always showed another spot, having a fluorescent property on U.V region, on t.l.c after getting as one spot. Because of that the yield of the isolated product is nearly 30%. (Fig. 4.14)

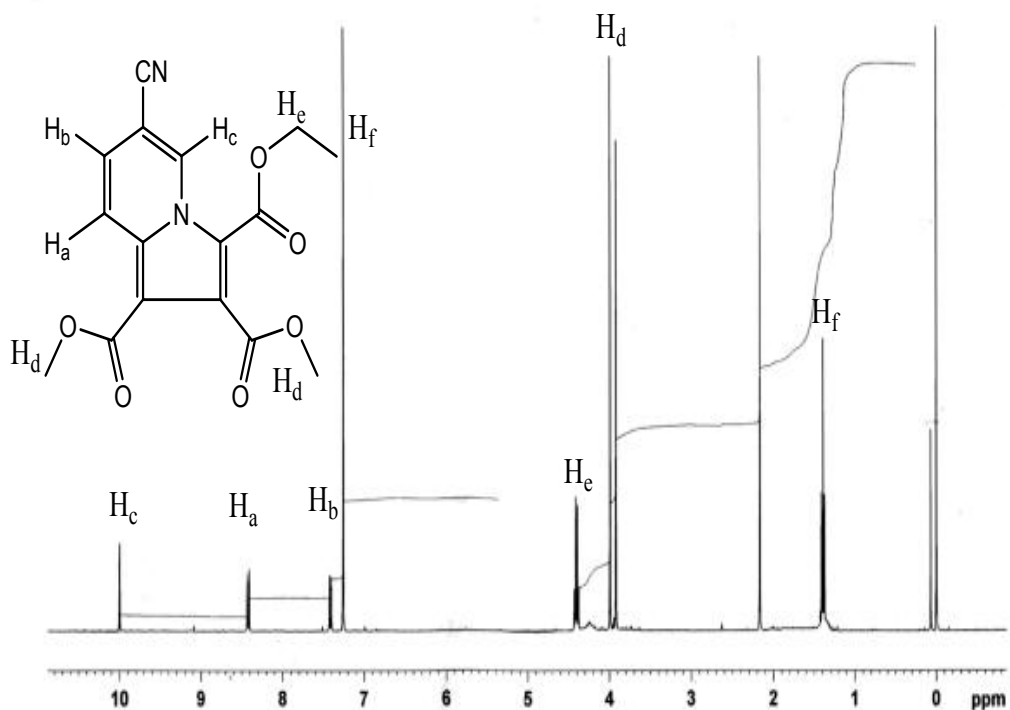


Figure 4.14. The ¹H NMR spectrum of cycloadduct **3i'**

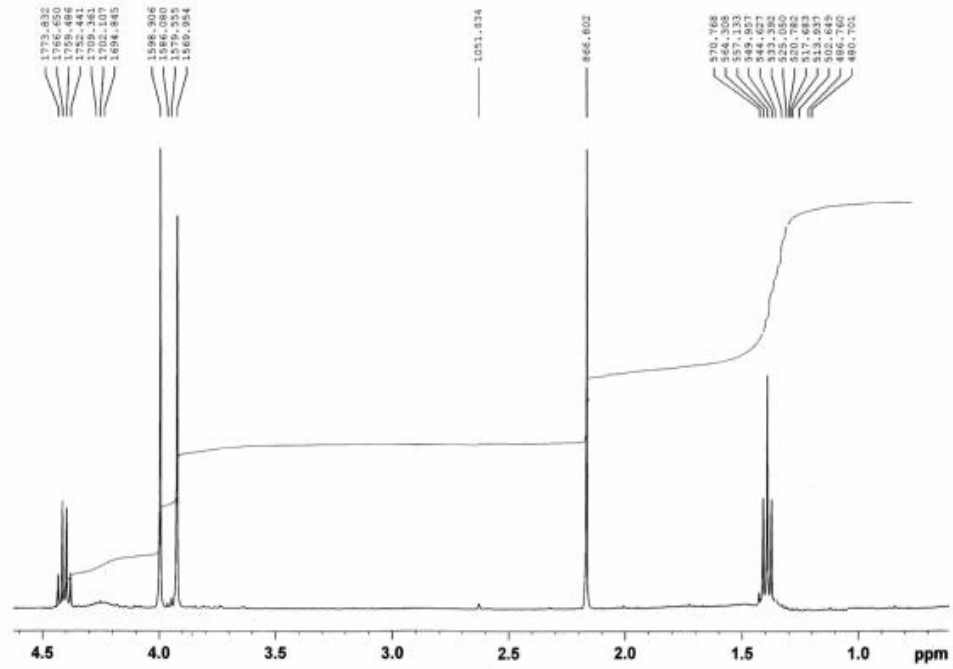


Figure 4.14. (Continued)

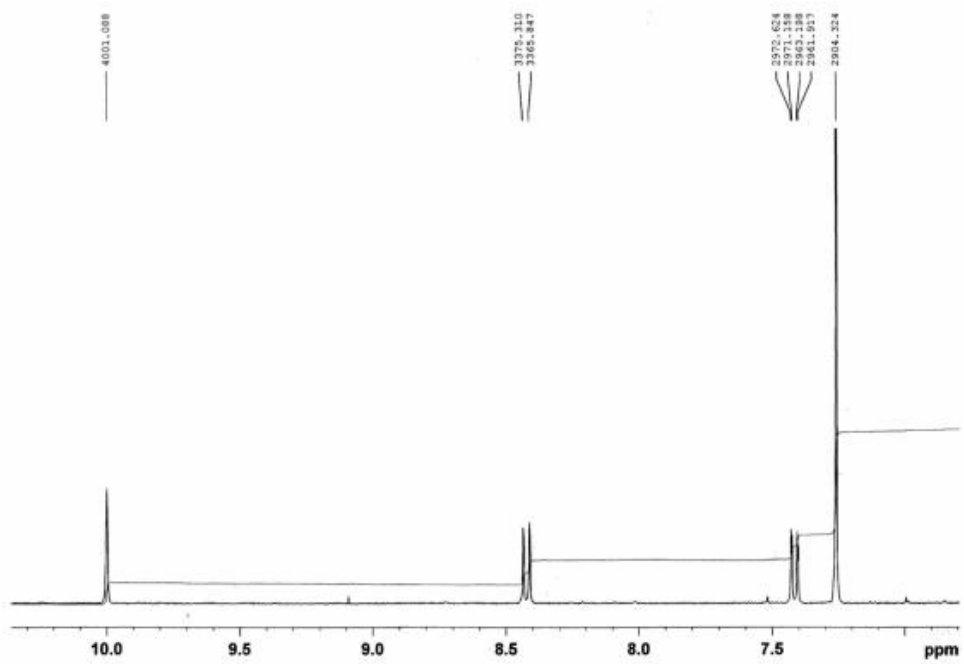


Figure 4.14. (Continued)

The cycloadduct **3k** is supported by the i.r. absorptions for α,β -unsaturated ester groups [$\nu(\text{nujol})$ (C=O) 1751 and 1740 cm^{-1}], a vinyl stretching band [$\nu(\text{nujol})$ (C=C) 1687] a nitrile band [$\nu(\text{nujol})$ (C \equiv N) 2232 cm^{-1}]. (**Fig. 4.15**)

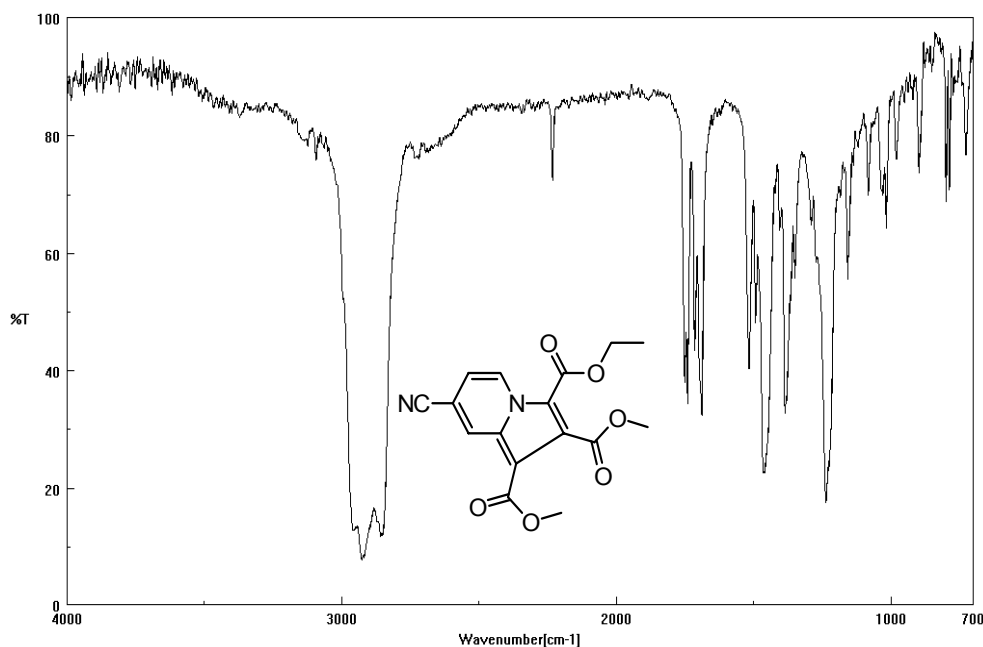


Figure 4.15. The i.r. spectrum of cycloadduct **3k** (In Nujol)

The ^1H NMR spectrum of cycloadduct **3k** shows one singlet related with H_a proton centered at 8.74 ppm, two singlets H_d protons almost having the same chemical shifts at 4.02 ppm and 3.98 ppm, two doublets for H_c and H_b protons centered at 9.63 ppm and 7.14 ppm, one triplet for H_f protons centered at 1.43 ppm and a quartet for H_e protons centered at 4.42 ppm. H_c proton only makes vicinal coupling with H_b ($J_{cb}=7.31$ Hz). H_b makes vicinal coupling with H_c ($J_{bc}=7.26$ Hz) and probably long range coupling with H_a ($J_{ba}=1.58$ Hz). In addition, the position of the signal for H_d protons change because of the side group effects on these protons.

The more shielded protons, near to ethyl ester group, comes at high field at 3.98 ppm. And also, we can decide by comparing the coupling constants, H_b and H_c are nearly cis to each other. (Fig. 4.16)

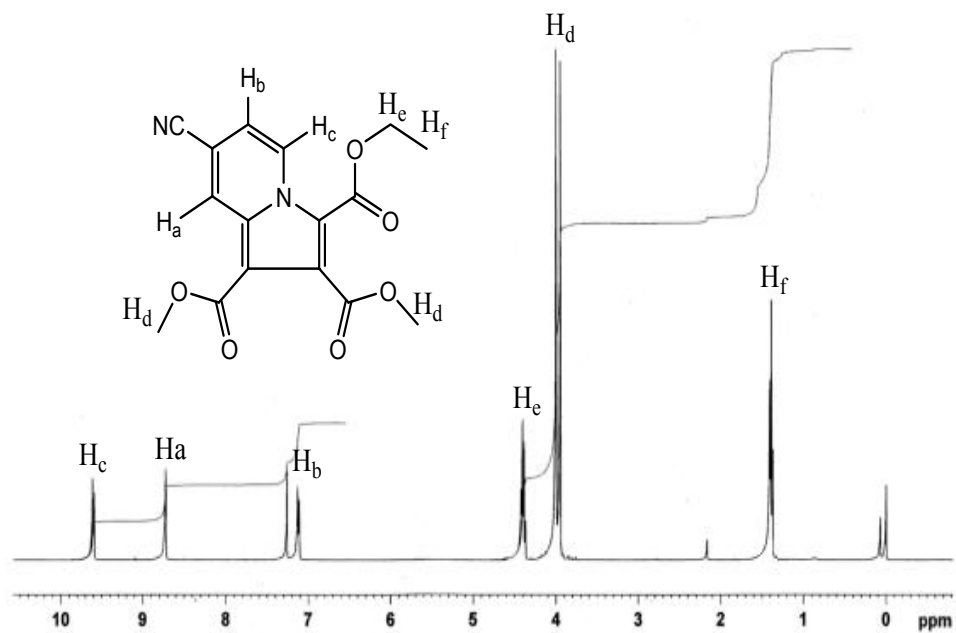


Figure 4.16. The ^1H NMR spectrum of cycloadduct 3k

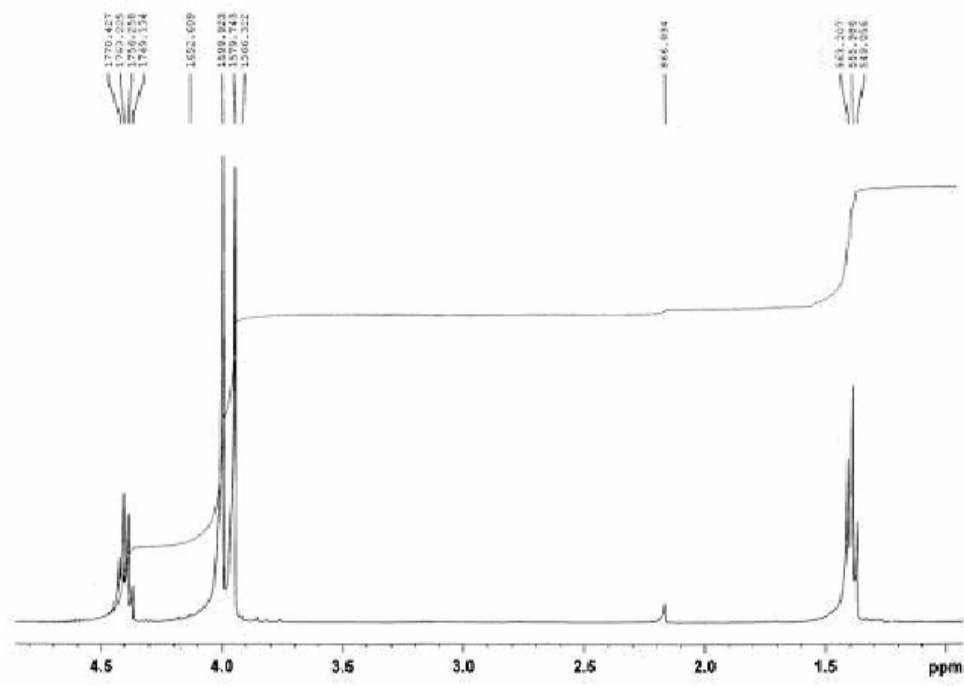


Figure 4.16. (Continued)

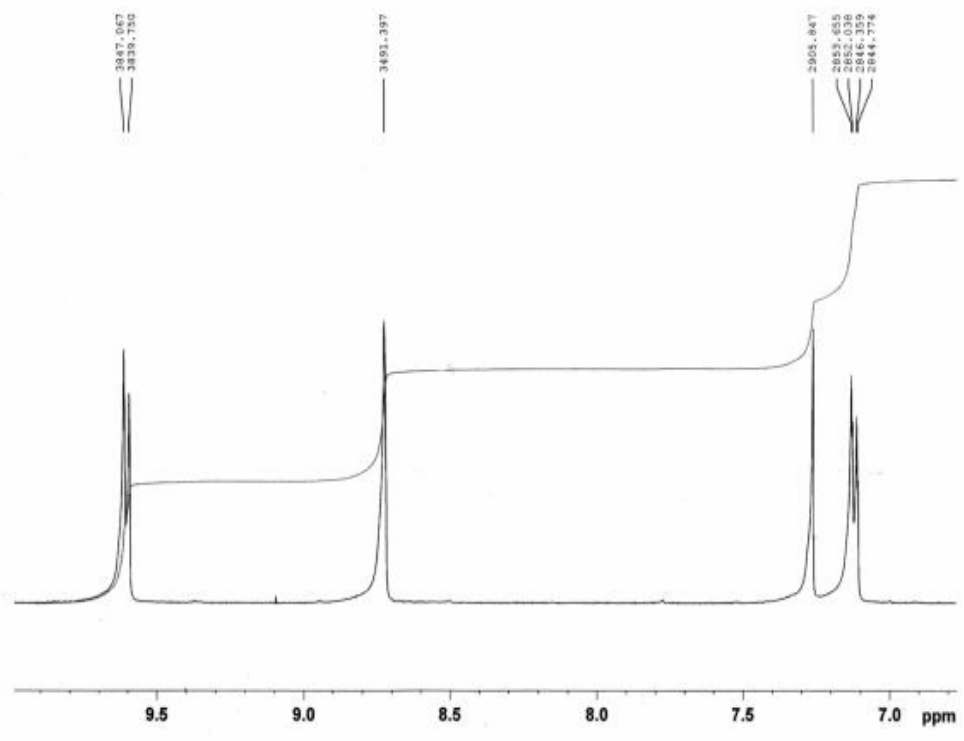


Figure 4.16. (Continued)

4.2.2. Molecular Orbital Considerations

The structural features of the cycloadducts obtained via the reactions of pyridinium ylides with dipolarophiles can also be deduced from theoretical evidences.

The MO method, EH, was used to find the corresponding orbital energies and coefficients. By this way, it has been possible to predict the regioselectivity of the ylides with the aid of the necessary equations given in introduction part. On this study, being used symmetrical dipolarophiles, the energies of FOs of both ylides and dipolarophiles gain importance to discuss how they react differently.

The present study offers the usage of EH method at the level of FMO to estimate qualitative correlations between theory and reactivity, regio-, and stereoselectivity in 1,3-dipolar cycloaddition reactions of pyridinium ylides towards acetylenic and olefinic dipolarophiles.

All calculations were performed using HyperChem-EH method to get HOMO and LUMO energies and the coefficients of the reaction sites of both ylides and dipolarophiles. Table 1 and table 2 show the HOMO and LUMO energies of them.

Table 1. The FMO energies of the azomethine ylides in eV.

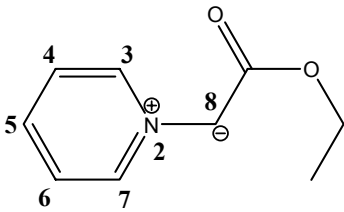
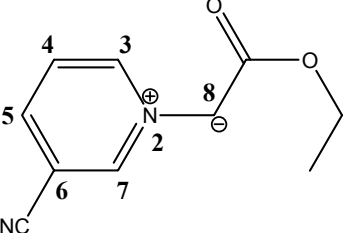
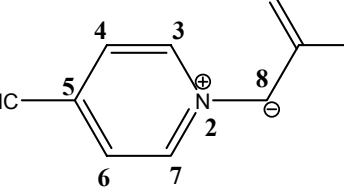
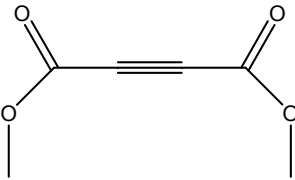
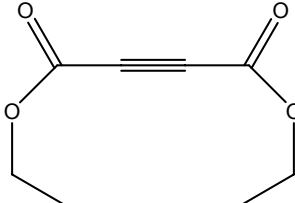
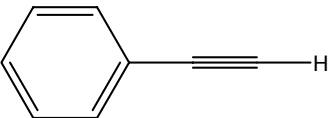
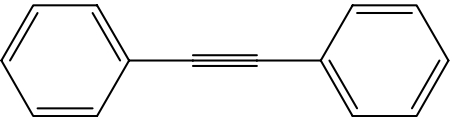
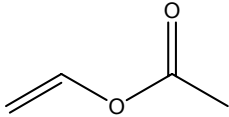
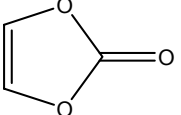
| <u>Azomethine ylides</u> | <u>HOMO</u> | <u>LUMO</u> |
|--|-------------|-------------|
|  | -11.50 | -9.306 |
|  | -11.79 | -9.422 |
|  | -11.85 | -9.764 |

Table 2. The HOMO and LUMO energies of dipolarophiles in eV.

| <u>Dipolarophiles</u> | <u>HOMO</u> | <u>LUMO</u> |
|---|-------------|-------------|
|  | -13.33 | -10.32 |
|  | -13.26 | -10.34 |
|  | -12.47 | -8.81 |
|  | -12.09 | -9.213 |
|  | -12.78 | -8.803 |
|  | -12.34 | -8.296 |

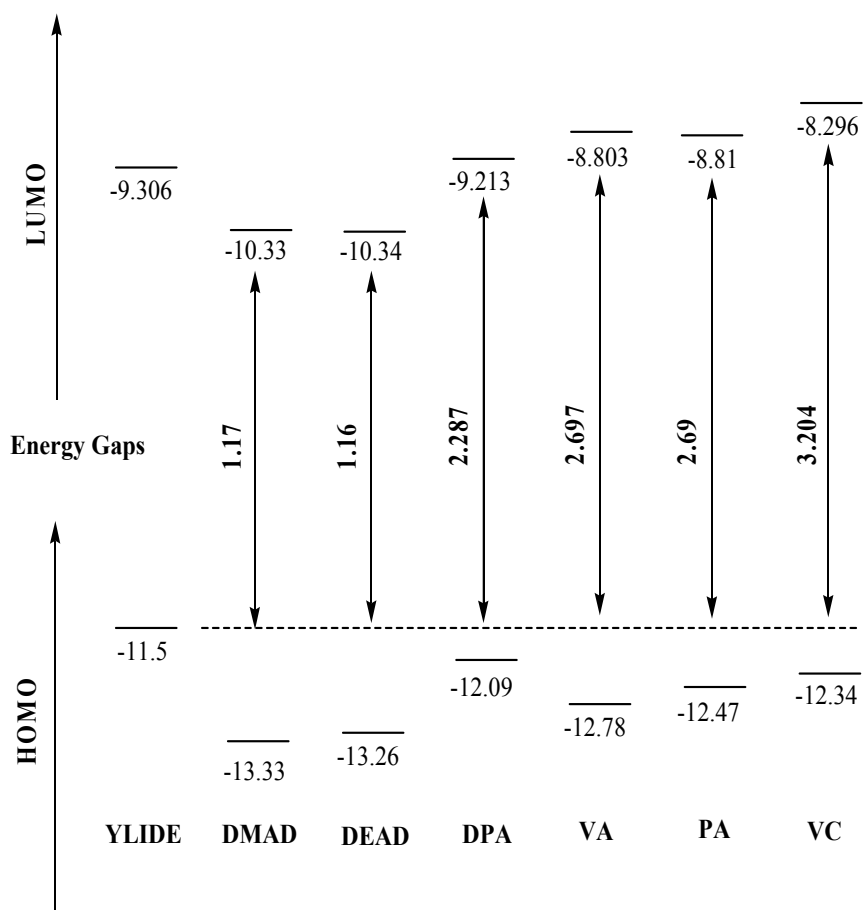


Figure 4.17. The relative energy gaps of the pyridinium ylide and dipolarophiles in eV.

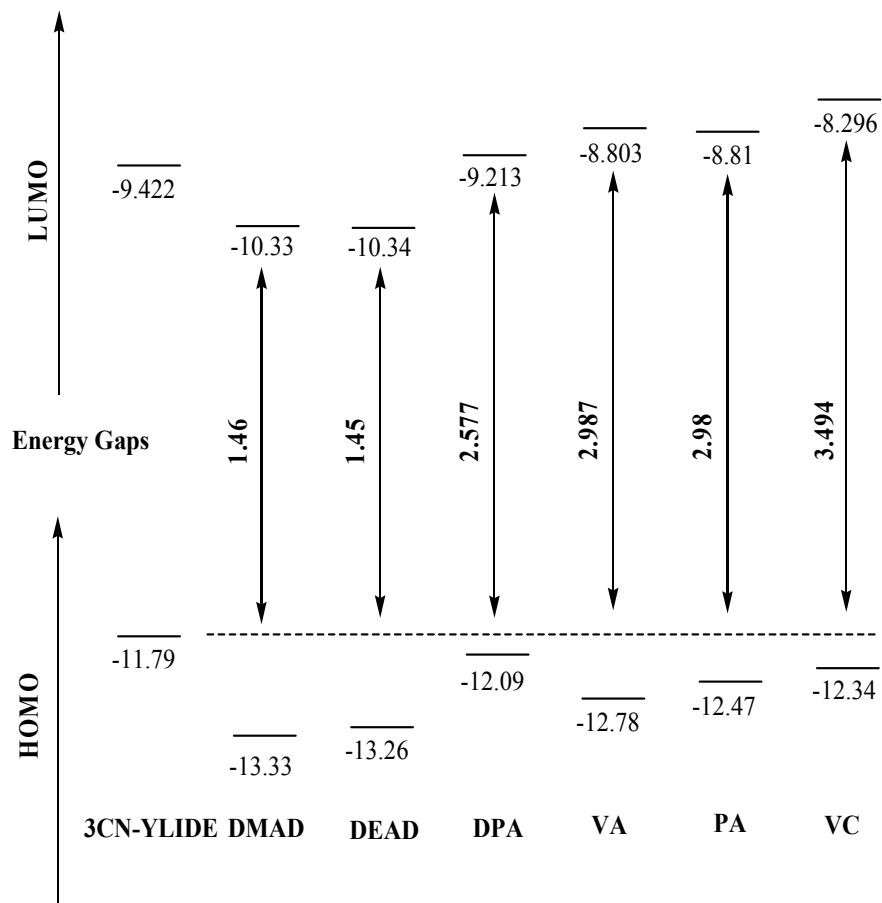


Figure 4.18. The relative energy gaps of the 3-cyanopyridinium ylide and dipolarophiles in eV.

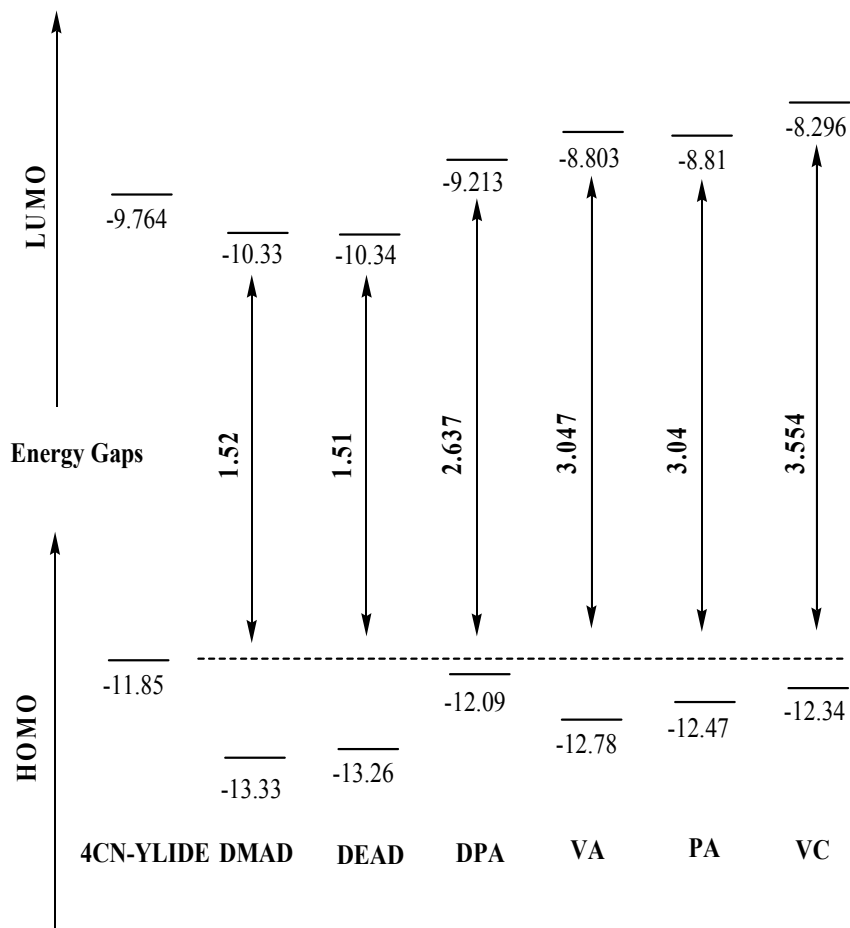


Figure 4.19. The relative energy gaps of the 4-cyanopyridinium ylide and dipolarophiles in eV.

Preliminary FMO calculations suggest that the cycloaddition reactions between pyridinium ylide, 3-cyanopyridinium ylide, 4-cyanopyridinium ylide and dipolarophiles (DMAD, DEAD) are $\text{HOMO}_{\text{dipole}}\text{-LUMO}_{\text{dipolarophile}}$ controlled. Because the energy gap is very low compared with $\text{LUMO}_{\text{dipole}}\text{-HOMO}_{\text{dipolarophile}}$. These dipoles and dipolarophiles give reaction at room temperature and does not need any additional energy to proceed. And also, this is the another core of our study. At room temperature, all the reactions, were done by DMAD and DEAD, are

proceeding by giving high yields nearly 75%. As we mentioned before, the other four dipolarophiles does not show any reactivity towards dipoles neither at room temperature nor at 60°C. Depending on FMO calculations, the reaction with DPA, VA, VC and PA may need more energy to overcome. Because the energy gaps between both HOMO and LUMO orbitals are quite higher than DMAD and DEAD. But, high temperatures were not tried to proceed reactions. Low temperatures were preferred. And also high temperature reactions will be tried by those dipolarophiles in future.

Table 3. The FMO coefficients of the azomethine ylides in eV.

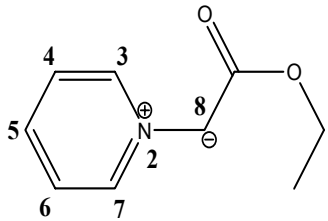
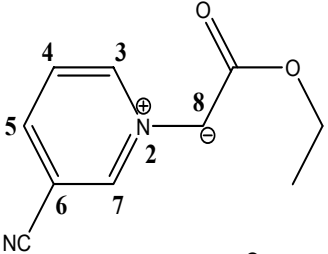
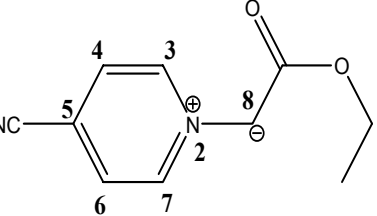
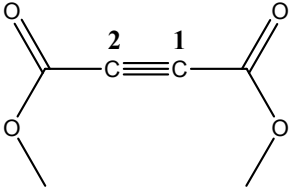
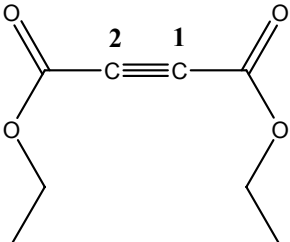
| <u>Azomethine ylides</u> | <u>Coefficients</u> | | | |
|---|---------------------|------------|------------|-------------|
| | <u>3</u> | <u>7</u> | <u>8</u> | |
|  | HOMO | 0.2877437 | 0.2912702 | -0.6544809 |
| | LUMO | -0.4100818 | -0.410926 | -0.07844152 |
|  | HOMO | 0.2411176 | 0.2683657 | -0.5820 |
| | LUMO | 0.5467275 | -0.2407864 | -0.2407864 |
|  | HOMO | 0.2580786 | 0.2591392 | -0.5752519 |
| | LUMO | 0.2249778 | 0.2192154 | 0.0262504 |

Table 4. The FMO coefficients of the dipolarophiles in eV.

| <u>Dipolarophiles</u> | <u>Coefficients</u> | |
|---|------------------------|------------|
| | <u>1</u> | <u>2</u> |
|  | <u>HOMO</u> -0.5870 | -0.5870 |
| | <u>LUMO</u> 0.407528 | -0.407528 |
|  | <u>HOMO</u> -0.5578759 | -0.5591276 |
| | <u>LUMO</u> -0.4011287 | 0.4013275 |

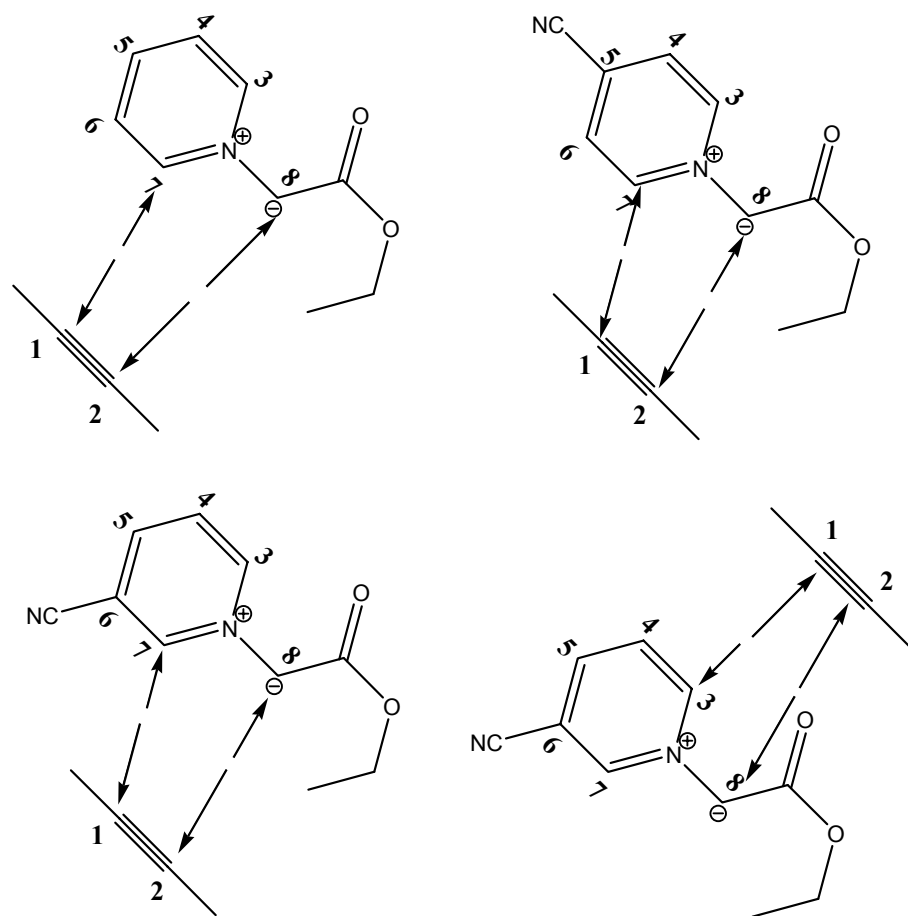
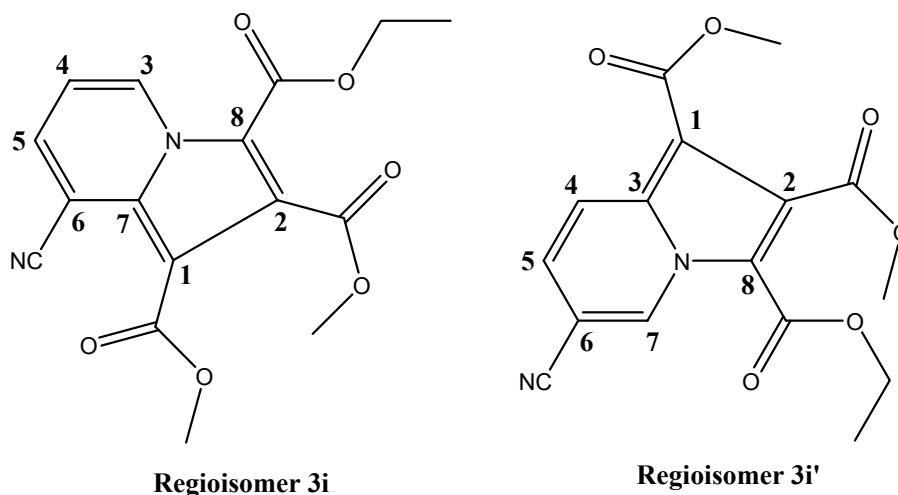


Figure 4.20. Bonding interactions between the ylides and dipolarophiles.

Bonding interactions between the ylides and dipolarophiles are like shown in figure 4.20. As we mentioned earlier, cycloaddition reactions between three ylides and dipolarophiles are $\text{HOMO}_{\text{dipole}}\text{-LUMO}_{\text{dipolarophile}}$ controlled. When we take figure 4.20 into account by comparing the coefficients of site 3 and site 7, the shapes of ylides can be symmetrical or non-symmetrical. Theoretical calculations show that the pyridinium ylide and 4-cyanopyridinium ylide are symmetrical, on the other hand, 3-cyanopyridinium ylide is non-symmetrical. As a result of this, two regioisomers seem to be possible from the reaction of 3-cyanopyridinium ylide and the dipolarophiles such as DMAD, DEAD.



But, the ratio of these regioisomers can vary comparatively. This reason can be explained by theoretical calculations. On the structure of 3-cyanopyridinium ylide, there are two possible reactive sites but, one of them is more energetic than the other. We can notice the energy difference by comparing the coefficients of sites. And so, regioisomer **3i** is formed by giving good yield due to the overlapping of larger coefficients at the reactive sites.

Also, experimental results support to the theoretical calculations. Because, at the end of the experiment, two regioisomers were obtained and purified by using column chromatography. Regioisomer **3i** gave relatively high yield compared to regioisomer **3i'**. However, one of the regioisomers (**3i'**) could be characterized. Because another new spot generated on the other regioisomer (**3i**) after purification. And, we decided that regioisomer **3i** seems not to be stable.

Generally, MO calculations at the level of FMO approach seem to be a powerful tool to explain the course of the cycloaddition reactions. The experimental findings are in well accord with the theoretical predictions. The structure of the

expected compounds and the reactivity of the cycloaddition reactions are easily estimated as seen in this work.

5. CONCLUSIONS

The following main topics can be deduced from this study.

Azomethine imines, being tried to prepare from pyromellitic dianhydride and the related substituted and unsubstituted phenylhydrazines, didn't show similar characteristic results of azomethine imines of 3-arylphthalazinium-1-olates. We didn't get any expected azomethine imine type betaines of them due to the rearrangement reactions upon heating at the final stage. The reasons of this have still been getting investigated.

At room temperature, by mixing pyridine and cyano substituted pyridines, we obtained easily the corresponding pyridinium bromides. From the bromides, in situ, azomethine ylides were prepared again in room temperature so they showed 1,3-dipolar cycloaddition reactions towards acetylenic dipolarophiles DMAD and DEAD.

The azomethine ylides failed to give any cycloadduct with olefinic dipolarophiles under various conditions. The reason may be lie on the fact that there would be the larger HOMO-LUMO energy gaps of the FMO's of the ylides and olefinic dipolarophiles.

The unsubstituted and 4-cyano substituted pyridinium ylides having symmetrical properties on the reactive sites led only one type of regioisomer. On the other hand, 3-cyano substituted ylide offered two kinds of regioisomers due to the unsymmetrical reactive sites.

The theoretical predictions of the regioisomers of 3-cyano substituted pyridinium ylide with the dipolarophiles upon cycloaddition reactions were well accord with the experimental findings. The major product of the experimental part was also the one of the theoretical calculations.

The reaction profiles of these cycloaddition reactions were also correctly predicted by using the extended Huckel MO calculations at the level of FMO approach.

Finally, the cycloadducts as well as the azomethine imines and ylides may show biological activity. This property will further make them important in the family of heterocyclic chemistry.

REFERENCES

1. Norman R.O.C., Principles of Organic Synthesis, Chapman and Hall L.t.d., London, p. 284, (1978).
2. Woodward R.B. and Hoffmann R., Jour. Of Am. Chem. Soc., 87:395, (1965)
3. Woodward, R.B.; Hoffmann, R. The Conservation of Orbital Symmetry, Academic Press Inc., (1970)
4. (a) 1,3-Dipolar Cycloaddition Chemistry; Padwa, A., Ed.; Wiley/Interscience: Newyork, 1984; Vols. 1-2. (b) Padwa, A. Comprehensive Organic Chemistry; Trost, B. M., Fleming, I., Eds.; Pergamon: Oxford, 1991; Vol. 4, pp 1069-1109.
5. Wasserman, A. Diels-Alder Reactions; Elsevier: Newyork, 1965.
6. Fleming, I. Pericyclic Reactions; Oxford University: Oxford, 1999.)
7. Huisgen R., Angew. Chem. Int. Ed. Engl., 1968, 7:321
8. Gilchrist, T. L.; Storr, R. C. Concerted Reactions, 1971; p 5-8
9. Woodward, R.B.; Hoffmann, R. The Conservation of Orbital Symmetry; Angew. Chem. Int. Edn. 8, 781 (1969)
10. Gilchrist, T. L.; Storr, R. C. Concerted Reactions, 1971; p 8.
11. (a) Padwa, A., Ed.; Wiley/Interscience: Newyork, 1984; Vols. 1.
(b) Torssell, K.B.G. Nitrile oxides, Nitrones and Nitronates in Organic Synthesis; VCH Weinheim, 1988.
12. (a) Huisgen, R. Angew. Chem. Int. Ed. Engl. 1967, 6, 16. (b) Huisgen, R.; Grashey, R.; Sauer, J. In The Chemistry of Alkenes; Patai, S., Ed.; Interscience: New York, 1964; p 739.

13. (a) Gothelf, K. V.; Jorgensen, K. A. *Chem. Rev.* 1998, 98, 863. (b) Gothelf K. V. In *Asymmetric Metal-Catalysed 1,3-Dipolar Cycloaddition Reactions*; Kobayashi, S.; Jorgensen, K. A., Eds.; Wiley/VCH: Weinheim, 2001; pp 211-248.
14. Hendrickson J.B., Cram D.J., Hammond G.S., p 855, McGraw-Hill Kogakusha, Ltd.
15. Sustmann R., *Tetrahedron Lett.*, 1971, 2717:20.27.
16. Woodward, R.B.; Hoffmann, R. *The conservation of orbital symmetry*, Verlag Chemie, Weinheim, 1970.
17. Houk, K.N.; Yamaguchi, K. in *1,3-Dipolar Cycloaddition Chemistry*; Padwa, A.(Ed.), Wiley, New York, 1984; Vol. 2, p. 407.
18. Houk, K.N.; Sims, J.; Watts, C.R.; Luskus, J. J. *Am. Chem. Soc.* 1973, 95, 7301.
19. Sustmann, R. *Tetrahedron Lett.* 1971, 2717.
20. Huisgen, R. in the *1,3-Dipolar Cycloaddition Chemistry*; Padwa, A. (Ed.), Wiley, New York, 1984; Vol. 1, p. 1.
21. Sustmann, R. *Pure Appl. Chem.* 1974, 40, 569.
22. Houk, K. N. *Top. Curr. Chem.* 1979, 79, 1.
23. Fukui K., Yonezawa T. and Shingu H., *J.Chem.Phys.*, 20:722, (1952).
24. Woodward-Hoffmann (1969). *Angew. Chem. Int. Ed. England.*, 8:781-853, (1969).
25. Fukui K., *Accounts Chem. Res.*, 4:57, (1971).
26. Salem L., *Jour. Of Am. Chem. Soc.*, 90:1968, (1968).
27. March J., *Adv. Org. Chem.*, p. 848, (1992)
28. Houk K.N., *Jour. Of Am. Chem. Soc.*, 94:8953, (1972).
29. Sustmann R. and Schubert R., (1972). *Angew. Chem. Int. Ed. Engl.*,11:840, (1972).

30. Sustmann R. and Trill H., *Angew. Chem. Int. Ed. England.*, 1:838, (1972).
31. Huisgen R., *Jour. Of Org. Chem.*, 2:565, (1963).
32. Sauer J., *Angew. Chem. Int. Ed. England*, 6:16, (1967).
33. Huisgen R., *Jour. Of Org. Chem.*, 41:403, (1976).
34. Huisgen R., *Angew. Chem. Int. Ed. England*, 2:633, (1963).
35. Woodward R.B. and Hoffmann R., *Jour. Of Am. Chem. Soc.*, 87:2046, (1965)
36. Woodward R.B. and Hoffmann R., *Jour. Of Am. Chem. Soc.*, 87:4388, (1965)
37. Fukui K., *Bull. of the Chem. Soc. Of Japan*, 39:498, (1966).
38. Pople J.A. and Segal G.A., *Jour. Of Chem. Phys.*, 43:29, (1965).
39. Pople J.A. and Segal G.A., *Jour. Of Chem. Phys.*, 43:136, (1965).
40. Dennis N., *Jour. Of Chem. Soc., Perkin I*, p. 2310, (1976)
41. Sustmann R. and Schubert R., (1972). *Angew. Chem. Int. Ed. Engl.*, 11:838, (1972).
42. Fukui K., Yonezawa T., Nagata C. and Shingu H., *J.Chem.Phys.*, 22:1433, (1964).
43. Anh N.T., Lefour J.M, Eisestein O. and Hudson R.F., *Tetrahedron*, 33:523, (1977)
44. Bestide J., Grandour E.N. and Rousseau O.H., *Tetrahedron Letters*, 4225, (1972)
45. Huisgen R., *Angewandte Chemie Int. Ed.*, Vol. 2, Number 10, p. 565-632, (1963)
46. Huisgen R., Fleischmann R., and Eckell A., *Tetrahedron Letters* 12, 1 (1960)
47. Huisgen R., and Eckell A., *ibid.* 12, 5 (1960)
48. Schmitz E., *Chem. Ber.* 91, 1495 (1958)
49. Huisgen R., Grashey R., Laur P., and Leitermann H., *Angew. Chem.* 72, 416 (1960)
50. Gösl R., and Meuwsen A., *Chem. Ber.* 92,2521 (1959)

51. Beyer H., Leverenz K., and Schilling H. *Angew. Chem.* 73,272 (1961)
52. Review: Baker W., and Ollis W. D., *Quart. Reviews* 11, 15 (1957)
53. Grashey R., Moriarty R. M., and Sun K. K., unpublished results, München, 1960-63
54. Huisgen R., Grashey R., and Steingruber E., *Tetrahedron Letters*, in the press; (1960)
55. Sakai N., Funabashi M., Hamada T., Minakata S., Ryu I., and Komatsu M., *Tetrahedron* 55 (1999) p 13703-13724.
56. Lund H., *Tetrahedron Lett.*, 1965, 3973.
57. Katritzky A.R.; Dennis N.; Ramaiah M., *J. Chem. Soc., Perkin 1*,1976, 2281.
58. Çelebi N., PhD Thesis, 1,3-Dipolar Cycloaddition Reactions of Kekule' and Non-Kekule 3-arylphthalazinium-1-olates, 1992, 50:129.

APPENDIX : IR , ¹H NMR, ¹³C NMR

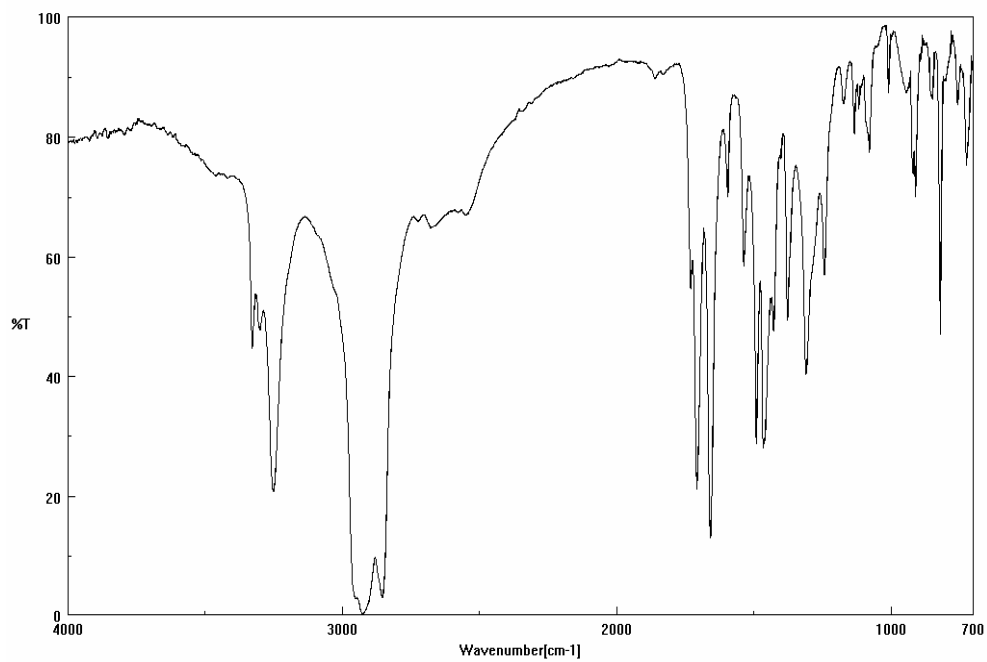


Figure 3.1. The i.r. spectrum of 2c,c' (In Nujol)

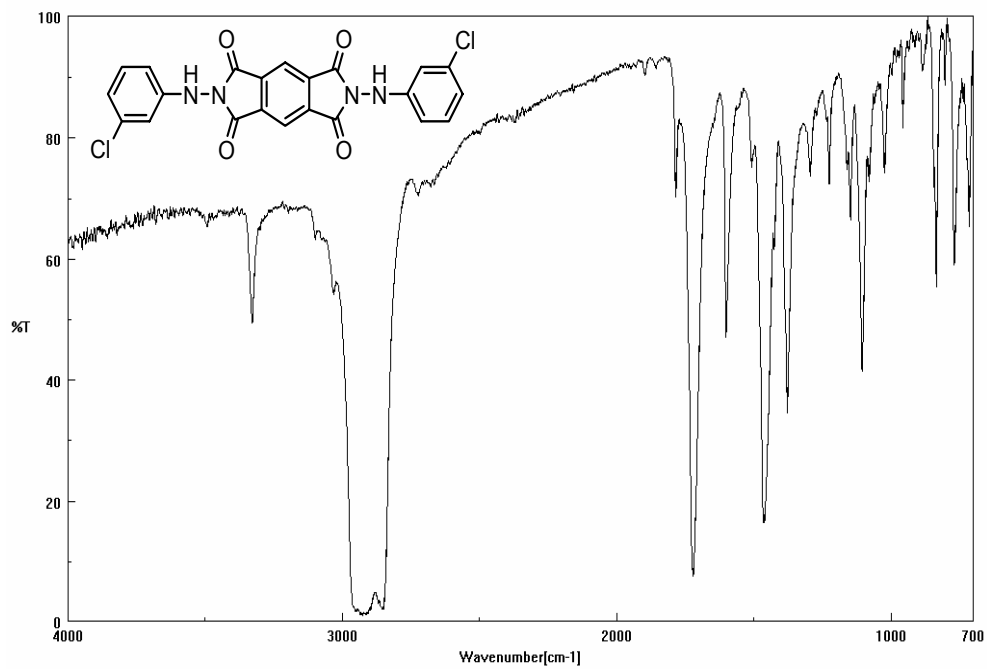


Figure 3.2. The i.r. spectrum of 2d (In Nujol)

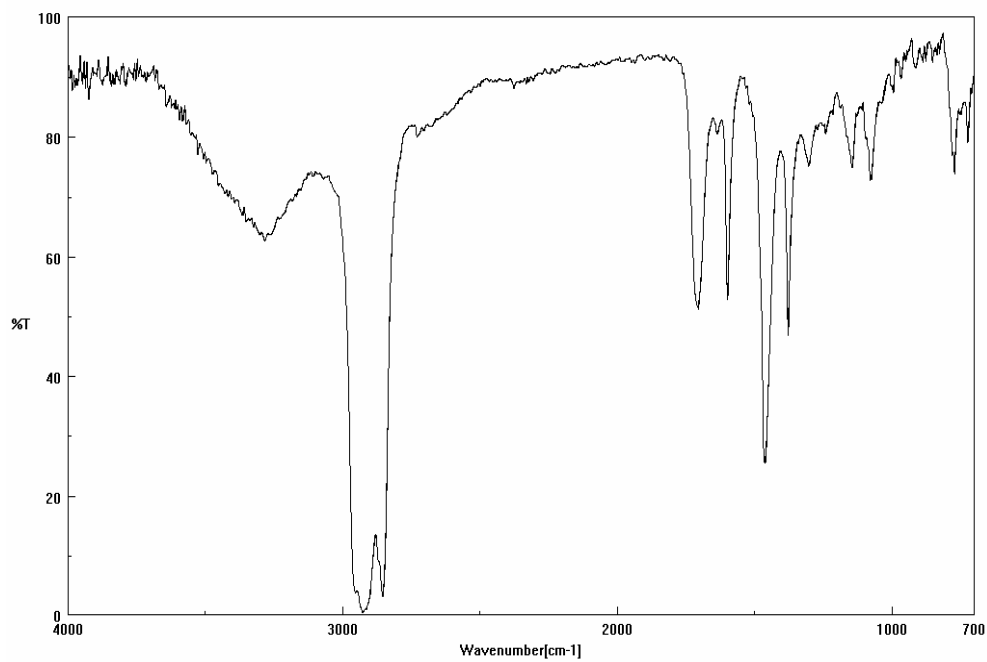


Figure 3.3. The i.r. spectrum of 2e,e' (In Nujol)

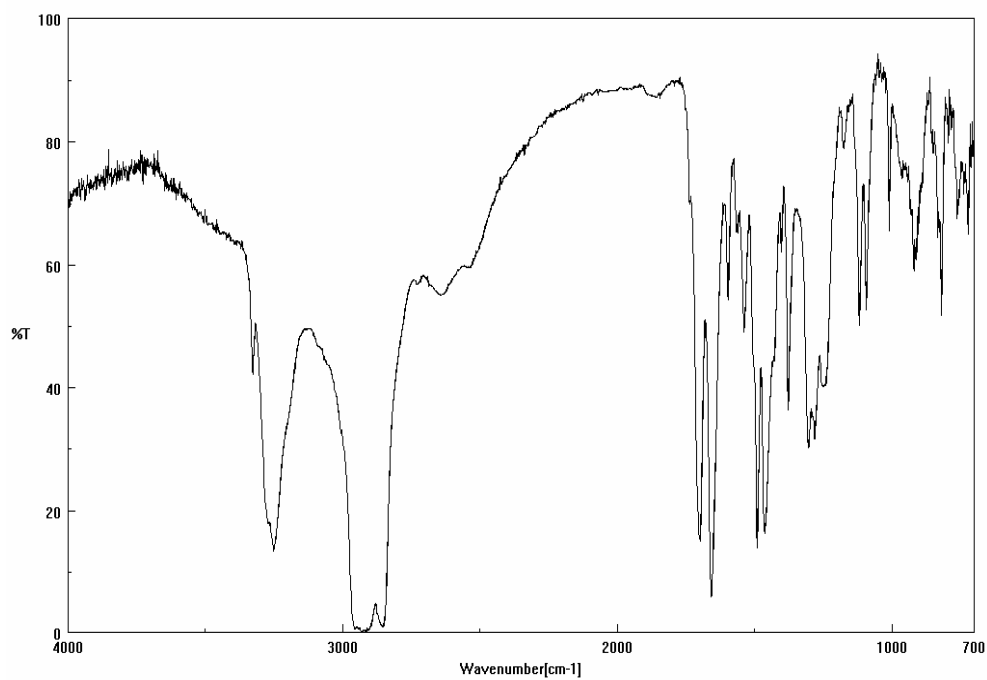


Figure 3.4. The i.r. spectrum of 2f,f' (In Nujol)

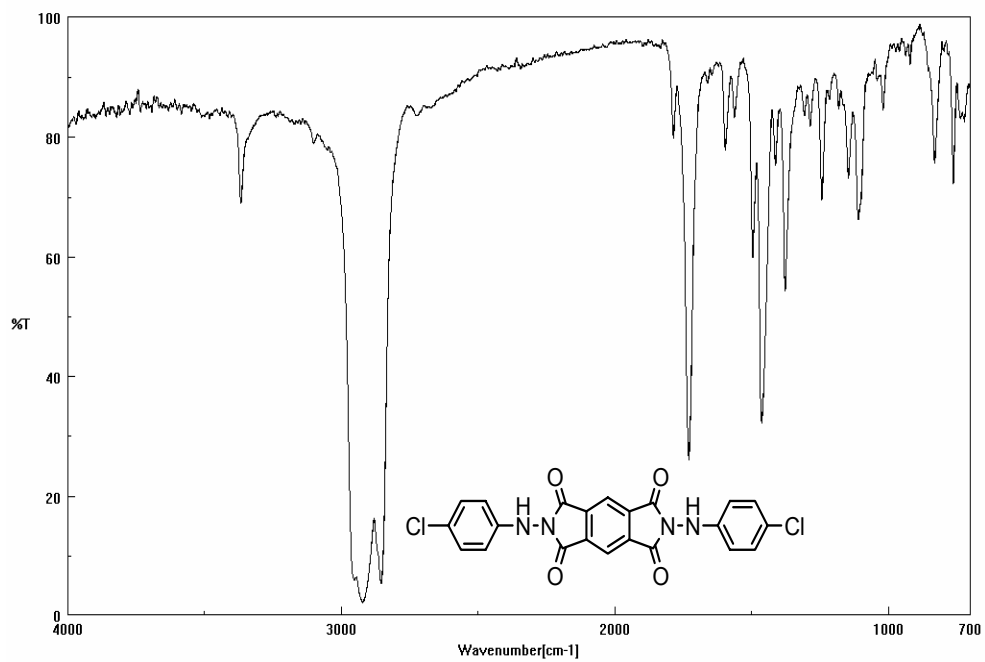


Figure 3.5. The i.r. spectrum of 2g (In Nujol)

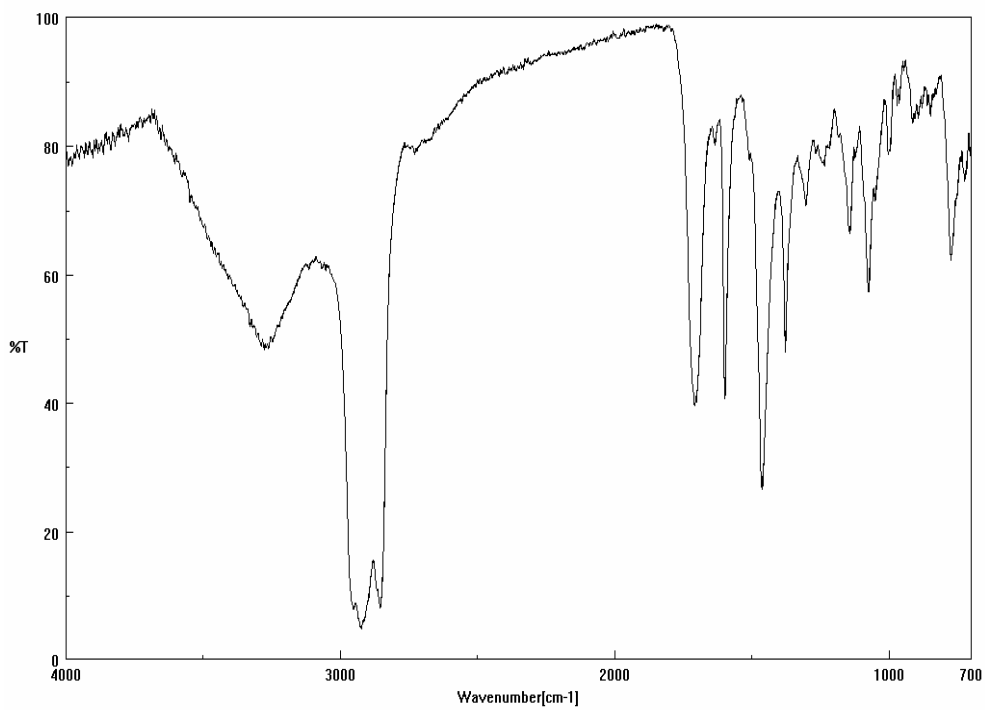


Figure 3.6. The i.r. spectrum of 2h,h' (In Nujol)

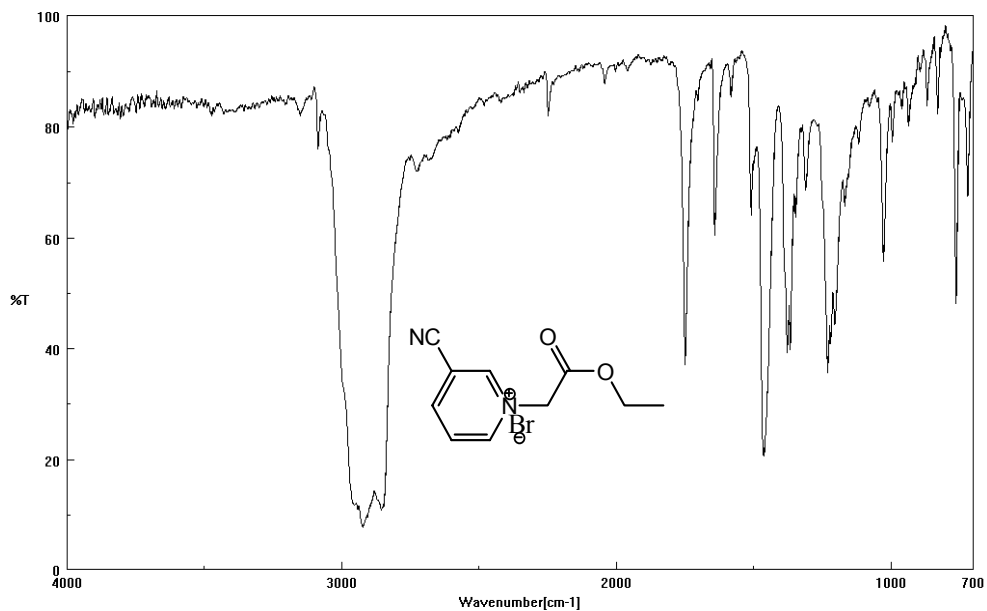


Figure 3.7. The i.r. spectrum of 3b (In Nujol)

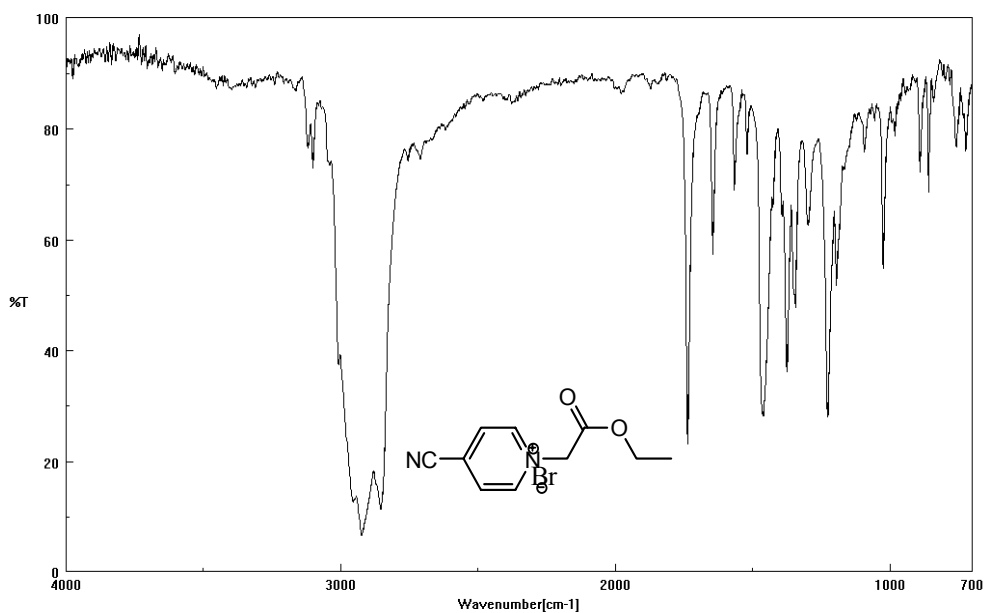


Figure 3.8. The i.r. spectrum of 3c (In Nujol)

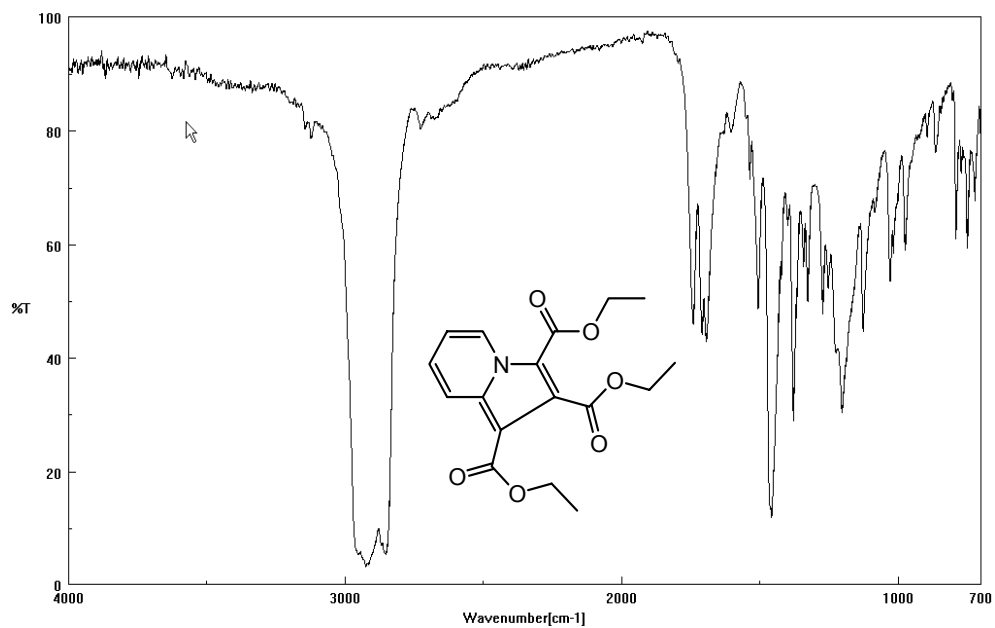


Figure 3.9. The i.r. spectrum of cycloadduct 3h (In Nujol)

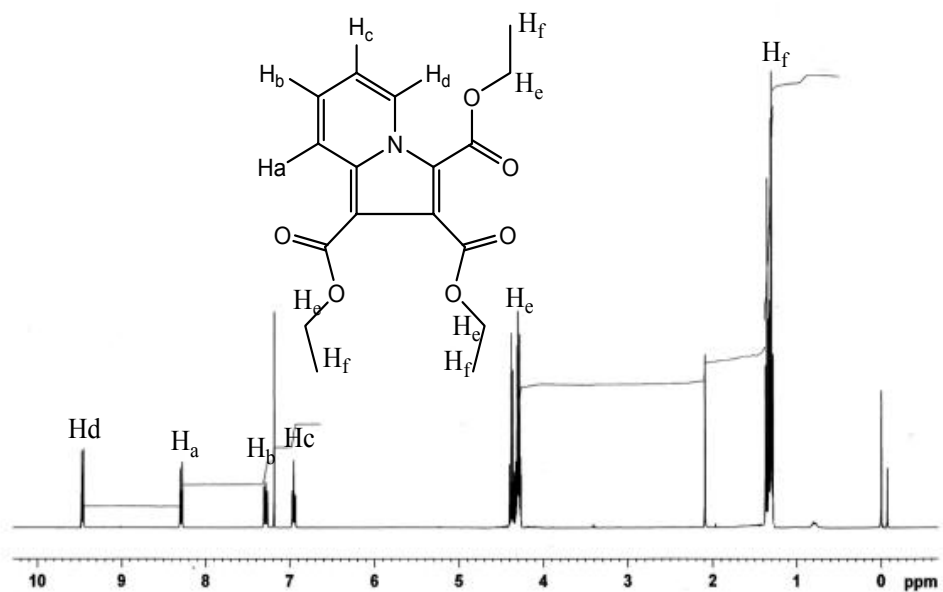


Figure 3.10. The ¹H NMR spectrum of cycloadduct 3h

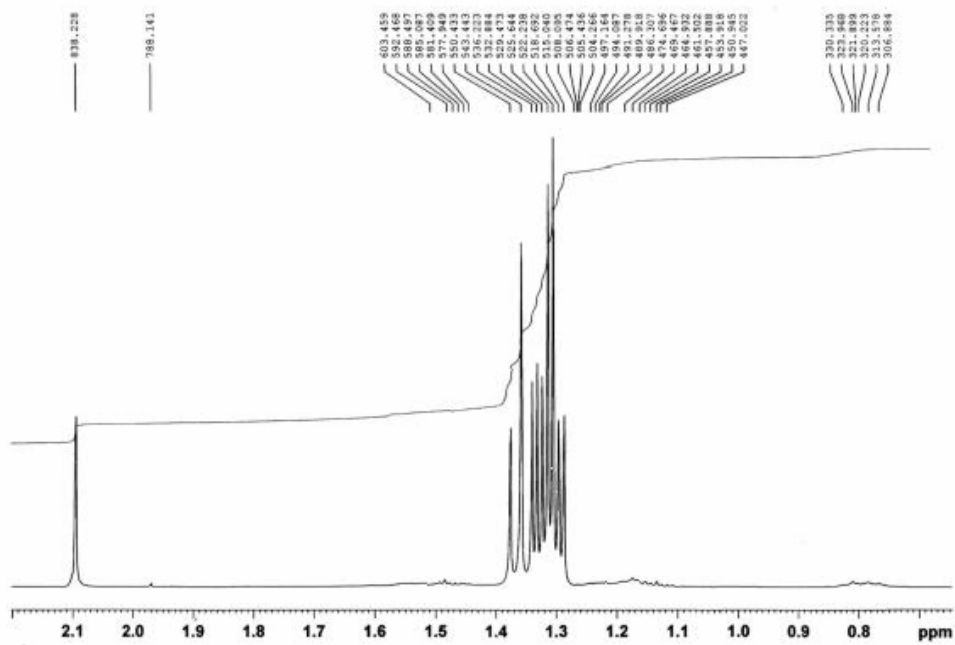


Figure 3.10. (Continued)

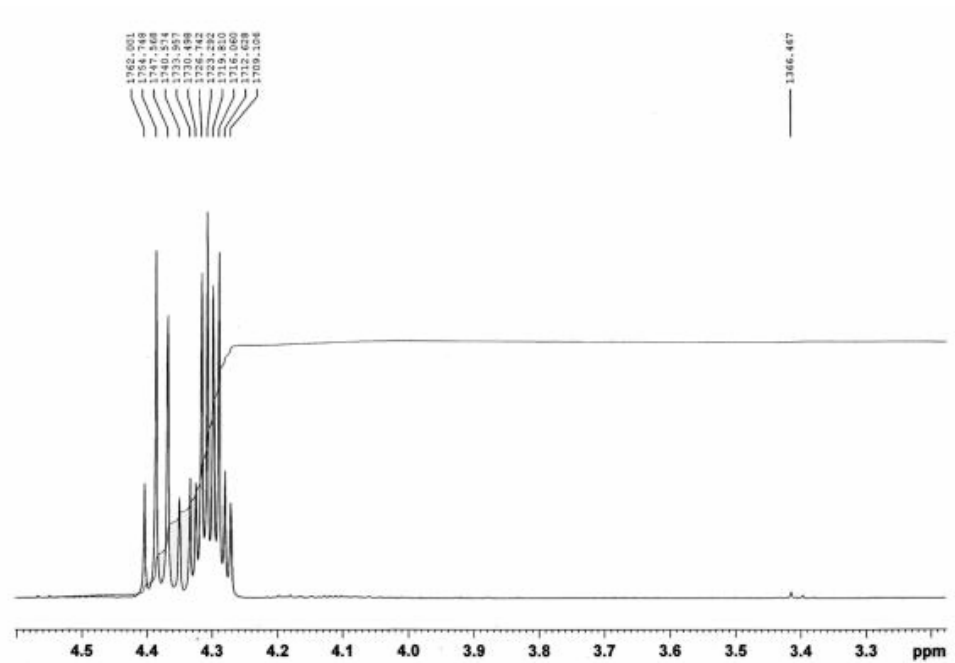


Figure 3.10. (Continued)

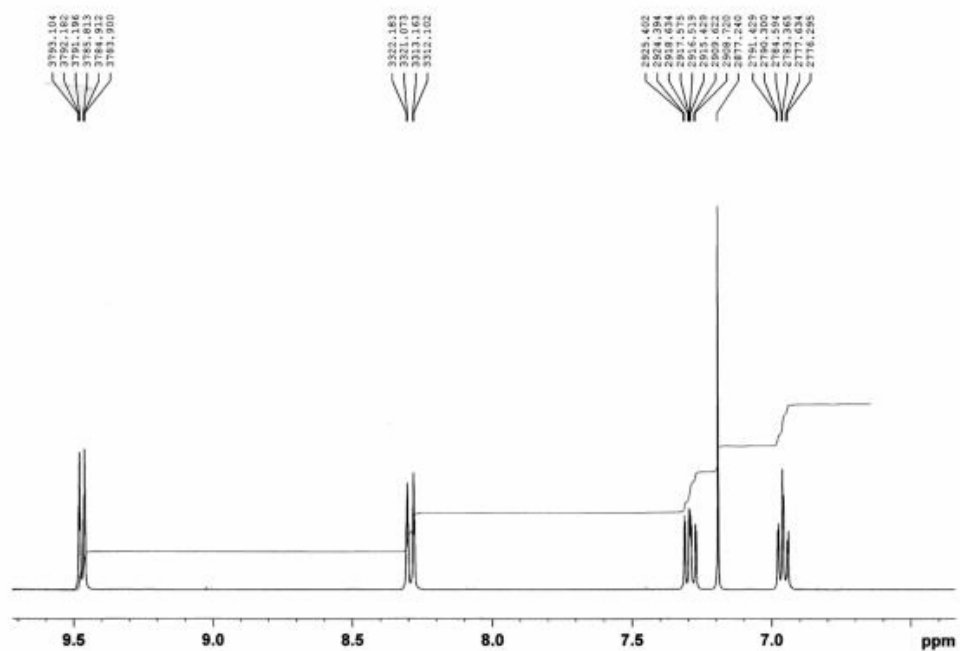


Figure 3.10. (Continued)

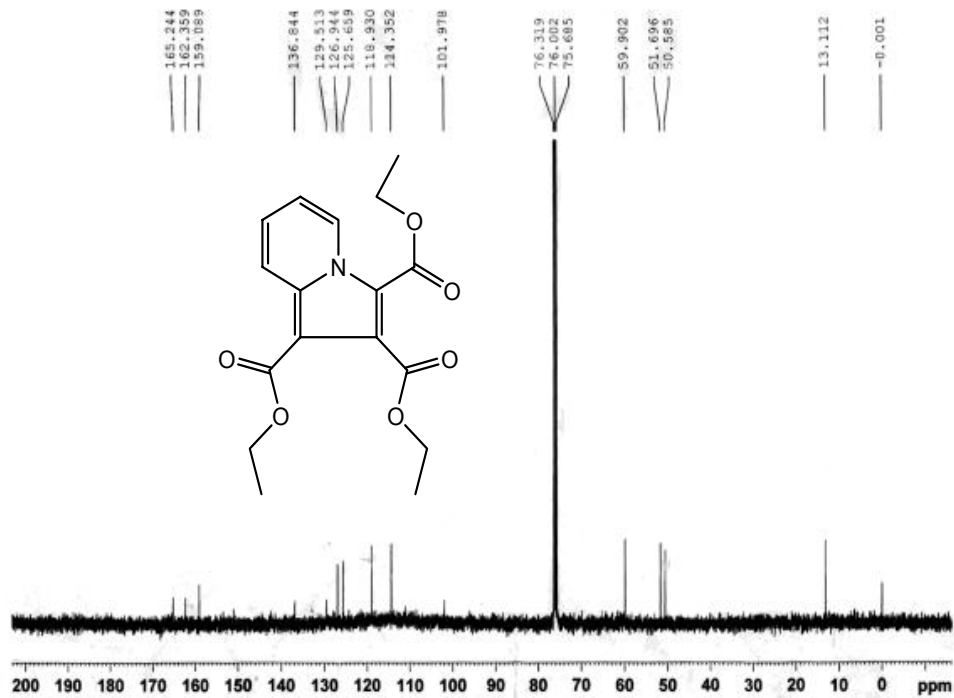


Figure 3.11. The ^{13}C NMR spectrum of cycloadduct 3h

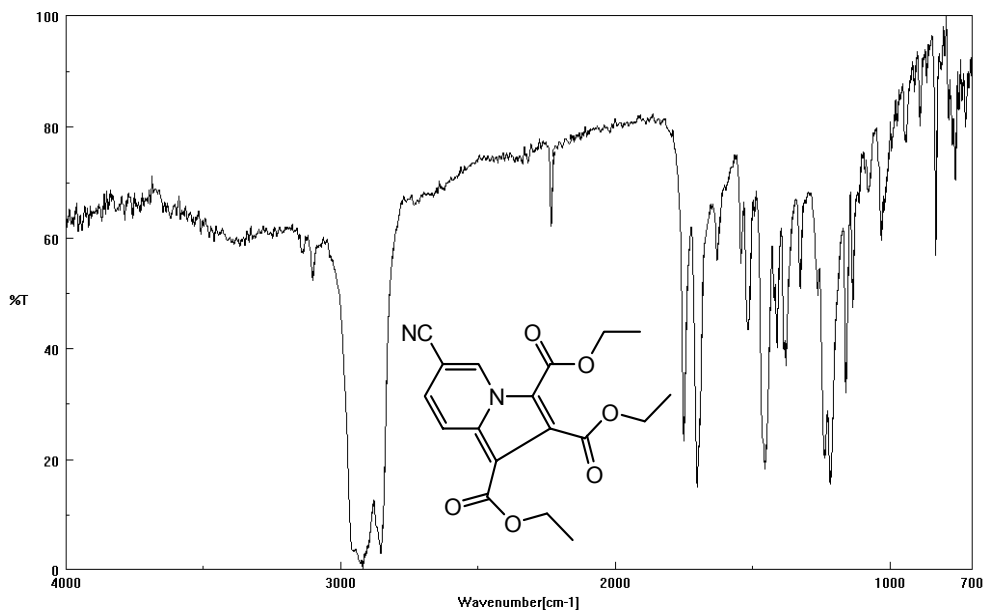


Figure 3.12. The i.r. spectrum of cycloadduct 3j' (In Nujol)

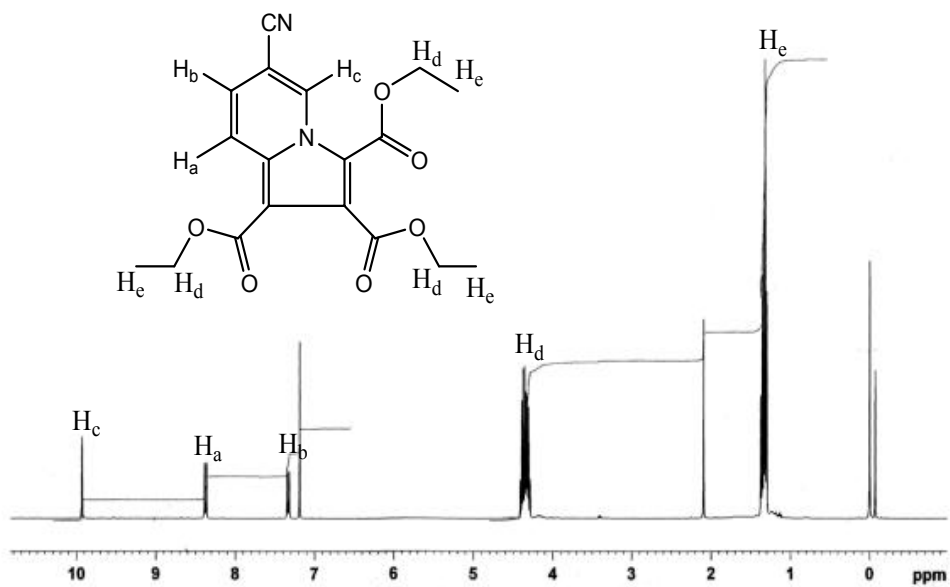


Figure 3.13. The ^1H NMR spectrum of cycloadduct 3j'

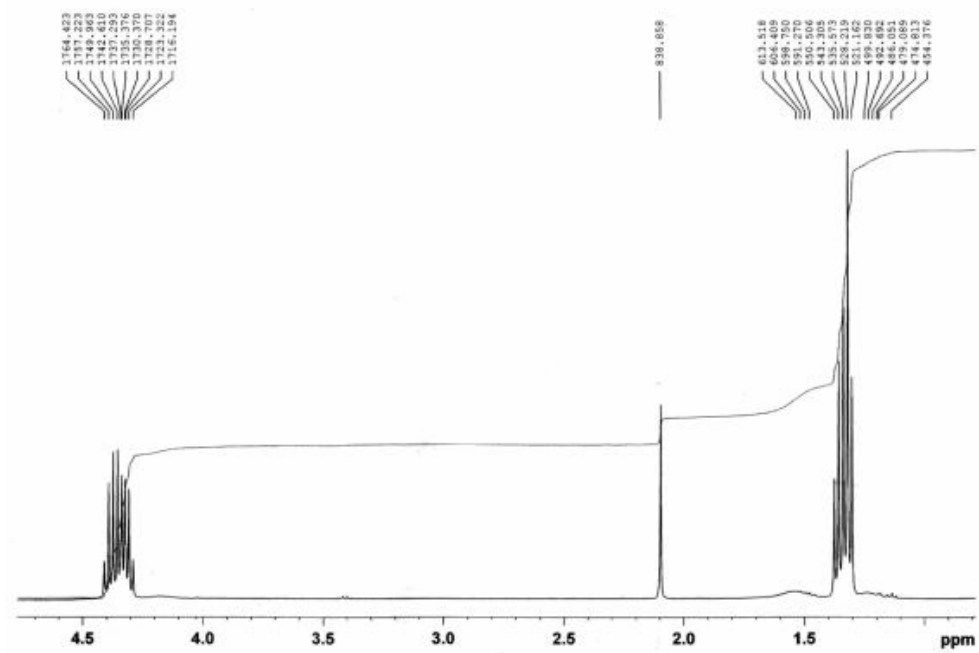


Figure 3.13. (Continued)

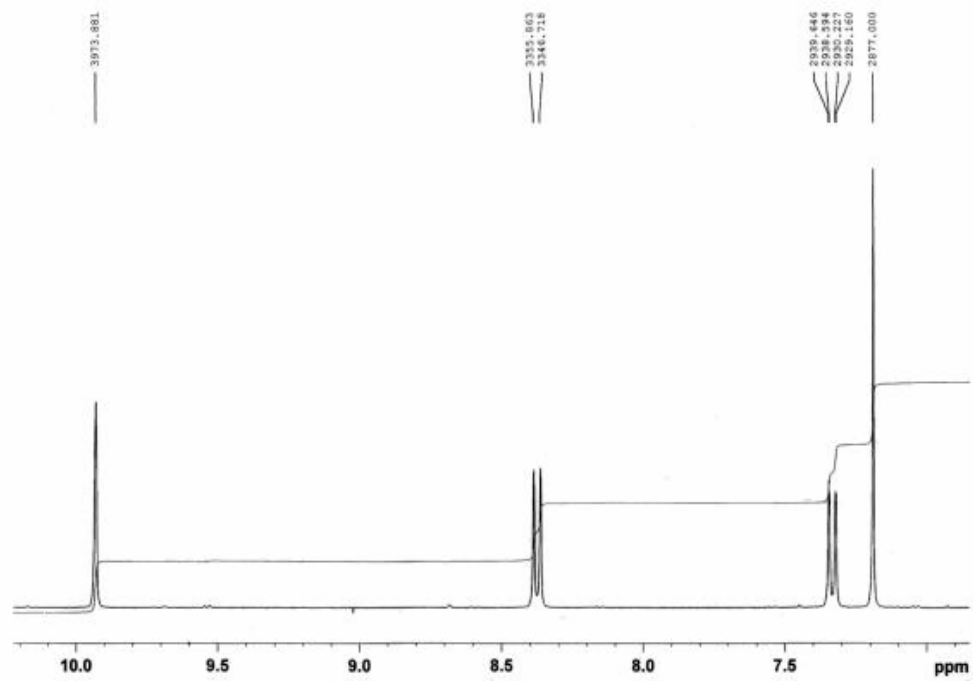


Figure 3.13. (Continued)

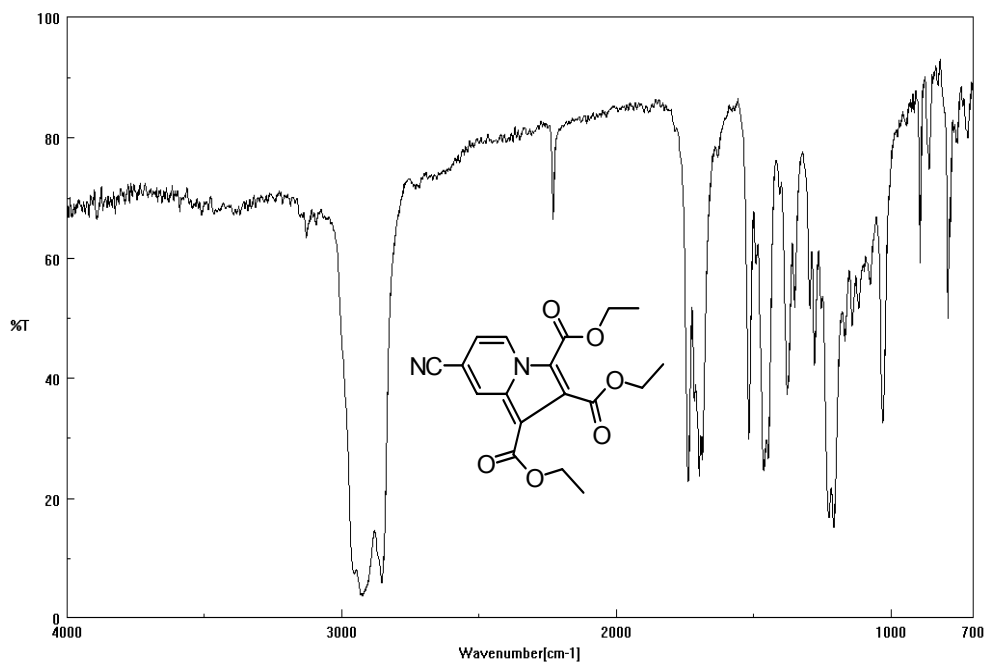


Figure 3.14. The i.r. spectrum of cycloadduct 31 (In Nujol)

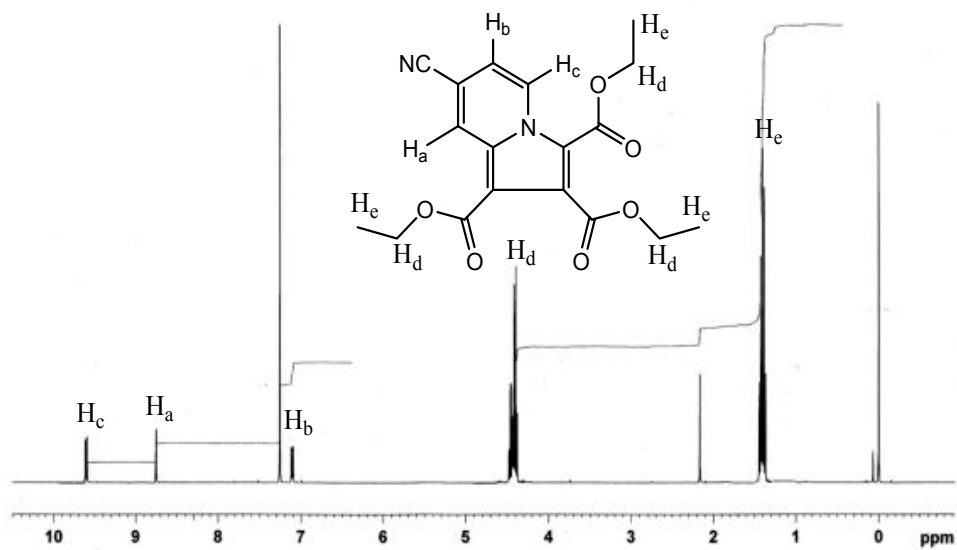


Figure 3.15. The ^1H NMR spectrum of cycloadduct 31

